CHARLES UNIVERSITY
FACULTY OF PHARMACY IN HRADEC KRÁLOVÉ
Department of Biochemical Sciences

UNIVERSITY OF HELSINKI
FACULTY OF PHARMACY
Division of Pharmaceutical Chemistry

SYNTHESIS OF EPITESTOSTERONE AND 4-HYDROXYESTRONE GLUCURONIDES USING RECOMBINANT HUMAN UDP-GLUCURONOSYLTRANSFERASES

Diploma thesis

Supervisors: Prof. RNDr. Lenka Skálová, Ph.D.

Erkka Järvinen, M.Sc. (Pharm.)

Hradec Králové 2018 Michaela Kašparová

Declaration

I declare that this thesis is my original author's work. All the literature and other sources I drew from are listed in the references and properly quoted in the text. The work has not been submitted for any other or the same academic degree.

Prohlášení

Prohlašuji, že tato práce je mým původním autorským dílem. Veškerá literatura a další zdroje, z nichž jsem při zpracování čerpala, jsou uvedeny v seznamu použité literatury a v práci řádně citovány. Práce nebyla využita k získání jiného nebo stejného titulu.

Hradec Králové 2018 ……...

Michaela Kašparová

Acknowledgement

The experimental part of this work was carried out at the Division of Pharmaceutical Chemistry, Faculty of Pharmacy, University of Helsinki with the support of the Erasmus+ programme of the European Union.

I would like to express my sincere gratitude to Doc. Moshe Finel, Ph.D. for providing me with an opportunity to join his research group, all his valuable advice, and professional guidance. My special thanks are due to Erkka Järvinen, M.Sc. (Pharm.) who guided me through this project with immense patience and support. I am also grateful to Johanna Mosorin for her skillful technical assistance and all my colleagues at the Division of Pharmaceutical Chemistry for creating such a positive working environment.

I would like to thank my supervisor in the Czech Republic, Prof. RNDr. Lenka Skálová, Ph.D., for her helpful and friendly attitude during completing this thesis.

My deepest gratitude goes to my family for their unconditional love and continuous support.

Finally, I want to thank my friends who were there for me and helped me stay positive and focused.

ABSTRACT

Charles University
Faculty of Pharmacy in Hradec Králové
Department of Biochemical Sciences

Candidate: Michaela Kašparová
Supervisors: Prof. RNDr. Lenka Skálová, Ph.D., Erkka Järvinen, M.Sc. (Pharm.)
Title of diploma thesis: Synthesis of epitestosterone and 4-hydroxyestrone glucuronides using recombinant human UDP-glucuronosyltransferases

Steroid hormones constitute an important part of the human endocrine system and are involved in a variety of physiological and pathological processes. Phase I and phase II biotransformation reactions convert these lipophilic, biologically active compounds to inactive, water-soluble metabolites that are readily excretable into bile or urine. One of the most common phase II biotransformation reactions is conjugation with glucuronic acid that is enabled by the catalytic activity of UDP-glucuronosyltransferases (UGTs). This study is focused on development and optimization of an enzymatic method for producing conjugates of glucuronic acid and two naturally occurring steroid hormones, epitestosterone and 4-hydroxyestrone. Recombinant human UGT2B7 was employed as a catalyst for the production of epitestosterone 17-glucuronide and 4-hydroxyestrone 4-glucuronide while synthesis of 4-hydroxyestrone 3-glucuronide was accomplished by UGT1A10 isoform. The synthesis reactions were scaled-up to yield milligrams of these glucuronide metabolites. The initial reaction product was subjected to liquid-liquid extraction, solid phase extraction and purification using high-performance liquid chromatography. The pure products of enzymatic syntheses ranged from 5.19 to 6.67 mg and accounted for 44.9 – 69.9 % of the theoretical yield. Final analyses using high-performance liquid chromatography and nuclear magnetic resonance spectroscopy confirmed predicted structures and indicated that the synthesized glucuronides are of a high purity. This method provides a basis for an efficient generation of highly pure steroid β-glucuronides, namely epitestosterone 17-glucuronide, 4-hydroxyestrone 3-glucuronide and 4-hydroxyestrone 4-glucuronide, which are suitable for use in future metabolic studies.

ABSTRAKT

Univerzita Karlova

Farmaceutická fakulta v Hradci Králové

Katedra biochemických věd

Kandidát: Michaela Kašparová

Školitelé: Prof. RNDr. Lenka Skálová, Ph.D., Erkka Järvinen, M.Sc. (Pharm.)

Název diplomové práce: Syntéza glukuronidů epitestosteronu a 4-hydroxyestronu pomocí rekombinantních lidských UDP-glukuronosyltransferas

Steroidní hormony tvoří důležitou součást lidského endokrinního systému a účastní se celé řady fyziologických i patologických procesů. Biotransformační reakce I. a II. fáze mění tyto lipofilní, biologicky aktivní látky na neaktivní, ve vodě rozpustné metabolity, které jsou snadno vylučitelné do žluči nebo moči. Jednou z nejběžnějších biotransformačních reakcí II. fáze je konjugace s kyselinou glukuronovou, která je umožněna katalytickou aktivitou UDP-glukuronosyltransferas (UGTs). Tato studie je zaměřena na vývoj a optimalizaci enzymatické metody využitelné pro produkci konjugátů kyseliny glukuronové a dvou přirozeně se vyskytujících steroidních hormonů, epitestosteronu a 4-hydroxyestronu. Jako katalyzátor pro produkci 17-glukuronidu epitestosteronu a 4-glukuronidu 4-hydroxyestronu byla použita rekombinantní lidská UGT2B7, zatímco syntéza 3-glukuronidu 4-hydroxyestronu byla uskutečněna pomocí izoformy UGT1A10. Měřítko syntetických reakcí bylo nastaveno tak, aby syntetizované metabolity dosahovaly miligramových množství. Výchozí reakční produkt byl podroben kapalinové extrakci, extrakci na pevné fázi a purifikaci pomocí vysokoúčinné kapalinové chromatografie. Čistý produkt enzymatické syntézy se pohyboval v rozmezí 5,19 – 6,67 mg a představoval 44,9 – 69,9 % teoretického výtěžku. Závěrečné analýzy provedené s využitím metod vysokoúčinné kapalinové chromatografie a spektroskopie nukleární magnetické rezonance potvrdily předpokládanou strukturu a indikovaly vysokou čistotu syntetizovaných glukuronidů. Tato metoda poskytuje základ pro účinnou produkci steroidních β-glukuronidů, jmenovitě 17-glukuronidu epitestosteronu, 3-glukuronidu 4-hydroxyestronu a 4-glukuronidu 4-hydroxyestronu, které svou vysokou čistotou vyhovují použití v budoucích metabolických studiích.

Contents

1. Introduction

Conjugation of a substrate with glucuronic acid is one of the most common biotransformation pathways in mammals and plays an important role in the metabolism of a whole range of both exogenous and endogenous substances. Introduction of a glucuronide moiety to a compound by UDP-glucuronosyltransferases (UGTs) generally results in its reduced biological activity and increased polarity which renders UGTs the major determinants of pharmacokinetic behavior of many drugs. Examination of glucuronidation activity of UGT isoenzymes *in vitro* may offer a basis for solid prediction of *in vivo* glucuronidation in drug discovery and development. Metabolic studies, as well as pharmacological and toxicological research, are often limited due to the lack of commercially available glucuronide metabolites. Employment of individual recombinant UGTs in the synthesis of glucuronides provides an alternative to the traditionally used chemical methods of glucuronidation, ineffective purification of glucuronide metabolites from biological samples, or ethically questionable syntheses employing animal enzymatic preparations.

The main aim of this study was to design an elegant method for producing well characterized, chemically pure steroid β-glucuronides using natural regio- and stereoselectivity of UGT enzymes. These steroid glucuronides will find application as a reference material for analytical method development and analyses determining presence and function of these phase II metabolites in biological materials. In addition, steroids and their glucuronide conjugates represent a convenient test material for enzyme kinetic studies of glucuronidation and transport of glucuronides. These studies help to elucidate the structure-function relationship of human UGTs and transporters that might be useful for understanding and prediction of the role of glucuronidation in the metabolism of many compounds.

2. Theoretical part

2.1 Biotransformation of xenobiotics and eobiotics

The human body is constantly exposed to a whole range of foreign chemicals, including food components, environmental pollutants, carcinogens, and pharmaceuticals. These exogenous compounds, also called xenobiotics, are often lipophilic substances, potentially harmful to human health. To prevent accumulation of xenobiotics to toxic levels, the human body has developed a multitude of biotransformation enzymes as a defense mechanism. Besides xenobiotics, many of these enzymes have an affinity for various endogenous substances, e.g. bile acids, steroid hormones, thyroid hormones, biogenic amines, or vitamins, and play an essential role in their biosynthesis and biotransformation (Gibson and Skett 2001). The biotransformation process enables excretion of xenobiotics and eobiotics from the organism by modifying their chemical structure and physiochemical properties (Ioannides, 2002). The major site of biotransformation reactions is the liver, other sites include intestines, kidneys, lungs, placenta, and blood (Rodwell et al. 2015).

The metabolic pathway includes conversion (phase I) and conjugative biotransformation reactions (phase II) (Gibson and Skett 2001). This phasing concept is sometimes extended by phase 0 and phase III transport processes which places emphasis on the importance of the interplay between enzymatic biotransformation and transport in the metabolism of drugs and other xenobiotics (Döring and Petzinger 2014).

2.1.1 Phase I biotransformation

Phase I enzymes catalyze a wide range of reactions which involve oxidation, reduction, hydrolysis, and isomerization. These reactions often result in the addition or uncovering of a hydrophilic group within the molecule (e.g. -OH, -SH, -NH_2) so the metabolites are more polar and can undergo phase II conjugative reactions (Gibson and Skett 2001).

The main phase I reaction is hydroxylation that is performed mainly by cytochromes P450 (CYP), a superfamily of heme-containing enzymes. These enzymes are extensively involved in the metabolism of xenobiotics, eobiotics, and some biosynthetic processes (Jancova et al. 2010).

2.1.2 Phase II biotransformation

In phase II reactions, an endogenous substance, which is often linked to a high-energy cofactor or substrate derivative, is added to the xenobiotic or endogenous substrate (or their phase I metabolite) to enhance its water solubility and excretability into bile or urine (Gibson and Skett 2001). The overview of the most common phase II reactions and corresponding transferase enzymes are shown in Table 1 (Rodwell et al. 2015, Meech et al. 2012). Other reactions ranked among phase II biotransformation processes are amino acid conjugation, fatty acid conjugation, and condensation (Gibson and Skett 2001).

Table 1. Phase II reactions and enzymes

Reaction	**Enzyme**
Glucuronidation	UGTs
Sulfation	Sulfotransferases
Glutathione conjugation	Glutathione S-transferases
Acetylation	Acetyltransferases
Methylation	Methyltransferases

2.1.2.1 Glucuronidation

Conjugation of a compound with glucuronic acid, also known as glucuronidation (Figure 1), is the most frequent glycosidation process in phase II biotransformation pathway in humans and it is responsible for the inactivation of nearly 35 % of clinically used drugs (Meech et al. 2012, Guillemette et al. 2014). Glucuronidation is a nucleophilic, bimolecular substitution (S_N2) catalyzed by UGTs. In this one-step process, a covalent linkage of glucuronic acid to a hydroxyl, carboxyl, carbonyl, sulfuryl, or amine group of a substrate is formed (Guillmette et al. 2014, Yang et al. 2017). The S_N2 reaction mechanism leads to an inversion of configuration, also referred to as 'Walden inversion', therefore, the formed glucuronide conjugate has the β-D configuration at C1 atom of the glucuronic acid moiety. Besides the glucuronide conjugate, uridine diphosphate (UDP), derived from the UDP-α-D-glucuronic acid (UDPGA), is also produced (Rowland et al. 2013, Wade and Simek 2016).

Although a few glucuronides of morphine, retinol, retinoic acid, and estrogens have the same or even higher biological activity, conjugation with the polar glucuronic acid predominantly leads to decreased biological activity and increased water solubility of the formed metabolite (Yang et al. 2017). Afterwards, glucuronide conjugates are recognized

by efflux transporters and exported to the extracellular space (Ge et al. 2016). Furthermore, glucuronides that are excreted into bile can undergo hydrolysis by bacterial β-glucuronidases which enables reabsorption of the parent compound from the intestine. This phenomenon, called enterohepatic circulation, results in an increased plasma exposure of the drug with possible implications for its therapeutic effect and toxicity (Guillemette et al. 2014). Therefore, glucuronidation and subsequent transporter-mediated excretion of glucuronide metabolites have a crucial impact on bioavailability and pharmacokinetics of many drugs and other xenobiotics (Yang et al. 2017).

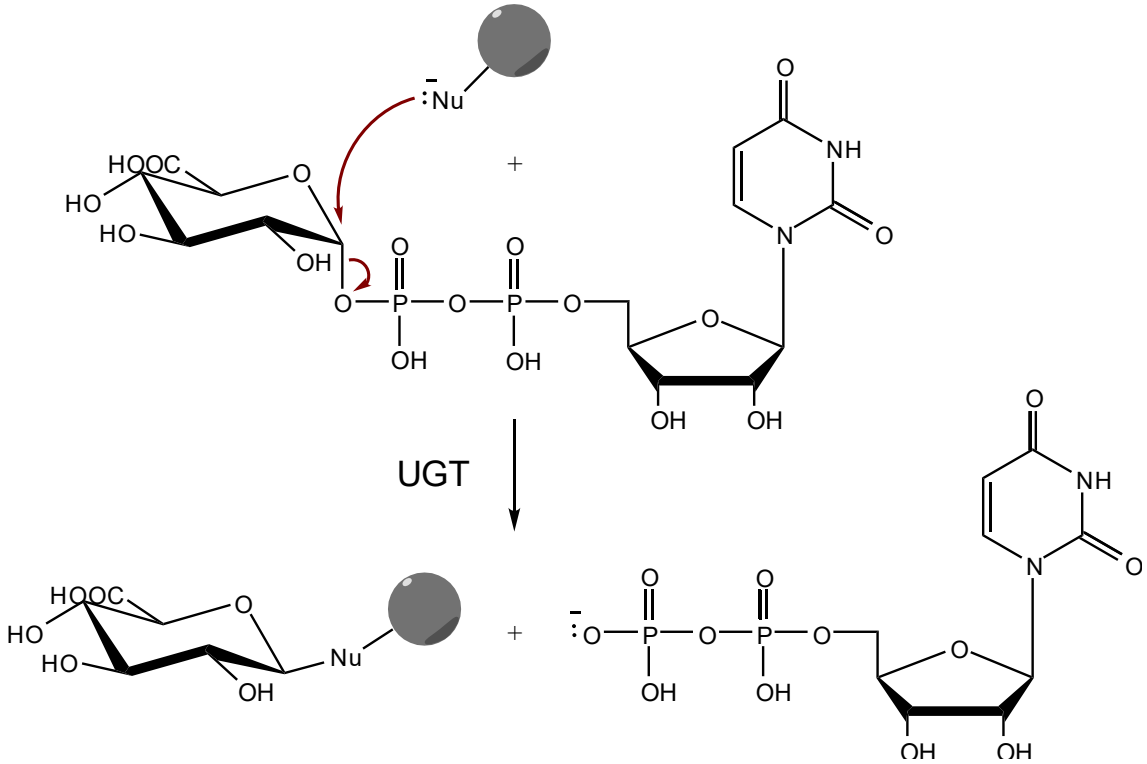

Figure 1. UGT-catalyzed glucuronidation

The UGTs catalyze the transfer of glucuronic acid from UDP-α-D-activated glucuronic acid to the nucleophilic group of a small organic molecule. The reaction product is β-D-glucuronide, a conjugate of the aglycone substrate with glucuronic acid. In addition to this product, UDP is formed. Symbol Nu represents the nucleophilic group on the small organic molecule.

2.1.3 Human UDP-glycosyltransferases

Human glycosyltransferases (GT) belong to the GT1 superfamily of inverting enzymes which are encoded by four *UGT* gene families, namely *UGT1*, *UGT2*, *UGT3* and *UGT8* (Mackenzie et al. 2005, Chang et al. 2011). Even though 22 UDP-glycosyltransferase isoforms have been identified in humans so far, the major role in the biotransformation of lipophilic chemicals is attributed to 19 glucuronidation enzymes of UGT1 and UGT2 family (Rowland et al. 2013). The members of UGT1 and UGT2 family are very active in the processing of a wide range of chemically diverse compounds and are involved in maintaining homeostasis of the entire organism. UGT8 family include a single enzyme that participates in the production of glycosphingolipids with no apparent function in drug metabolism (Meech et al. 2012).

In general, UDP-glycosyltransferases transfer sugar moiety from an activated sugar donor to a small molecule. UDP-α-D-glucuronic acid, UDP-α-D-glucose, UDP-α-D-galactose, and UDP-α-D-xylose can be used as a hexose moiety donor in glycosidation reactions (Meech et al. 2012). This thesis deals with enzymes of UGT1 and UGT2 family that utilize mainly UDP-α-D-glucuronic acid as a sugar co-substrate. These enzymes are called UDP-glucuronosyltransferases even though their sugar specificity may not be absolute (Meech et al. 2012, Rowland et al. 2013).

2.1.3.1 The human UGT families 1 and 2

Based on protein sequence identity, evolutionary divergence, and historical reasons, human UGTs (EC 2.4.1.17) are classified into two families, UGT1A and UGT2 (Figure 2). The latter can be further divided into two subfamilies, UGT2A and UGT2B (Mackenzie et al. 2005, Rowland et al. 2013, Oda et al. 2015).

UGT1A isoforms are encoded by a single *UGT1A* locus on human chromosome 2q37.1 that comprises variable first exons (n = 13) and four shared common exons. Nine functional UGT1A isoenzymes are translated from the thirteen possible mRNA isoforms (UGT1A1, UGT1A3, UGT1A4, UGT1A5, UGT1A6, UGT1A7, UGT1A8, UGT1A9, and UGT1A10) with identical carboxyl termini and different amino-terminal domains (Rowland et al. 2013, Guillemette et al. 2014, Fujiwara et al. 2016). Remaining four gene isoforms do not encode functional proteins (UGT1A2p, UGT1A11p, UGT1A12p, and UGT1A13p) (Guillemette et al. 2014). Recently, a new terminal exon, referred to as exon 5b, was localized in intron 4 within the *UGT1A* gene and thus alternative splicing among the common exons of the gene can occur. In addition to nine classic UGT1A proteins,

known as UGT1A isoforms 1 or UGT1A_i1, these new splice variants generate nine shorter UGT1A protein isoforms, named as UGT1A_i2. It is suggested that these enzymatically inactive UGT1A_i2 proteins are involved in the regulation of glucuronidation processes by interacting with enzymatically active UGT1A_i1 enzymes (Girard et al. 2007).

The *UGT2A* and *UGT2B* genes occur in a gene cluster on chromosome 4q13.2 (Fujiwara et al. 2016). Two members of *UGT2A* gene family (*UGT2A1* and *UGT2A2*) are comprised of two unique first exons with corresponding promoters and shared common exons 2 – 6. On the contrary, UGT2A3 and all UGT2B isoforms are encoded by single genes of six unique exons (Oda et al. 2015, Yang et al. 2017). Similarly to the *UGT1A* gene family, transcriptional diversity has been reported in *UGT2A* and *UGT2B* locus leading to novel isoforms of UGT enzymes. It is beyond doubt that alternative splicing contributes to interindividual UGT-mediated metabolism, however, the physiological and pharmacological function of this genomic mechanism remains poorly understood (Guillemette et al. 2010, Tourancheau et al. 2016).

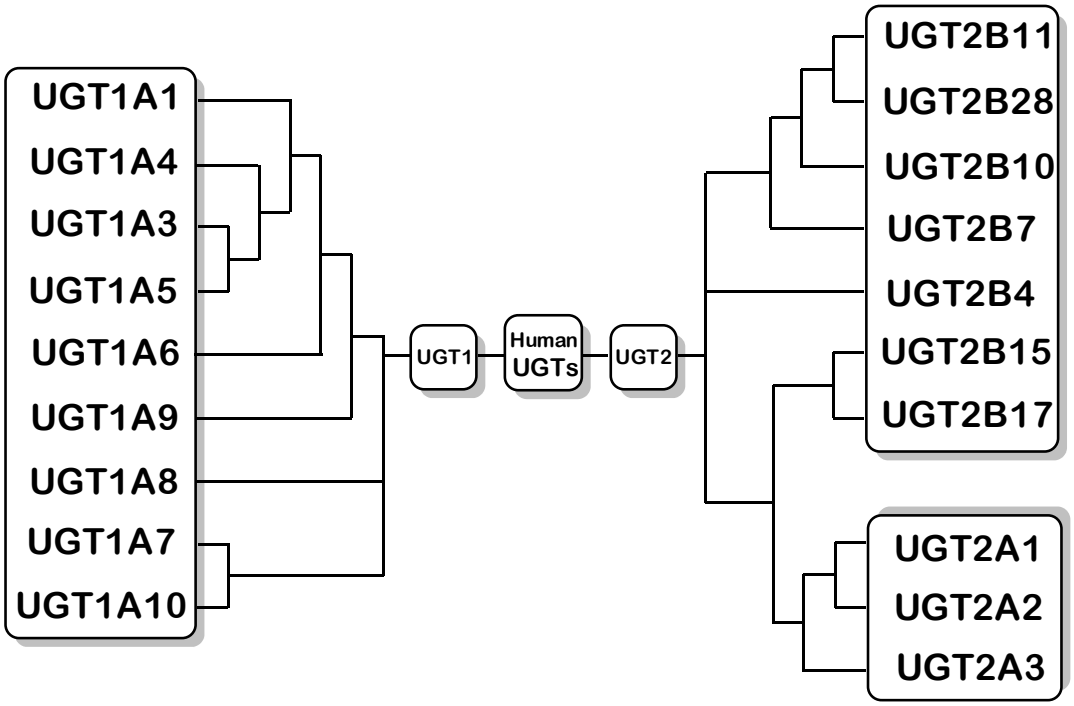

Figure 2. Phylogenetic tree of human UGTs (modified from Guillemette et al. 2010)

2.1.3.2 Molecular structure and cellular localization of human UGTs

UGTs are membrane-bound glycoproteins situated in the endoplasmic reticulum (ER). The UGT polypeptide is comprised of two parts, an amino-terminal domain and a carboxy-terminal domain (Oda et al. 2015). N-terminal domain and most of the C-terminal domain is localized on the luminal side of the ER. The rest of the C-terminal domain consists of a short C-terminal transmembrane part of 17 hydrophobic residues and a long cytoplasmic tail comprised of 19 – 24 residues (Magdalou et al. 2010, Radominska-Pandya et al. 2010, Rowland et al. 2013). Due to the intraluminal orientation of catalytic cleft and cytosolic synthesis of UDPGA from UDP-glucose by UDP-glucose 6-dehydrogenase (UGDH), transport of this hydrophilic co-substrate is essential for glucuronidation reaction. Although the exact mechanism of this uptake remains unknown, it is assumed that one or more members of the solute carrier group of membrane transport proteins (SLC) are involved in the UDPGA transport to the UGT active site (Kobayashi et al. 2006, Meech et al. 2012, Rowland et al. 2015). The carboxyl group of the formed glucuronide is predominantly ionized at the pH of the ER lumen, therefore, a glucuronide efflux transporter is needed to remove glucuronide conjugates from the ER. Suggested hypothetical mechanism of this transport is a facilitated diffusion performed by multiple transporters (Figure 3). Besides UDPGA import, the glucuronide export could be another rate-limiting factor for glucuronidation reactions (Csala et al. 2004).

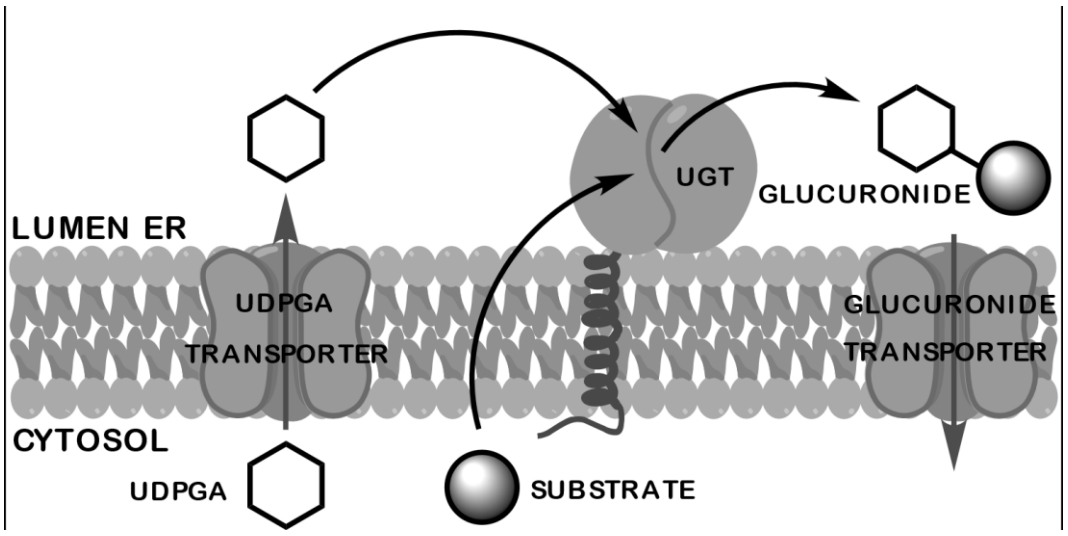

Figure 3. Schematic model of human UGT in the membrane of the ER

UDPGA uptake into the ER lumen is mediated by specific protein transporter(s), whereas the lipophilic substrate crosses the ER membrane by diffusion. The substrate is conjugated with glucuronic acid by UGT and the formed hydrophilic glucuronide conjugate is transported into cytosol (Rowland et al. 2013).

The barrier function of the ER membrane lay the foundations for one of the three major hypotheses explaining *in vitro* UGT activity latency. This hypothesis suggests that the latency phenomenon is caused mainly by the limited access of UDPGA to the intraluminal active site of UGT enzymes. In addition, adenine nucleotide inhibition effect and hydrophobic lipid environment influence on UGT conformation have also been proposed as an explanation of UGT activity latency (Liu and Coughtrie 2017). Disruption of the ER membrane *in vitro* is achievable by many treatments including sonication, grinding in sand and the addition of detergents, phospholipase A or C, or staphylococcal α-toxin. Both disruptive agent and preparative method of the microsomal fractions can have a significant effect on UGT activities *in vitro* and alter the accuracy of *in vitro-in vivo* extrapolation. (Fisher et al. 2000, Liu and Coughtrie 2017). The pore-forming peptide alamethicin seems to be a disruptor of choice in avoiding UGT *in vitro* latency in UGT assays since it does not affect the enzyme activity (Fisher et al. 2000).

UGT enzymes are expressed as precursors containing a cleavable N-terminal signal peptide that is important for controlling the integration into the ER, although other parts of the enzyme and various mechanisms can be involved in the targeting process (Magdalou et al. 2010). After membrane integration, the signal peptide is cleaved and the N-terminal domain is glycosylated. The mature protein consists of about 505 amino acids (Radominska-Pandya et al. 2010).

C-terminal tail of the mature UGT enzyme contains a common sequence of about 50 amino acids, also referred to as UGT signature sequence, which is shared across all human glycosyltransferases (Guillemette et al. 2014). In general, the C-terminal domain of human UGT family members exhibits high sequence homology and is regarded to be responsible for UDPGA binding (Fujiwara et al. 2016). Nevertheless, the N-terminal end was also reported to participate in sugar binding (Radominska-Pandya et al. 2010). In contrast to the C-terminal part of UGT proteins, the N-terminal domain is very divergent and gives rise to a substrate aglycone specificity of human UGT isoforms (Guillemette et al. 2014).

Since obtaining crystal structures of membrane-bound proteins is problematic, the complete three-dimensional structure of an active human UGT has not been resolved to date. However, the UDPGA binding domain of human UGT2B7, as well as soluble forms of plant and bacterial UGTs, have been crystallized and used as templates in modelling and structural characterization of human UGTs (Miley et al. 2007, Fujiwara et al. 2016). Results from the crystallography and modelling experiments contribute to the hypothesis

that the human UGTs are GT-B fold enzymes composed of two linked β/α/β Rossmann-like domains with a catalytic site positioned at their interface (Miley et al. 2007, Radominska-Pandya et al. 2010, Fujiwara et al. 2016).

Homology modelling is a valuable source of information about substrate binding, substrate specificity, and catalytic mechanism of human UGTs and contributes to a better understanding of oligomerization of UGT proteins and protein-protein interactions affecting the enzymatic activity of these important biotransformation enzymes (Fujiwara et al. 2016). Nevertheless, due to significant sequence and structural differences between the template and human UGT enzymes, the reliability of the modelled protein structures is still questionable. Therefore, a crystal structure of a mammalian UGT is needed to obtain a complex and reliable structural information about human UGT enzymes (Radominska-Pandya et al. 2010, Fujiwara et al. 2016).

UGT enzymes can form dimers and higher oligomers *in vitro*, both hetero- and homo-oligomers (Finel and Kurkela 2008, Fujiwara et al. 2016). Recently, extensive protein-protein interactions of UGT2B7 were revealed using immunoprecipitation indicating that UGTs also interact with other microsomal or even cytoplasmic enzymes and may form a functional unit with these biotransformation proteins (Fujiwara and Itoh 2014, Fujiwara et al. 2016). It is evident that both oligomerization and other protein-protein interactions may have a significant influence on the function of UGT enzymes *in vitro*, however, no evidence of oligomerization of intact UGTs *in vivo* have been acquired so far (Fujiwara et al. 2016).

2.1.3.3 Tissue distribution of human UGTs

Human UGT expression profiles display significant differences among tissues (Rowland et al. 2013). Evaluation of tissue distribution of the individual UGT isoforms is important for understanding their physiological and/or pathological role as well as for predicting *in vivo* glucuronidation and clearance models (Oda et al. 2012, Oda et al. 2015). Due to the similar primary structure of human UGTs (up to 97% amino acid sequence similarity), preparation of UGT isoform-specific antibodies for a direct immunochemical detection is a difficult task (Oda et al. 2015). Only a few specific antibodies were developed for measurements of protein levels using Western blot analysis (Oda et al. 2012, Oda et al. 2015).

Besides immunochemical techniques, semiquantitative reverse transcription-polymerase chain reaction (RT-PCR) and quantitative reverse transcriptional-polymerase

chain reaction (qRT-PCR) analyses were used to assess the expression of individual UGTs. Nevertheless, tissue distribution of UGT isoforms that was determined at mRNA levels does not necessarily correlate with the actual protein levels (Oda et al. 2012, Oda et al. 2015). For instance, extremely high and predominant mRNA contents of isoform UGT2B4 (34.5 – 55.7 % of total UGT mRNA expression) in human liver samples does not reflect protein contents of UGT2B4 (13 % of total) (Izukawa et al. 2009, Ohno and Nakajin 2009, Court et al. 2012, Oda et al. 2015). Recent analytical techniques, especially targeted peptide-based quantification using liquid chromatography-tandem mass spectrometry (LC-MS/MS), allow direct quantification of UGT isoforms (Sato et al. 2014, Oda et al. 2015).

Absolute UGT protein contents in human liver microsomes (HLM), human intestinal microsomes (HIM), and human kidney microsomes (HKM), quantified by liquid chromatography-mass spectrometry (LC-MS) or LC-MS/MS, were previously summarized in a review (Oda et al. 2015). Combined and averaged data of five studies showed that the isoforms of UGT2B subfamily constitute 54 % of total UGT proteins expressed in the liver with the highest contents of UGT2B7 (22 %, 98 pmol/mg protein). Other isoforms detected in the liver microsomes were UGT2B4 > UGT1A4 > UGT2B15 > UGT1A1 > UGT1A6 > UGT1A3 > UGT1A9 > UGT2B10 > UGT2B17 (Oda et al. 2015, Fallon et al. 2013). On the other hand, very low or no protein or mRNA levels of UGT1A5, UGT1A7, UGT1A8, UGT1A10, UGT2A1, and UGT2A2 were detected in human liver (Izukawa et al. 2009, Ohno and Nakajin 2009, Court et al. 2012, Oda et al. 2015). UGT1A9, UGT2B7, and UGT1A6 have a major role in renal drug metabolism (Rowland et al. 2013) and UGT2B7, UGT2B17, UGT1A10, UGT1A1, and UGT1A6 are the most abundant isoforms in the small intestine according to their mRNA levels (Ohno and Nakajin 2009, Court et al. 2012).

In addition to extensive expression in the liver, kidney and small intestine, human UGT mRNAs were detected in many other tissues including colon, stomach, oesophagus, lung, trachea, brain, thymus, heart, bladder, spleen, placenta, cervix, ovaries, testis, mammary gland, prostate, and adipose tissue (Ohno and Nakajin 2009, Court et al. 2012).

2.1.3.4 Genetic polymorphism of UGTs and clinical relevance

More than 200 alleles of human *UGT1A* and *UGT2* genes have been identified to date (UGT Nomenclature Committee 2005). In the case of the widely studied gene *UGT1A1* with 113 described alleles, genetic polymorphism has a crucial effect on the enzymatic

function and results in phenotypes with reduced or even absent enzymatic activity associated with severe forms of unconjugated hyperbilirubinemia (Crigler-Najjar types I and II syndromes) as well as mild forms of unconjugated hyperbilirubinemia (Gilbert's syndrome) (Radominska-Pandya et al. 2005, UGT Nomenclature Committee 2005). Furthermore, altered function of UGT1A1 can cause decreased glucuronidation of clinically used drugs (e.g. atazanavir, ezetimibe, etoposide, irinotecan) that can lead to the manifestation of their toxicity (Stingl et al. 2014). UGT polymorphism is clinically relevant especially when glucuronidation significantly contributes to the elimination of a drug or active glucuronide conjugates are formed (Stingl et al. 2014). Many case-control studies have proposed that genetic polymorphism of *UGT1* and *UGT2* genes is associated with an increased risk of cancer development. As UGT enzymes participate in the elimination of many carcinogens and cancer-promoting molecules (e.g. androgens, estrogens, dietary and tobacco carcinogens), altered expression or enzymatic activity can play a role in carcinogenesis, however, more data are needed to evaluate the risk of cancer development in association with UGT polymorphisms (Hu et al. 2016). A comprehensive list of UGT alleles can be found at the Pharmacogenomics Laboratory website (UGT Nomenclature Committee 2005).

2.1.3.5 Substrate specificity of human UGTs

UGT enzymes catalyze the transfer of glucuronic acid from UDPGA to an oxygen, nitrogen, sulfur, or acidic carbon atom of a wide range of diverse, structurally unrelated substrates (Rowland et al. 2013). O-glucuronides and N-glucuronides are most commonly formed glucuronide conjugates. More than one UGT isoform usually participate in glucuronidation of a single compound with different kinetic parameters, however, every UGT isoform is unique in its substrate selectivity and some compounds are specifically conjugated by a single UGT isoform (e.g. bilirubin) (Oda et al. 2015, Yang et al. 2017).

In general, O-glucuronides of small phenols are formed mainly by UGT1 family apart from UGT1A4. Similarly, larger phenols, some anthraquinones, and flavonoids are efficiently conjugated by UGT1 excluding UGT1A6. UGT1A3 and UGT1A9 can form acyl-O-glucuronides. N-glucuronidation of primary or secondary amines is catalyzed mostly by UGT1A1, UGT1A3, UGT1A4, UGT1A6, UGT1A8 and UGT1A9, whereas UGT1A3, UGT1A4, and UGT2B10 are responsible for glucuronidation of tertiary amines (Oda et al. 2015, Yang et al. 2017). An overview of typical substrates of human UGT enzymes is shown in Table 2.

Table 2. Examples of xenobiotic and eobiotic substrates of human UGTs (modified from Oda et al. 2015)

UGT enzyme	Typical substrates
UGT1A1	bilirubin, 17β-estradiol (E_2), etoposide, ezetimibe, SN-38 (an active metabolite of irinotecan)
UGT1A3	bile acids, polyaromatic hydrocarbons, amines, nonsteroidal anti-inflammatory drugs (NSAIDs), statins
UGT1A4	tertiary amines (e.g. midazolam, ketoconazole, *S*-nicotine, *S*-cotinine, lamotrigine, tamoxifen, trifluoperazine)
UGT1A6	planar phenols (α-naphtol, 4-nitrophenol), paracetamol, serotonin
UGT1A7	carcinogens (e.g. hydroxylated benzo[α]pyrenes), SN-38, mycophenolic acid
UGT1A8	catechol estrogens, coumarins, flavonoids, anthraquinones, phenols, troglitazone, mycophenolic acid, raloxifene
UGT1A9	large phenols, steroids, fatty acids, propofol, sorafenib, mycophenolic acid, NSAIDs, fibrates
UGT1A10	phenols, nitrosamines, flavonoids, estrogens, polycyclic aromatic hydrocarbons, troglitazone, raloxifene, dopamine
UGT2B4	bile acids (hyocholic acid, hyodeoxycholic acid), opioid drugs (codeine, morphine), zidovudine
UGT2B7	opioid drugs (morphine, codeine, buprenorphine, naloxone), antiviral drugs, NSAIDs, bile acids, fatty acids, steroids
UGT2B10	tertiary amines (amitriptyline, imipramine, clomipramine, trimipramine, diphenhydramine)
UGT2B11	orphan enzyme
UGT2B15	*S*-oxazepam, hydroxytamoxifen (an active metabolite of tamoxifen), lorazepam, sipoglitazar
UGT2B17	dihydrotestosterone, testosterone, androsterone, vorinostat

Despite substrate promiscuity, UGT enzymes exhibit substrate regio- and stereoselectivity towards many compounds (Sten et al. 2006, Sten et al. 2009, Wu et al. 2011). For instance, distinctive substrate regioselectivity of several UGT isoforms was observed in a study on the glucuronidation of various estrogens (Lépine et al. 2004).

Although there may be some general principles (e.g. preference of phenol glucuronidation over alcohol glucuronidation), prediction of regioselectivity is very difficult since it appears to be isoform- and substrate-dependent (Wu et al. 2011). Even though many *in vitro* and *in silico* approaches have been employed to understand substrate stereoselectivity and regioselectivity of human UGTs, knowledge of these phenomena is limited (Miners et al. 2004, Sten et al. 2009).

2.1.3.6 Experimental models for evaluating glucuronidation *in vitro*

Drug metabolism directly influences the overall therapeutic and toxic profile of a drug. Conjugation with glucuronic acid is an important biotransformation process involved in the elimination of drugs from many therapeutic classes. *In vitro* glucuronidation data together with knowledge of factors that modulate UGT activity *in vivo* (e.g. age, diet, ethnicity, liver and intestinal diseases, genetic polymorphism, drugs, hormonal factors, alcohol abuse) can help estimate the relative contribution of glucuronidation on drug clearance *in vivo*. *In vitro-in vivo* extrapolation enables selecting drug candidates with favorable pharmacokinetic and toxicological properties in drug metabolism studies preceding clinical trials. Therefore, assessment of drug glucuronidation *in vitro* can be used for preclinical drug development but also for clinical practice (e.g. individual drug dosing and evaluation of the risk for drug interactions) (Brandon et al. 2003, Miners et al. 2004, Ge et al. 2016).

UGT function and properties are frequently studied using *in vitro* activity and inhibition assays (Miners et al. 2004). Generally, *in vitro* assays can be carried out on several kinds of *in vitro* models including intact perfused organs, tissue slices, isolated cells, subcellular fractions, and isolated enzymes (Brandon et al. 2003). Microsomal fractions are probably the most common source of UGT enzymes and can be obtained by differential centrifugation of tissue homogenates. Microsomes contain enzymes bounded to vesicles of the ER, mainly CYP and UGT proteins. Besides extensively used HLM, other extrahepatic tissues can serve as a source of microsomal fractions (Venkatakrishnan et al. 2003). In contrast to microsomes, models that comprise of intact cells contain soluble enzymes, transporter proteins, and cytosolic cofactors and therefore can provide more realistic information about *in vivo* drug metabolism and elimination (Brandon et al. 2003). On the other hand, since several UGT enzymes are present in these models and specific inhibitors and substrates are not known for each UGT isoform, studying the effect of individual isoenzymes and genetic polymorphism on glucuronidation reaction is very

complicated (Brandon et al. 2003, Miners et al. 2004, Oda et al. 2015). Together with inhibition studies using microsomal preparations, recombinant human isoenzymes are employed in reaction phenotyping studies of glucuronidation. Reaction phenotyping study can determine specific isoform(s) involved in glucuronidation of a compound (Oda et al. 2015).

Recombinant human UGT enzymes have been expressed in mammalian cells including COS (monkey kidney cells), V79 (Chinese hamster lung fibroblast cells), and HEK293 (human embryonic kidney cells). In addition to mammalian cells, *Escherichia coli*, yeasts (*Pichia pastoris*, *Saccharomyces cerevisiae*), and baculovirus-infected Sf9 insect cells from the ovarian tissue of the fall armyworm *Spodoptera frugiperda* have been used to express recombinant UGT enzymes (Radominska-Pandya et al. 2005, Zhang et al. 2012). Besides studying drug biotransformation, drug-drug interactions, and genetic polymorphism, recombinant human UGTs can be used for isolation and synthesis of glucuronides (Stachulski and Meng 2013).

Baculovirus-infected Sf9 insect cell system is capable of high-level expression of recombinant proteins. UGT enzymes produced by the recombinant baculovirus-infected insect cells can form up to 5 – 10 % of total cellular protein. This expression system was used to generate UGT enzymes with six histidine residues (His-tag) attached on the C-terminal end (Kurkela et al. 2003, Radominska-Pandya et al. 2005). His-tagged fusion proteins can be easily purified by immobilized metal-chelating chromatography (e.g. using nickel-containing column). Moreover, commercially available monoclonal antibodies against His-tag enable evaluation of UGT expression levels and thus comparison of the glucuronidation activity in different preparations with respect to the expression (Kurkela et al. 2003). Recombinant UGTs expressed in baculovirus-infected insect cells demonstrated decreased normalized activity (velocity of metabolite formation per unit of UGT protein) compared to HLM. This decrease in normalized activity led to the hypothesis that overexpression of the enzyme negatively influences its activity per protein unit, perhaps due to the accumulation of inactive enzyme (Zhang et al. 2012, Oda et al. 2015).

Despite the significant advantages of *in vitro* studies including complexity, simple interpretation, ethical acceptability, and relative inexpensiveness, *in vivo* application *of in vitro* data is problematic (Brandon et al. 2003). Numerous studies have focused on improving the in *vitro-in vivo* correlation by optimizing experimental conditions of *in vitro* assays and by taking transport processes into considerations (Ge et al. 2016).

However, *in vivo* studies are still needed to give a complex representation of true *in vivo* situation (Brandon et al. 2003).

2.1.3.7 Experimental conditions of *in vitro* UGT assays

In vitro studied enzymatic activity of UGT enzymes can be greatly affected by numerous factors including pH of the incubation mixture, buffer type, ionic strength, concentration of organic solvent, UDPGA concentration, UDP product inhibition, as well as inclusion of divalent ions, saccharolactone, or bovine serum albumin (BSA) (Oleson and Court 2008, Walsky et al. 2012, Manevski et al. 2013, Liu and Coughtrie 2017, Walia et al. 2017). Optimization of incubation conditions is essential for glucuronidation experiments and can significantly enhance the reliability of *in vivo-in vitro* extrapolation (Manevski et al. 2013).

Incubations are often conducted with 5 mM UDPGA in 50 mM to 100 mM phosphate buffer (PB) or tris(hydroxymethyl)aminomethane (TRIS) buffer at pH of approximately 7.4 (Walsky et al. 2012, Walia et al. 2017). Comparison between TRIS buffer and PB showed that use of the former can positively affect the formation of glucuronide conjugate in HLM and recombinant UGT incubations (Walsky et al. 2012). In another study on azidothymidine (AZT) glucuronidation in liver microsomes, various physiological and non-physiological systems were tested. The highest rates of AZT glucuronidation were obtained with bicarbonate buffer and William's E medium (bicarbonate-based) (Engtrakul et al. 2005). The effect of buffer type is most likely substrate- and isoform-dependent (Engtrakul et al. 2005, Walsky et al. 2012). Alteration of pH to higher values can be beneficial for basic substrates, whereas lowering pH values can positively influence glucuronidation of acidic substrates, possibly by modifying charge on the substrate molecule (Chang et al. 2009).

Magnesium chloride ($MgCl_2$) is often added to an incubation mixture in concentrations ranging from 2 mM to 10 mM. $MgCl_2$ is a source of divalent ions Mg^{2+} that stimulate UGT activity in a concentration-dependent manner (Walsky et al. 2012). The inclusion of 10 mM Mg^{2+} was reported to reverse the inhibition of UGT activity by UDP in alamethicin-disrupted HLM, possibly by Mg^{2+}-UDP complex formation (Walia et al. 2017). On the other hand, 10 mM $MgCl_2$ caused a decreased activity of recombinant UGT1A4, therefore the $MgCl_2$ concentration of 5 mM is generally recommended (Walsky et al. 2012).

Dimethyl sulfoxide (DMSO), a polar aprotic solvent, is frequently used in concentrations up to 10 % to improve substrate solubility in an incubation mixture. DMSO can have a beneficial effect on glucuronidation rates, especially in case of high substrate hydrophobicity. However, higher concentrations of DMSO (20 %) were shown to inhibit or even abolish the enzyme activity. The ultimate effect of different DMSO concentrations on glucuronidation probably depends on the studied substrate and source of UGTs (microsomes/recombinant enzymes/cell homogenates), therefore preliminary assays to optimize DMSO concentration are recommended in each case (Zhang et al. 2011).

Inclusion of a pore-forming antibiotic alamethicin in optimal concentrations into assays helps to avoid UGT latency in microsomal preparations, perhaps due to enhanced flow of substrate and UDPGA to the active site of UGT enzyme and better drainage of products (glucuronides and UDP) through alamethicin-formed pores in the microsomal membrane (Fisher et al. 2000, Walsky et al. 2012, Walia et al. 2017). In contrast to microsomal preparations, the addition of alamethicin has no effect on the activity of recombinant UGT enzymes (Zhang et al. 2011, Walsky et al. 2012).

It has been reported that a reducing agent dithiothreitol (DTT) is capable to activate glucuronidation towards p-nitrophenol in rat hepatic microsomes without membrane perturbation. The suggested molecular mechanism responsible for this activation is a DTT-mediated reduction of the intramolecular disulfide bond between two cysteine residues in rat UGT1A6 resulting in a conformational change and loss of latency. However, recombinant rat UGT1A6 expressed in COS cells is insensitive to DTT treatment proposing that this enzyme expressed in cultured cells is already in the reduced state with high catalytic activity (Ikushiro et al. 2002).

Saccharolactone is a β-glucuronidase inhibitor frequently used to prevent enzymatic hydrolysis of the glucuronide conjugates. Data from a study evaluating the addition of saccharolactone to glucuronidation incubations showed measurable but limited impact on glucuronidation activity of human tissue microsomes and recombinant human UGTs (Oleson and Court 2008). Moreover, saccharolactone was reported to have no or even negative effect on glucuronidation catalyzed by HLM and recombinant human UGTs in another study (Walsky et al. 2012). Therefore, routine inclusion of saccharolactone is not recommended and, if used, pH of the saccharolactone solution should be adjusted before use to avoid decrease of UGT activity due to lowered pH (Oleson and Court 2008).

Inhibitory effect of unsaturated fatty acids released from disrupted membranes can be eliminated by BSA. Addition of fatty acid-free BSA enhances *in vitro* activities of UGTs by decreasing K_m and/or increasing V_{max} of glucuronidation reactions. A significant stimulatory effect was observed in assays including 0,1 % BSA, higher concentrations (1 %, 2 % BSA) may be disadvantageous, mainly due to high nonspecific binding of substrates. Albumin effect on enzyme kinetics seems to be aglycone substrate and UGT isoform-dependent (Manevski et al. 2013). Fatty acid-free human serum albumin (HSA) and human intestinal fatty acid binding protein (IFABP) may be an alternative to BSA in sequestering fatty acids (Rowland et al. 2007, Rowland et al. 2009). Moreover, IFABP was demonstrated to bind substrates and other molecules to a lesser extent than BSA (Rowland et al. 2009).

2.2 Steroid hormones

Human steroid hormones are biologically active substances controlling a variety of vital physiological functions. All endogenous steroid hormones (glucocorticoids, mineralocorticoids, estrogens, androgens, and progestins) are biosynthesized from cholesterol and exhibit remarkable structural similarity based on the common 4-ring cyclopentanoperhydrophenanthrene framework (Figure 4) (Greaves et al. 2015).

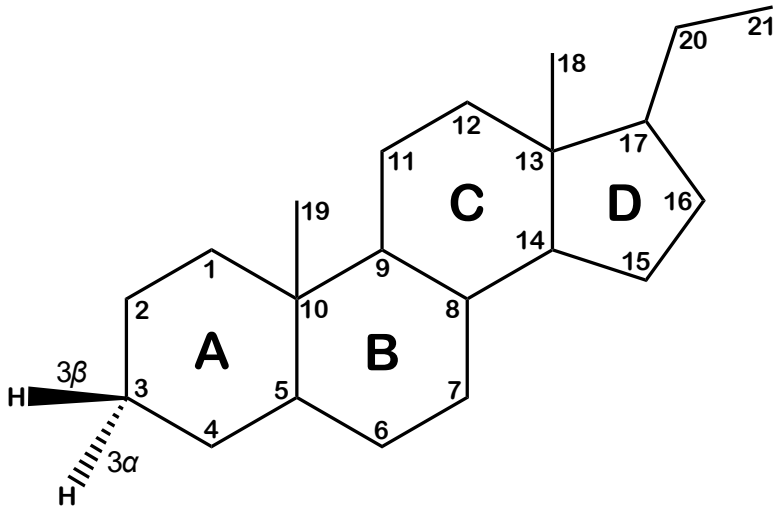

Figure 4. Graphical illustration of a fully saturated steroid skeleton consisting of four rings named in alphabetical order and 21 carbons numbered sequentially according to a standard convention. Hydrogens or substituents attached to a ring are designated as α (dashed line) if they lie below the plane of the ring or β (solid line) if they are positioned above the plane of the ring. Steroid hormones can be derived from estrane, androstane or pregnane skeleton with 18, 19 and 21 carbon atoms, respectively (modified from Greaves et al. 2015).

Human steroidogenesis takes place in several tissues including adrenal cortex (zona glomerulosa, zona fasciculata, and zona reticularis), testis (Leydig cells), ovaries (theca cells and granulosa cells), brain, and placenta (Miller and Auchus 2011, Greaves et al. 2015). These steroidogenic tissues express cholesterol side-chain cleavage enzyme (CYP11A1, formerly known as P450scc) that is involved in the first rate-limiting and hormonally controlled step of steroidogenesis – the conversion of cholesterol to pregnenolone in mitochondria. Local biosynthesis of steroid hormones is controlled by enzyme expression and cofactors which variability leads to different steroidogenic pathways and thus unique hormone production in each tissue type (Miller and Auchus 2011, Niwa et al. 2015).

Steroid hormones can be classified into three groups by a number of carbon atoms in their structure. Estrane-based hormones contain 18 carbons and are mainly produced in female ovarian tissue, but also in placenta, male testes, and adrenal gland in both males and females. Androstane-based steroids with 19 carbon atoms are synthesized primarily in male testes (testosterone) and zona reticularis of the adrenal gland (mainly dehydroepiandrosterone sulfate) in both genders. In females, the minority of androgens is produced in ovarian theca cells. Steroid hormones consisting of 21 carbon atoms are produced mainly in the adrenal gland (Greaves et al. 2015). Zona glomerulosa of the adrenal gland is involved in aldosterone production, whereas in zona fasciculata, steroidogenic pathway results in corticosterone and cortisol. Progesterone is synthesized in corpus luteum during the luteal phase, in the placenta during pregnancy, and as a step in androgen and mineralocorticoid synthesis in the adrenal gland (Ghayee and Auchus 2007, Greaves et al. 2015). After entering systemic circulation, steroid hormones bind to plasma transport proteins and are transported to the site of action. Binding to the transport proteins enhances their poor solubility and plasma half-life. The free form of a hormone is biologically active, can traverse lipophilic membranes, and encounter intracellular cytosolic or nuclear receptor (Rodwell et al. 2015). Steroid hormones are subjects to both phase I and phase II biotransformation reactions. Reduced hydrophobicity of steroid conjugates, mostly glucuronides, allow their excretion from the body. Only a minority of some steroid hormones is excreted unchanged (Greaves et al. 2015).

Steroid hormones are a part of the endocrine system that controls vital functions and provides homeostatic responses to a constantly changing environment (Rodwell et al. 2015). As for UGT enzymes, steroid hormones are significantly involved in the regulation of UGT expression in hormone-dependent tissues. For instance, the *UGT2B15* gene is up-regulated by E_2 in estrogen receptor-positive breast cancer cell lines. On the contrary, dihydrotestosterone bounded to the androgen receptor in prostate carcinoma cells promotes down-regulation of *UGT2B15* and *UGT2B17* genes (Starlard-Davenport et al. 2008, Rowland et al. 2013). Interestingly, *UGT1A10* gene is up-regulated by low concentrations of E_2 and down-regulated by increasing E_2 concentrations. The regulation of UGT enzymes by steroid hormones might play a significant role in the pathogenesis of cancer since the above mentioned UGT isoforms control the exposure of several hormone-responsive tissues to steroid hormones (Starlard-Davenport et al. 2008).

2.2.1 Epitestosterone (EpiT)

EpiT (17α-hydroxyandrost-4-en-3-one) is a 17α stereoisomer (epimer) of testosterone (17β-hydroxyandrost-4-en-3-one), a steroid hormone with androgenic and anabolic properties (Stárka 2003, Kuuranne et al. 2014). Both epimers are naturally present in the human body and biosynthesized from the same steroid precursor, cholesterol. Although the exact biosynthetic pathway of EpiT is still unknown, some hypotheses were reported. It was suggested that EpiT is synthesized by 3β-hydroxysteroid dehydrogenase (HSD) from 5-androsten-3β,17α-diol, a side-product formed from pregnenolone by CYP17A1 (16-ene synthase) competitively to the formation of 16-ene steroids (Weusten et al. 1989, Stárka 2003). Nevertheless, the more recent study proposed that EpiT most likely originates from the conversion of pregnenolone to dehydroepiandrosterone catalyzed by CYP17 followed by formation of 4-androstenedione by 3β-HSD and EpiT by 17α-HSD. An alternative pathway of EpiT synthesis from DHEA comprises conversion to 5-androstene-3α,17α-diol catalyzed by the enzyme 17α-HSD and subsequent formation of EpiT by 3β-HSD (Bellemare et al. 2005). In some mammal species with high activity of 17α-HSD, EpiT is formed by interconversion of testosterone. In humans, however, EpiT does not originate from testosterone and conversion of exogenously administered EpiT to testosterone was found negligible (Stárka 2003, Bellemare et al. 2005).

EpiT occurs in an ovarian follicular fluid, mammary cyst fluid, testes, and prostate (Stárka 2003, Zamrazilová et al. 2012). It is assumed that the main site of production of EpiT is testes (over one half of daily secretion). In addition to testes, adrenal gland and ovaries were reported to secrete EpiT (Stárka 2003). EpiT production is assumed to be only 3 % of testosterone formation in adult men, by the age of 10 years, however, plasma levels of EpiT reach higher values than those of testosterone. Average plasma concentration of EpiT is 2.5 nmol/l in men and 1.2 nmol/l in women. Plasma levels exhibit a peak around 20 years in females and 35 years in males followed by a continuous decrease with an increase in postmenopausal women (Stárka 2003, Bellemare et al. 2005).

EpiT appears to be a natural antiandrogen, exhibits antigonadotrophic activity and potential neuroprotective effect, nevertheless, the biological role of EpiT remains unclear (Stárka 2003). EpiT is a subject to phase II biotransformation reactions, predominantly glucuronidation and to a lesser extent sulfation prior to its excretion into urine (Sten et al. 2009). Urinary excretion of epitestosterone glucuronide (ETG) increases after intravenous testosterone administration, oral androstenedione intake, or stimulation by

adrenocorticotropic hormone or human chorionic gonadotropin, whereas long-term testosterone administration dramatically decreases urinary levels of EpiT conjugates, possibly due to decreased secretion of luteinizing hormone (Catlin et al. 2002, Stárka 2003).

2.2.1.1 Glucuronidation of EpiT

The major elimination pathway of EpiT and testosterone is conjugation with glucuronic acid (Sten et al. 2009). The role of individual UGT isoforms in testosterone and EpiT conjugation is fundamentally affected by the configuration of the 17-hydroxy group. Glucuronidation assay with 19 recombinant human UGT enzymes demonstrated the dominant role of UGT2B7 in the formation of ETG that was followed by glucuronidation rates of UGT2A1 and UGT2A2, and detectable activities of UGT1A4 and UGT2B4. On the contrary, the most active enzyme in testosterone glucuronidation was UGT2B17 with UGT2A1 as the second most active isoform. Whereas UGT2B7 was capable to catalyze glucuronidation of both epimers (with the clear preference of EpiT), EpiT was not glucuronidated by UGT2B17 and additional experiments showed that EpiT acts as a competitive inhibitor of UGT2B17. Even though isoform UGT2A1 glucuronidated both stereoisomers at similar and noticeable rates, this isoform is supposed to play a minor role in testosterone and EpiT glucuronidation *in vivo*. The main reason for this assumption is that UGT2A1 expression is limited mainly to the nasal epithelium and the olfactory mucosa (Sten et al. 2009, Court et al. 2012).

Although UGT2B7 His268Tyr polymorphism was reported to influence activity towards some substrates, UGT2B7*1 (His) and UGT2B7*2 (Tyr) do not appear to differ in EpiT glucuronidation rates (Chatzistefanidis et al. 2012, Rane and Ekström 2012).

2.2.1.2 EpiT in anti-doping control

Anabolic androgenic steroids (AAS), both endogenous and exogenous, are widely abused by athletes and other sportsmen to enhance muscle strength and sport performances. Androgenic steroids regulate muscle protein metabolism, bone metabolism, sexual and cognitive functions, erythropoiesis, and plasma lipid concentrations via intracellular androgen receptor (Rane and Ekström 2012). Exogenous administration of AAS is prohibited and both testosterone and EpiT are on the 2018 List of Prohibited Substances and Methods published by the World Anti-Doping Agency (World Anti-Doping Agency 2018). The misuse of AAS was banned in 1974 by the

International Olympic Committee and started to be tested at the 1976 Olympic Games in Montreal via radio-immunoassays. Although a significant progress in analytical methods allowed to detect abuse of several exogenous steroids, misuse of testosterone and its prohormones remained unprovable until the introduction of the urinary testosterone to EpiT (T/E) ratio in 1983 (Eenoo and Delbeke 2006). Since testosterone and EpiT are usually present in urine in similar concentrations (mainly as glucuronide conjugates), T/E ratio was used to distinguish between the endogenous synthesis of testosterone and its exogenous administration (Kaur-Atwal et al. 2011). T/E ratio started to be assessed by gas chromatography-mass spectrometry (GC-MS) after enzymatic hydrolysis of glucuronide conjugates and later by direct measurement of testosterone and ETG with LC-MS/MS (Fabregat et al. 2013, Kuuranne et al. 2014). The population-based cut-off values were initially set to 6/1 and from 2004 to 2013, the threshold value indicating possible steroid abuse and requiring further investigation by isotope ratio mass spectrometry was 4/1 (Strahm et al. 2015). Nevertheless, large interindividual variations that affect T/E ratio led to both false positive and false negative results. Most notably, genetic polymorphism of *UGT2B17*, encoding the major UGT enzyme involved in testosterone glucuronidation, significantly affect T/E ratio and can result in a false negative outcome in individuals being homozygous for the gene deletion. Other genetic polymorphisms with influence on T/E levels were founded in *CYP17* and *PDE7B* (phosphodiesterase 7B) genes (Rane and Ekström 2012). To avoid misinterpretations of T/E ratio, a new steroidal module of the athlete biological passport was introduced in 2014. The steroid profile of testosterone, EpiT, androsterone, etiocholanolone, 5α-androstane-3α,17β-diol, and 5β-androstane-3α,17β-diol is monitored over time, statistically evaluated, and an individual-based reference range is determined. Although individual steroid profiling provides a sensitive tool in anti-doping control, variables influencing individual steroid profiles (e.g. hormonal fluctuations during the menstrual cycle in women) must be understood and taken into consideration to avoid misinterpretation (Kuuranne et al. 2014, Mullen et al. 2017).

2.2.2 Estrone (E_1) and 4-hydroxyestrone (4-OHE_1)

E_1 is one of the most abundant endogenous estrogens in female's blood circulation (Rezvanpour and Don-Wauchope 2017). Similarly to endogenous estrogens, E_1 originates from oxidative demethylation of androgens by the enzyme aromatase (CYP19A1). The biosynthesis of estrogens takes place primarily in the ovaries of premenopausal women,

however, in postmenopausal women and men, the absolute majority of estrogens are produced in extragonadal sites that are dependent on external source of androgenic precursors. The extragonadal sources of estrogens expressing aromatase comprise mesenchymal cells of adipose tissue (including mammary adipose tissue) and skin, vascular endothelial cells, aortic smooth muscle cells, osteoblasts and chondrocytes of bone, liver, and brain. Furthermore, estrogens produced in these sites act in a paracrine or even intracrine manner rather than as endocrine hormones and their plasma concentrations merely reflect the sum of locally formed estrogens (Simpson et al. 1999, Simpson 2003, Ghayee and Auchus 2007, Greaves et al. 2015, Rezvanpour and Don-Wauchope 2017).

E_1 is an oxidative product of E_2 metabolism mediated by 17β-HSD type 2 in the endometrium and breast tissue. E_1 can also directly arise from 4-androstene-3,17-dione by the action of aromatase and undergo subsequent conversion to E_2 by 17β-HSD type 1 in the placenta and ovarian granulosa cells (Blair 2010). In this pathway, E_1 acts as a precursor of the most biologically active estrogen, E_2, therefore the interconversion of E_1 and E_2 is believed to be an important regulatory mechanism of estrogen action (Zhu and Conney 1998, Blair 2010).

E_1 metabolic pathways include irreversible oxidative phase I biotransformation through regioselective hydroxylation at A-ring or D-ring by human cytochrome P450 enzymes. Products of phase I reactions, most importantly 2-hydroxyestrone, 4-OHE_1 and 16α-hydroxyestrone, can further undergo conjugation by phase II biotransformation enzymes (Fuhrman et al. 2012, Niwa et al. 2015, Rezvanpour and Don-Wauchope 2017).

Hydroxylated estrogen metabolites have a different potential to activate estrogen receptors, exhibit unique estrogen receptor-independent biological actions, and thus have a distinct effect on tissue proliferation (Zhu and Conney 1998). While 4- and 16-hydroxylation pathways lead to a formation of genotoxic metabolites that are related to high breast cancer risk mainly in postmenopausal women, 2-hydroxylated metabolites lack the tumorigenic activity and are associated with normal cell differentiation and apoptosis (Zhu and Conney 1998, Fuhrman et al. 2012). The negative association of 2-hydroxylated metabolites with the carcinogenic process is most likely caused by their low hormonal activity, rapid biotransformation to 2-methoxyestrogens, and immediate urinary excretion. Furthermore, 2-methoxyestrogens were reported to inhibit tumour cell proliferation and angiogenesis (Samavat and Kurzer 2015).

4-OHE_1 is an oxidative metabolite of E_1 and belongs among potentially carcinogenic catechol estrogens (Fuhrman et al. 2012). While 2-hydroxylation is a dominant metabolic pathway in the liver with 2-hydroxyestrone being the predominant circulating catechol estrogen, in several extrahepatic target tissues mainly 4-hydroxylated estrogen metabolites are formed (Zhu and Conney 1998). Unlike 2-hydroxyestrone with little or no estrogenic activity, 4-OHE_1 have an estrogenic action on body weight and a tissue-specific estrogenic effect in the uterus, mammary gland, and bone (Westerlind et al. 2000). The ability to activate the estrogen receptor together with the potential to undergo metabolic redox cycling and form mutagenic DNA adducts implicate 4-OHE_1 as a carcinogenic metabolite. This suggestion is in line with the observation that 4-hydroxylase activity, caused presumably by up-regulation of CYP1B1, is elevated in human breast cancer tissue compared to normal breast tissue (Liehr and Ricci 1996, Zhu and Conney 1998, D'Uva et al. 2018).

Metabolism of estrogens is being extensively investigated with an effort to reveal exogenous and genetic factors which influence biotransformation pathways of estrogens (Fuhrman et al. 2012). To standardize estrogen measurements across laboratories in epidemiological studies and use research results in clinical practice, an accurate bioanalytical method for quantifying estrogens and their metabolites in urine, serum, and tissues with high specificity, sensitivity, and reproducibility is essential (Blair 2010, Fuhrman et al. 2015).

2.2.2.1 Estrogen-mediated carcinogenesis

There is a growing evidence that endogenous estrogens and their catechol metabolites are implicated in cancer initiation, promotion, and progression. Two complementary pathways of estrogen-mediated carcinogenesis have been suggested (Yager 2015). The original paradigm is based on the interaction of the estrogenic compound with estrogen receptor that results in altered gene expression, increased cell proliferation, decreased apoptosis, and accumulation of genetic damage. However, several experiments confirmed a significant role of estrogens in the carcinogenic process even in the absence of estrogen receptor and another mechanism independent of estrogen receptor has been proposed. This mechanism involves the oxidative metabolism of estrogens by cytochrome P450 enzymes to 2- and 4-hydroxycatechol estrogens and their further oxidation to reactive quinone estrogens. The 3,4-quinone estrogens are suspected as mutagens since these electrophiles constitute a great amount of unstable DNA adducts, 4-$OHE_{1/2}$-1-N3 adenine

and 4-$OHE_{1/2}$-1-N7 guanine, which are released from DNA leaving apurinic sites (Cavalieri et al. 2006, Yager 2015). The burst of apurinic sites leads to induction of erroneous base excision repair that generates cancer-initiating mutations (Cavalieri et al. 2006, Fuhrman et al. 2012). Both 2- and 4-catechol estrogens may also initiate a process of redox cycling that initiates the formation of reactive oxygen species (ROS). ROS cause oxidative stress and further damage of cellular macromolecules such as DNA, lipids, and proteins and thus contribute to the carcinogenic potential of catechol estrogens (Gestl et al. 2002, Samavat and Kurzer 2015). In addition, 4-hydroxycatechol estrogens boost cancer invasiveness and metastatic processes by activation of matrix metalloproteinases that are involved in disruption of the extracellular matrix, a barrier to tumour growth (Mitra et al. 2009).

Phase II biotransformation pathways including methylation, sulfonation, and glucuronidation prevent oxidation of catechol estrogens and the associated formation of DNA adducts and ROS. O-methylation of catechol estrogens by catechol-O-methyltransferase is considered to have a major protective function, however, further phase II enzymes are needed for the inactivation of 4-hydroxycatechol estrogens in tissues in which both 2- and 4-catechol estrogens are generated (Gestl et al. 2002, Samavat and Kurzer 2015). Glucuronidation can effectively eliminate native estrogens and their hydroxylated metabolites from circulation and target tissues, therefore, UGT enzymes seem to impede both hypothetical mechanisms of estrogen-related carcinogenesis (Starlard-Davenport et al. 2007). The significance of glucuronidation is further supported by accumulating data that indicate the presence of estrogen-conjugating UGT enzymes and significant amounts of estrogen glucuronides in steroid target tissues (Lépine et al. 2004, Thibaudeau et al. 2006).

2.2.2.2 Glucuronidation of 4-OHE_1

4-OHE_1 contains two possible sites of glucuronidation, 3- and 4-hydroxy groups of aromatic ring A. Both 4-hydroxyestrone 3-O-(β-D-glucuronide) (4-OHE_1-3G) and 4-hydroxyestrone 4-O-(β-D-glucuronide) (4-OHE_1-4G) are formed in site-specific reactions catalyzed by different UGT isoenzymes. Results of 16-hour experiments with microsomal fractions of 15 recombinant UGTs expressed in HEK293 cell system and a commercial microsomal fraction of UGT1A10 examining the activity of 16 UGT isoenzymes showed that 5 UGT isoforms, namely UGT1A1, UGT1A3, UGT1A8, UGT1A9, and UGT2B7 catalyze the conjugation of 4OHE_1 with glucuronic acid. In

contrast to UGT2B7, the active isoforms of UGT1A family were reported to conjugate the substrate at both glucuronidation sites. Based on kinetic parameters from the same study, it was concluded that glucuronidation of 4-OHE_1 is catalyzed more efficiently at position 4 compared to conjugation at position 3. UGT2B7 was the predominant isoform involved in the formation of 4-OHE_1-4G, whereas glucuronidation at position 3 was preferentially catalyzed by UGT1A8 (Lépine et al. 2004).

Another study on 4-OHE_1 glucuronidation by nine recombinant human UGTs, which were expressed as His-tagged proteins in baculovirus-infected Sf9 insect cells, was conducted. Incubations lasting 20 minutes demonstrated the highest catalytic activity of UGT1A10 towards 4-OHE_1. 4-OHE_1 was also effectively conjugated by UGT2B7 and UGT1A8 isoforms and activities of UGT1A9, UGT1A7, UGT1A1, and UGT1A3 were detected as well (Starlard-Davenport et al. 2007). The identification of UGT1A10 as the major UGT isoform responsible for *in vitro* glucuronidation of 4-OHE_1 is in stark contrast to the former experiments with commercially available UGT1A10 in which no glucuronides of 4-OHE_1 were detected in the case of this isoform (Lépine et al. 2004, Starlard-Davenport et al. 2007).

Since it is assumed that UGT2B7 serve as a potential tumour-suppressor factor against genotoxic 4-hydroxycatechol estrogens in breast and uterine tissue (Gestl et al. 2002, Lépine et al. 2004), the effect of genetic polymorphism in *UGT2B7* gene was investigated. Even though *in vitro* enzymatic assays demonstrated enhanced inactivation of 4-hydroxycatechol estrogens by UGT2B7*2 allozyme compared to UGT2B7*1 protein, neither *UGT2B7*1* allele (His268) nor *UGT2B7*2* allele (Tyr268) was related to breast cancer risk (Thibaudeau et al. 2006, Hu et al. 2016).

In summary, these observations indicate that several UGT isoenzymes are capable of conjugation of 4-OHE_1, knowledge of 4-OHE_1 glucuronidation and involvement of individual UGT isoforms in this process as well as their expression in steroid target tissues is limited to date.

2.3 Synthesis of glucuronides

2.3.1 Glucuronides in research and medicine

In general, glucuronidation belongs among the most important detoxification pathways of drugs and results in glucuronide conjugates with decreased biological activity (Guillemette et al. 2014). However, many biologically active O-alkyl and O-aryl glucuronides of drugs have been described and some reactive O-acyl glucuronides and N-glucuronides have been associated with adverse drug reactions suggesting their implication in drug toxicity (Stachulski and Meng 2013). International guidance on nonclinical safety studies recommends nonclinical characterization of human metabolites that account for more than 10 % of total drug-related exposure and were observed at significantly higher levels in humans than in the toxicity studies (The International Conference on Harmonisation of Technical Requirements for Registration of Pharmaceuticals for Human Use, 2009). Therefore, glucuronide metabolites may be needed for the safety assessment of drugs and new drug development processes. Besides, glucuronides have recently attracted attention as potential water-soluble and less toxic prodrugs of anticancer agents with high tumour selectivity that is enhanced by increasing β-glucuronidase enzyme levels in tumour tissue (Stachulski and Meng 2013). Higher levels of β-glucuronidases in tumours have also enabled development of promising radionuclide-labeled glucuronide imaging agents in nuclear medicine (Stachulski and Meng 2013).

For analysis of trace components in complex biological matrices, high-purity samples of glucuronide conjugates are required as analytical standards. Stable isotope-labeled glucuronides enable precise and accurate quantitative analyses by GC-MS and LC-MS (Sanaullah and Bowers 1996).

Taken together, since commercial sources of glucuronide standards are limited or unavailable, efficient methods for production of satisfactory amounts of these conjugates are required for analytical purposes, metabolism studies, and in other fields of drug research and development (Kaspersen and Boeckel 1987, Stachulski and Meng 2013).

2.3.2 Chemical synthesis of glucuronides

Chemical synthesis of glucuronide conjugates is considered much more difficult than any other chemical preparation of glucosides because glucuronidation requires the highest activation energy for the corresponding aglycone (Stachulski and Jenkins 1998). Despite

this fact, many successful chemical syntheses of structurally diverse glucuronides have been described using various activated sugar intermediates (Stachulski and Meng 2013). The Königs-Knorr reaction which employs methyl ester of acyl-protected 1-bromo-α-D-glucuronate is the most applied method for the synthesis of O-alkyl and O-acyl glucuronides. The reaction is mostly catalyzed by silver salts, such as Ag_2CO_3 followed by the occasional use of mercury and cadmium salts. The β-D-glucuronide is acquired after deprotection hydrolysis step which may generate undesirable elimination products (Stachulski and Meng 2013). The yield of β-anomer strongly depends on reaction conditions, used solvent, catalyst, and aglycon, mainly its complexity and stability (Kaspersen and Boeckel 1987, Stachulski and Meng 2013). Low yields and the necessity of multiple protection and deprotection steps are the main disadvantages of the chemical production of glucuronides (Stachulski and Meng 2013). Among further drawbacks of chemical methods belong many side-reactions resulting in a high formation of by-products, most often the corresponding α-anomer, *ortho* ester, or *C*-glucuronides of phenols, which requires additional purification steps (Kaspersen and Boeckel 1987). To reduce side-reactions and increase the formation of β-glucuronide, many other activated sugar donors, catalysts, and methods of chemical syntheses have been developed (Stachulski and Jenkins 1998, Stachulski and Meng 2013).

2.3.3 Enzymatic synthesis of glucuronides

The enzymatic synthesis of glucuronides provides an alternative approach to produce glucuronides. The application of enzymes enabled many highly regioselective and stereoselective syntheses of β-D-glucuronides under mild conditions in one step. These features are considered essential, particularly taking complex aglycons with more possible glucuronidation sites and unstable compounds into consideration (Stachulski and Jenkins 1998, Stachulski and Meng 2013).

Many methods of enzymatic syntheses have been conducted so far and their resulting milligram yields are usually sufficient for laboratory use. Nevertheless, chemical methods are still required for larger, preparative scale syntheses (Stachulski and Jenkins 1998, Stachulski and Meng 2013).

Conventional batch-wise syntheses employs tissue homogenates, microsomes from several tissues, or recombinant UGTs as catalysts and quite expensive UDPGA as a sugar donor (Stachulski and Meng 2013). As individual UGT expression levels differ among enzymatic preparations, the yields of enzymatic syntheses strongly depend on the source

used. Moreover, enzymatic sources can vary in glucuronidation regioselectivity and stereoselectivity and produce structurally diverse glucuronide/s (Stachulski and Jenkins 1998, Stachulski and Meng 2013).

Liver microsomes are the most favored source of enzymes but they can be isolated from kidneys and intestines as well. Both HLM and animal liver microsomes can be utilized for synthetic purposes. To increase enzyme expression levels and glucuronide yields, liver microsomes are often exposed to various inducing agents (e.g. Aroclor 1254, a polychlorinated biphenyl mixture). Nevertheless, microsomal preparations do not contain UGT isoforms expressed in other tissues and their usage may encounter some ethical issues (Stachulski and Meng 2013, Ma et al. 2014).

The employment of purified UGT enzymes in the synthesis of glucuronides is limited because membrane-bound UGTs are challenging to isolate and purify. On the other hand, recombinant UGTs are commonly used as convenient glucuronidation catalysts. Rapid improvement of genetic engineering techniques allowed cloning and expression of numerous recombinant UGT isoenzymes and their application in glucuronide production (Radominska-Pandya et al. 2005, Stachulski and Meng 2013). However, poor enzyme stability, low expression levels, and low normalized activities per unit of UGT protein are often encountered problems (Drăgan et al. 2010).

Recently, glucuronylsynthase derived from *Escherichia coli* β-glucuronidase by single-point mutation has been used for efficient and stereoselective *in vitro* glucuronide production. Unlike UGT isoforms, the soluble bacterial glucuronylsynthase can be easily purified and uses α-D-glucuronyl fluoride as a sugar co-substrate. Favorably, this sugar donor can be synthesized in four steps from D-glucose. Milligram amounts of several steroid glucuronides were obtained for common analytic applications, however, some substrates demonstrated very low conversion. In the case of EpiT, the conversion to the corresponding glucuronide was only 28 % (Ma et al. 2014).

2.3.3.1 Whole-cell biotransformation system

A novel approach of synthesis of glucuronides is based on the co-expression of UGT enzyme and UGDH within a recombinant yeast cell. In these recombinant yeast strains, sugar cofactor UDPGA is generated from glucose by UGDH. UDPGA is then conjugated to an aglycone by chosen co-expressing UGT isoform and exported to the reaction medium (Drăgan et al. 2010). This method is capable of scalable and efficient glucuronide production without the need for the expensive UDPGA co-substrate (Drăgan et al. 2010,

Ikushiro et al. 2016). The fission yeast, *Schizosaccharomyces pombe*, were used for the syntheses of unlabelled and isotopically labeled glucuronides (Drăgan et al. 2010). Later, a biotransformation system involving budding yeast, *Saccharomyces cerevisiae,* was developed and proved to be more efficient for the production of various glucuronide conjugates including unstable acyl glucuronides (Ikushiro et al. 2016).

2.3.3.2 Immobilized enzymes

Application of immobilized microsomes for the synthesis of glucuronides enables easier separation of glucuronide products from the reaction mixture. Moreover, higher stability of immobilized enzymes with the possibility to extend the incubation time or reuse the enzymes has been reported (Stachulski and Meng 2013). The microsomal enzymes have been entrapped in alginate beads, immobilized on Sepharose 4B beads, the phospholipid-coated octadecyl silica particles, or phospholipid high-performance liquid chromatography (HPLC) column (Kamimori et al. 2003). Solid phase extraction (SPE) column loaded with microsomes and coupled to an automated preparative HPLC system has allowed full automatization of synthesis and purification processes. In addition, glucuronide yields using microsomes immobilized on the SPE column were higher compared to glucuronide productivities of free microsomes (Kashima et al. 2010).

Development of on-line drug metabolism system employing immobilized enzyme phospholipid columns, known as immobilized enzyme reactors (IMERs), allowed enzymatic synthesis and subsequent analysis of produced metabolites by liquid chromatography-nuclear magnetic resonance spectroscopy (LC-NMR) (Kashima and Okabayashi 2010). Alternatively, a capillary electrophoresis system containing microsomes encapsulated in a monolithic capillary was used for on-line production, separation, and determination of drug glucuronides (Sakai-Kato et al. 2002).

2.3.4 Detection and structural characterization of glucuronides

Sample isolation and purification are often conducted after synthesis to avoid an interfering effect of the complex reaction mixture prior to further analyses. During sample pre-treatment, an appropriate pH and temperature should be wisely selected based on glucuronide stability. Liquid-liquid extraction (LLE), SPE, and preparative HPLC purification are most commonly employed procedures (Stachulski and Meng 2013).

Nowadays, HPLC, mass spectrometry (MS), tandem mass spectrometry (MS/MS), and their combinations (LC-MS, LC-MS/MS) enable direct glucuronide qualitative and

quantitative analysis (Sanaullah and Bowers 1996, Stachulski and Meng 2013). Glucuronides are often ionized by soft electrospray ionization technique. Molecular ion observed in MS spectra provides information about molecular weight and characteristic fragment ions together with MS/MS spectra fragmentation pattern derived from selected molecular ion help to elucidate glucuronide structure (e.g. the type of glycosidic bond). The main advantage of this technique is that only a very small quantity of the analyzed sample is needed (Kaspersen and Boeckel 1987, Stachulski and Meng 2013).

Complete structural characterization of the synthesized molecule is usually obtained with nuclear magnetic resonance (NMR) spectroscopy (Kaspersen and Boeckel 1987). The site of conjugation can be determined by comparing the ^{1}H NMR spectra of glucuronide and aglycon with the most significant changes in chemical shifts near the glucuronidation site (Stachulski and Meng 2013). In ^{1}H NMR spectra, β-D-glucuronide can be distinguished from α-D-glucuronide using chemical shift and coupling constant. The axial proton of β-anomer come into resonance at a lower frequency (higher field) than the equatorial proton of α-anomer and the H1-H2 coupling constant observed in β-D-glucuronide is greater (7-10 Hz) than in its α-anomer (2-4 Hz) (Kaspersen and Boeckel 1987). Two-dimensional NMR techniques such as homonuclear correlation spectroscopy (COSY), heteronuclear multiple-bond correlation spectroscopy (HMBC) and heteronuclear single-quantum correlation spectroscopy (HSQC) are needed for complete assignment of ^{1}H and ^{13}C NMR spectra (Luukkanen et al. 1999, Stachulski and Meng 2013).

3. Aims of the study

The main aims of this study were:

- to select isoforms with the highest activity and regioselectivity for syntheses of 4-OHE_1-3G and 4-OHE_1-4G, respectively, and for this purpose, to examine glucuronidation of 4-OHE_1 by a set of recombinant human UGT enzymes.

- to optimize the catalytic activity of UGT-enriched membranes to achieve the highest possible glucuronide production.

- to develop and optimize enzymatic procedures easily applicable in laboratories to produce milligrams of glucuronides of EpiT and 4-OHE_1.

- to isolate pure glucuronides and confirm their chemical structure with modern analytical methods.

4. Materials and methods

4.1 Chemicals

The list of used chemicals is presented in Table 3.

Table 3. Chemicals

Chemical	CAS RN	Manufacturer
4-OHE$_1$ ≥ 90 % (HPLC)	3131-23-5	Sigma Aldrich
4-OHE$_1$ ≥ 98 % (TLC)	3131-23-5	MP Biomedicals
Acetonitrile for HPLC	75-05-8	Sigma-Aldrich
Albumin from bovine serum (≥ 96 %, essentially fatty acids free)	9048-46-8	Sigma-Aldrich
Ammonia solution 25%	1336-21-6	VWR International
Dichloromethane (≥ 99.8 %)	75-09-2	Honeywell
Dimethyl sulfoxide p.a.	67-68-5	Sigma-Aldrich
Dimethyl sulfoxide-d_6	2206-27-1	Sigma-Aldrich
EpiT	481-30-1	Sigma-Aldrich
Ethylenediaminetetraacetic acid disodium salt dihydrate	6381-92-6	Sigma-Aldrich
Formic acid for MS (~ 98 %)	64-18-6	Fluka
Magnesium chloride hexahydrate (99.0 – 102.0 %)	7791-18-6	Sigma-Aldrich
Methanol LC-MS	67-56-1	Fluka
Sodium hydroxide p.a.	1310-73-2	Sigma-Aldrich
Sodium phosphate dibasic dihydrate (98.5 – 101.0 %)	10028-24-7	Sigma-Aldrich
Sodium phosphate monobasic dihydrate (≥ 99.0 %)	13472-35-0	Sigma-Aldrich
Perchloric acid (70 %)	7601-90-3	Sigma-Aldrich
Trizma® hydrochloride	1185-53-1	Sigma-Aldrich
Trizma® base	77-86-1	Sigma-Aldrich
UDPGA ammonium salt (98 – 100 %)	43195-60-4	Sigma-Aldrich

Water for assays and analyses was purified using a Milli-Q water purification system (MilliporeSigma). Other chemicals used in the laboratory were acquired from commercially available sources and solvents were of LC-MS grade.

4.2 Stock solutions and other material

50 mM 4-OHE_1 solution

In case of need, solid compound (Mr = 286.37) was dissolved in an appropriate volume of DMSO in a microtube and stored at -20 °C.

10 mM EpiT solution

7.56 mg of EpiT (Mr = 288.42) was dissolved in 2.620 ml of DMSO and stored at -20 °C.

100 mM $MgCl_2$ solution

2.033 g of $MgCl_2 \cdot 6H_2O$ (Mr = 203.30) was dissolved in 100 ml of Milli-Q water in a 100-ml volumetric flask and stored in a bottle with a screw cap at 4 °C.

200 mM PB pH 7.4

Solution A: 3.560 g of $Na_2HPO_4 \cdot 2H_2O$ (Mr = 177.99) was dissolved in 100 ml of Milli-Q water in a 100-ml volumetric flask. Solution B: 3.120 g of $NaH_2PO_4 \cdot 2H_2O$ (Mr = 156.01) was dissolved in 100 ml of Milli-Q water in a 100-ml volumetric flask. Solution B was gradually added to solution A under pH meter until a pH of 7.4 was reached. The resulting buffer was kept in a bottle with a screw cap at 4 °C.

50 mM solution of UDPGA

A fresh 50 mM solution of UDPGA ammonium salt was prepared for 4-OHE_1 glucuronidation assay by dissolving 11.53 mg of the solid compound (Mr = 580.29) in 397.4 µl of Milli-Q water and stored at -20 °C. For other purposes, 50 mM stock solution of UDPGA ammonium salt prepared earlier in the laboratory was used.

500 mM TRIS-HCl buffer pH 7.5

Solution A: 7.880 g of Trizma® hydrochloride (Mr = 157.60) was dissolved in 100 ml of Milli-Q water in a 100-ml volumetric flask. Solution B: 6.057 g of Trizma® base (Mr = 121.14) was dissolved in a 100-ml volumetric flask. Solution B was gradually added to

solution A under pH meter until a pH of 7.5 was reached. The prepared buffer was kept in a bottle with a screw cap at 4 °C.

4 M perchloric acid (PCA)

1.501 ml of 70% PCA (Mr = 100.46, ρ = 1.664 g/ml at 25 °C) was carefully added to 2.85 ml of Milli-Q water and stored in a vial at 4 °C until use.

5 M Sodium hydroxide solution

19.999 g of sodium hydroxide (Mr = 40.00) was dissolved in 100 ml of Milli-Q water in a 100-ml volumetric flask and stored at a room temperature.

Hypotonic buffer (0.1 mM EDTA, 0.5 mM PB pH 7.4)

Hypotonic buffer for each membrane isolation by osmotic lysis was prepared by mixing 250 µl of 200 mM ethylenediaminetetraacetic acid (EDTA) solution and 250 µl of 1 M phosphate buffer (both prepared earlier in the laboratory) in a 500-ml volumetric flask, eventually filled in with Milli-Q water, transferred to a bottle with a screw cap and stored at 4 °C.

Phosphate buffered saline (PBS) was diluted from 10 X stock which was prepared by The Media Kitchen, Institute of Biotechnology, University of Helsinki.

For insect Sf9 cell culturing, HyClone SFX-Insect cell culture medium (Thermo Fisher Scientific) supplemented with 5% heat-inactivated HyClone™ Fetal Bovine Serum (FBS, Thermo Fisher Scientific) was used.

Pierce bicinchoninic acid (BCA) Protein Assay Kit (Thermo Fisher Scientific) was employed in quantification of protein concentration. The kit contains:

BCA Reagent A (sodium carbonate, sodium bicarbonate, BCA and sodium tartrate in 0.1 M sodium hydroxide)

BCA Reagent B (4% cupric sulfate)

BSA Standard Ampules 2 mg/ml (20 % BSA in 0,9% saline and 0,05% sodium azide)

BSA standard solutions

Set of BSA standard aqueous solutions (at concentrations of 0; 0,4; 0,08; 0,2; 0,28; 0,40; 0,48; 0,6 mg/ml) was prepared earlier in the laboratory and stored at -20 °C.

BCA working reagent

Fresh BCA working reagent was prepared by mixing 50 parts of BCA reagent A and a part of BCA reagent B before every protein quantification procedure.

pH-indicator strips from MilliporeSigma were used to test the approximate pH.

4.3 Equipment

The list of used devices is presented in Table 4.

Table 4. Devices

Device	Model	Manufacturer
Analytical scale	CP-225 D	Sartorius Mechatronics Corporation
Centrifuge	5415 D	Eppendorf
Centrifuge	5810 R, 5804 R	Eppendorf
Dry block heater	QBD2	Grant Instruments
Freeze dryer	LyoPro3000	Heto Lab
HPLC system	Agilent 1100 Series	Agilent Technologies
Incubator	Series B	Termaks
Incubator shaker	Classic Series C25	New Brunswick Scientific
Microplate photometer	Model 550	Bio-Rad
Microplate reader	Varioskan™ LUX	Thermo Fisher Scientific
Microplate nephelometer	Nepheloskan Ascent	Thermo Labsystems
NMR spectrometer	Ascend™ 400 MHz	Bruker
pH meter	AB 150	Fisher Scientific
Rocker	CR100	FinePCR
Rotavapor system	R-200 (V-800, V-500, B-490)	Büchi
Shaker and incubation hood	Certomat R and Certomat HK	Sartorius
Ultracentrifuge	Optima L-80 XP	Beckman Coulter
Ultrasonic bath	GS13	GeneralSonic
Ultrasonic cell disruptor	450	Branson Ultrasonic Corporation
Vortex	Genie 2	Scientific Industries

4.4 Synthesis of ETG

Recombinant human UGT2B7, the most active isoform in glucuronidation of EpiT (Sten et al. 2009), was selected for optimization of synthesis of ETG.

4.4.1 Recombinant human UGT2B7

The P4 viral stock of recombinant baculovirus containing full-length complementary DNA (cDNA) encoding the His-tagged UGT2B7*2 protein was generated according to manufacturer's instructions (Bac-to-Bac® Baculovirus Expression System, Invitrogen) as described previously (Kurkela et al. 2003). In brief, recombinant baculovirus particles were generated by transposition of the UGT2B7*2 cDNA into the bacmid propagated in the competent DH10Bac™ *E.coli* cells and subsequent transfection of Sf9 cells with isolated bacmid DNA using Cellfectin® reagent. The initial P1 viral stock was isolated after transfection and the P4 baculoviral stock, used for *UGT2B7*2* gene expression, was prepared by sequential amplification of the initial P1 viral stock.

4.4.1.1 Preparation of UGT2B7 cell homogenates

In order to maximize the expression of active UGT, the optimal conditions (infection volume and incubation time) for UGT2B7 enzyme production were determined. Parallel 10-ml Sf9 cell suspensions cultured in HyClone SFX-Insect medium enriched with 5 % of FBS were infected with four different amounts of the P4 baculoviral stock (0.5, 1.0, 2.0, 3.0 µl of virus stock per ml of cell suspension) in two sets. The infection was conducted at the cell density of $2x10^6$ cells/ml as counted with a cell counting chamber using optical microscopy. The infected cells were cultured in 100-ml Erlenmeyer flasks in an incubator shaker at 27 °C and 120 rpm, either for 48 h (first set) or 72 h (second set). The cell suspensions were transferred into centrifuge tubes and centrifuged (1,000 g, 5 min, 16 °C). The cell pellets were washed twice with 3 ml of PBS and after last centrifugation, the pellets were resuspended in 600 µl of PBS and stored in 1.5-ml microtubes at -20 °C.

4.4.1.2 Protein concentration of UGT2B7 cell homogenates

To standardize the amount of protein in the activity assay, total protein concentrations of cell homogenates were assessed by the BCA method. This method is based on the reduction of cupric cation (Cu^{2+}) to cuprous cation (Cu^{1+}) by protein in alkaline medium. The cuprous cation is chelated by two molecules of BCA resulting in a purple-colored

complex which gives a strong absorbance at 562 nm (540 – 590 nm), increasing linearly with protein concentration (Thermo Fisher Scientific Inc. 2013).

100-fold dilutions of cell suspensions (25 µl) were pipetted in duplicate into microplate wells alongside with BSA standards (25 µl) in duplicate, 200 µl of BCA working reagent was added, and the plate was placed on a plate shaker for 30 s. Then, the plate was covered with aluminum foil and incubated at 37 °C for 30 min. The plate was cooled to room temperature and the absorbance at 562 nm was measured on a microplate reader. The average absorbance measurement of the blank was subtracted from each value and a standard curve was generated using linear regression in GraphPad Prism (Section 4.9).

4.4.1.3 UGT2B7 expression optimization assay

The reaction mixtures contained 50 mM PB, 5 mM $MgCl_2$, 20 µM EpiT, 50 µg total protein of cell homogenate, and 5 mM UDPGA in a final volume of 100 µl and total DMSO concentration of 0,2 % (v/v). The activity assays were conducted in duplicate and included single control incubation (lacking UDPGA) for each enzyme source. The conditions were adjusted to keep substrate consumption under 20 %.

The basic reaction mixture was prepared by mixing 1494 µl of water, 750 µl of 200 mM PB, 150 µl of 100 mM $MgCl_2$, and 6 µl of 10 mM EpiT in a 5-ml tube. 80 µl of the basic reaction mixture was pipetted into 1.5-ml microtubes placed in an ice rack. 10 µl of diluted cell homogenates, prepared in microtubes in an ice rack according to Table 5, was added to the basic reaction mixture, gently vortexed and kept at 4 °C for 15 min. The samples were pre-incubated at 37 °C for 5 min in a dry block heater and the reaction was started by the addition of 10 µl of warmed (37 °C, 5 min) 50 mM UDPGA followed by gentle vortexing and incubation in the dry block heater (37 °C, 20 min). In control incubations, the co-substrate UDPGA was replaced by 10 µl of pre-warmed water. After 20 min, the reactions were terminated by the precipitation of the enzymatic protein with 10 µl of 4 M PCA, the tubes were thoroughly vortexed, and kept in the ice rack at 4 °C for 15 min. Finally, the samples were centrifuged at 16,000 g for 10 min and the supernatants were subjected to HPLC analysis using the injection volume of 60 µl (Section 4.8.11).

Table 5. Dilution of cell homogenates to 5 mg/ml preceding the activity assay

Sample	Virus stock [µl/ml]	Incubation time [h]	Protein concentration [mg/ml]	Cell homogenate [µl]	Water [µl]
1	0.5	48	25.1	10	50.2
2	1.0	48	25.3	10	50.6
3	2.0	48	24.7	10	49.4
4	3.0	48	24.0	10	48
5	0.5	72	23.9	10	47.8
6	1.0	72	23.6	10	47.2
7	2.0	72	27.6	10	55.2
8	3.0	72	23.4	10	46.8

4.4.1.4 Preparation of UGT2B7-enriched membranes

After determination of the optimal expression conditions, 600 ml of Sf9 insect cell suspension ($2x10^6$ cells/ml) was equally divided into six 250-ml Erlenmeyer flasks, infected with 1.0 µl of the P4 baculoviral stock per ml of cell suspension and incubated at 27 °C on a rotating shaker at 120 rpm for 72 h. The cells were transferred into twelve centrifuge tubes (50 ml each) and collected by centrifugation (1,200 g, 8 °C 5 min). The cell pellets were washed twice with 10 ml of PBS, centrifuged under the same conditions after each wash, and stored in the centrifuge tubes at -20 °C. To select an optimal method for membrane isolation, osmotic lysis and sonication were employed.

A cell pellet obtained by centrifugation of 300 ml of cell culture was resuspended in a hypotonic buffer (approx. 60 ml). The resulting cell suspension was transferred to a 500-ml beaker placed in an ice bath and filled in with hypotonic buffer to a total volume of 300 ml. The contents of the beaker were being stirred on the magnetic stirrer for 1 h and then centrifuged (1,000 g, 4 °C, 5 min). The supernatant was transferred to six 5804 R centrifuge suitable tubes (42 ml each) and the rest of the supernatant was used for resuspension of the cell pellet. The resulting suspension was homogenized by hand with a glass Potter-Elvehjem homogenizer (10 strokes), followed by centrifugation at 1,000 g at 4 °C for 5 min. The supernatant was mixed with the supernatant from the preceding centrifugation in the six 5804R centrifuge suitable tubes and the membranes were collected by centrifugation at 15,963 g at 4 °C for 75 min. The membrane-containing

pellet was resuspended in 3.5 ml of cold 25 mM TRIS-HCl buffer (pH 7.5), homogenized, divided into aliquots, and stored at -80 °C until use.

A cell pellet corresponding to 300 ml of cell culture was resuspended in 60 ml of hypotonic buffer and equally divided into two 100-ml beakers placed on ice. The cell homogenates were then sonicated seven times with 10-s bursts using an ultrasonic cell disruptor. The sonicated mixture was centrifuged (3,220 g, 4 °C, 10 min) to remove cell debris and the resulting supernatant was transferred into six pre-cooled ultracentrifuge tubes. The volume of supernatant in each ultracentrifuge tube was adjusted with hypotonic buffer to a total volume of 20 ml and the membrane pellet was isolated by ultracentrifugation (100,000 g, 4°C, 1 h 15 min). After resuspension of the pellet with 4.5 ml of cold 25 mM TRIS-HCl buffer pH 7.5, the membrane preparations were homogenized in a glass Potter-Elvehjem homogenizer (3 strokes) and stored in microtubes at -80 °C until use.

4.4.1.5 Activity comparison of UGT2B7 membrane preparations

To standardize the protein amount in the activity comparison test, total protein concentrations of membrane preparations were assessed in duplicate by the BCA method as described in Section 4.4.1.1. The activity of UGT2B7 membrane preparations was determined in small-scale incubations (100 µl) containing 5 mM $MgCl_2$, 50 mM PB, 20µM EpiT, 25 µg of total protein of membrane preparation, and 5 mM UDPGA. The samples were tested in triplicate and included one control incubation (lacking UDPGA) for both membrane preparations. The activity assay was conducted in the same manner as described in 4.4.1.1. The reaction time was reduced to 10 min to keep substrate consumption under 20 %. The samples were analyzed using HPLC with the injection volume of 60 µl.

4.4.2 Determination of the optimal conditions for the synthesis of ETG

Since the activity of both UGT2B7 membrane preparations was comparable, the membranes were combined (1:1) and the resulting membrane preparation (24.1 mg/ml) was used as an enzyme source in the following optimization and synthesis reactions. All preparatory reactions were initiated by the addition of UDPGA, incubated on a rotating base at 190 rpm at 37 °C and terminated with 4 M PCA (10 % of the reaction volume). The sample pre-treatment before HPLC analysis was done as described in 4.1.1.1 and 5 µl of the supernatant was analyzed (see 4.8.1.1 for HPLC method).

4.4.2.1 Buffer type and DMSO concentration

Optimal DMSO concentration was determined in small-scale 24-h incubations (100 µl) in the presence of 5%, 7% or 10% DMSO (v/v). The incubation mixtures contained 10 % of membrane preparation (v/v), 500 µM EpiT, 5 mM $MgCl_2$, 5 mM UDPGA, and a buffer, either 100 mM TRIS-HCl pH 7.5 or 50 mM PB pH 7.4.

4.4.2.2 UDPGA concentration

To ensure the most effective utilization of the costly UDPGA in the milligram-scale reaction, test reactions were started with three different concentrations of UDPGA, namely 3 mM, 4 mM, and 5 mM. Based on the previous 24-h incubations, DMSO concentration was 7.5 % (v/v), substrate concentration was increased to 750 µM, and 100 mM TRIS-HCl pH 7.5 was used. The glucuronidation was catalyzed by 10 % of UGT2B7 membrane preparation (v/v) and was terminated after 17 h on a rotating base at 37 °C.

4.4.2.3 UGT2B7 membrane contents

In the end, the contents of microsomal preparation were optimized by small-scale 24-h incubations containing 6 %, 8 % or 10 % of the enzyme source (v/v). On the ground of former observations, the reaction mixtures consisted of 100 mM TRIS-HCl pH 7.5, 5 mM $MgCl_2$, 7.5 % DMSO (v/v), 750 µM EpiT, and 4 mM UDPGA in a total volume of 150 µl.

4.4.3 Milligram-scale synthesis of ETG

4.4.3.1 Synthesis reaction

Based on the small-scale incubations, the reaction volume was scaled up to produce milligram amounts of ETG. The milligram-scale synthesis was carried out in a sealed, light-protected 50-ml Erlenmeyer flask in the presence of 100 mM TRIS-HCl buffer pH 7.5, 5 mM $MgCl_2$, 750 µM EpiT, 7.5 % of DMSO (v/v), 8 % of the enzyme source (v/v, 48.1 mg of total protein of UGT2B7-enriched membrane homogenate), and 4 mM UDPGA in a total volume of 25 ml (Table 6). The reaction was protected from light and incubated at 37 °C on a rotating base at 140 rpm for 24 h. Then, the mixture was directly centrifuged at 15,963 g for 10 min to remove insoluble proteins. The resulting precipitates were washed twice with several milliliters of water, centrifuged after each wash (15,963 g, 10 min), and the supernatants were combined.

Table 6. The final composition of the reaction mixture

Stock	Added volume	Final concentration
500 mM TRIS-HCl buffer pH 7.5	5.000 ml	100 mM
100 mM $MgCl_2$	1.250 ml	5 mM
10 mM EpiT in DMSO	1.875 ml	750 µM (7.5 % DMSO)
UGT2B7 membranes	2.000 ml	8 % (v/v)
50 mM UDPGA	2.000 ml	4 mM
Milli-Q water	12.875 ml	-

4.4.3.2 LLE

The unconsumed aglycone was removed from the mixture by alkalization of the supernatant with 5 M sodium hydroxide solution to pH 10 using pH-indicator strips and extracting it two times with dichloromethane in amounts equal to the reaction mixture. 200 µl of the dichloromethane fraction was evaporated, redissolved in a mixture of methanol (25 µl) and water (25 µl) and subjected to HPLC analysis with the injection volume of 20 µl to assure that the ionized ETG remained unextracted in the aqueous phase.

4.4.3.3 SPE

The aqueous phase obtained after LLE was acidified with formic acid to pH 2 (below the pKa of the ETG that is 2.8 ± 0.7) using pH-indicator strips to ensure the retention of the unionized form of steroid glucuronide on the reversed-phase sorbent.

For SPE, two Oasis HLB cartridges (200 mg, 6 ml, Waters) were used with a vacuum manifold. The cartridges were pre-conditioned with 3 ml of methanol and equilibrated with 3 ml of 2% formic acid in Milli-Q water. After loading of the acidified sample (approx. 14 ml per cartridge), polar impurities were removed with 4 ml of wash solvent containing 2 % of formic acid in 35% methanol-water mixture. The elution of glucuronides was performed with 4 ml of 75% aqueous methanol solution including 0.8 ml of 25% aqueous ammonia solution (w/w). 4 ml of methanol including 0.8 ml of 25% aqueous ammonia solution was used to flush out the cartridges. An eluate was collected to 5-ml tubes, analyzed with HPLC (5 µl injection), and the fractions containing glucuronides were combined. The glucuronide fraction was evaporated to dryness with a rotary evaporator and the residue was reconstituted in 3 ml of a mixture composed of

methanol, water, and DMSO in a ratio of 8:6:1. Dissolution process was accelerated in an ultrasonic bath and the solution was filtered through a syringe filter (Acrodisc®, PTFE Membrane, pore size 0.2 μm) prior to HPLC purification.

4.4.3.4 HPLC purification

Time-based collection of HPLC fractions was optimized by injecting 1, 25, 50, and 100 μl of the sample. Chromatograms monitored at four wavelengths (210, 244, 254, and 280 nm) were analyzed to eliminate impurities in the collected fractions. After optimization, the whole volume of the sample was gradually fractionated in 100-μl injections and the glucuronide fractions were collected at a retention time of 2.29 – 2.56 min (approx. 90 % of the peak area, see 4.8.1.1 for HPLC method).

4.4.3.5 Reaction yield, purity and structural confirmation

The glucuronide fractions were combined and lyophilized. The lyophilized product was solvated in a mixture of acetone, methanol and trace 25% ammonia solution (w/w), transferred to pre-weighed vials, concentrated under nitrogen, and kept under vacuum overnight to give ammonium salt of ETG. The vial with the sample was weighed and the reaction yield was calculated by subtracting the weight of the empty vial from the weight of the vial with the sample.

6.31 mg of ETG ammonium salt (Mr = 481.59) was dissolved in 262 μl of deuterated DMSO to obtain 50 mM stock solution and NMR spectra were recorded (see 4.8.2).

The chromatographic purity was characterized using HPLC with a diode array detector. For the purity analysis, the 50 mM stock of ETG was diluted to a 50 μM solution with Milli-Q water. Blank sample containing pure Milli-Q water was parallelly analyzed with the test sample. The injection volume was 5 μl. See Section 4.8.1.1 for details about used HPLC method.

4.5 4-OHE_1 glucuronidation activity assay

4.5.1 Solubility of 4-OHE_1 and calibration curve

Samples for solubility experiment represented the composition of test samples for glucuronidation assay excluding UDPGA and enzyme source. The samples contained 5 mM $MgCl_2$, 100 mM TRIS-HCl buffer 7.5, and 4-OHE_1 in a concentration range from 0 to 300 µM. Due to lipophilicity of the aglycone, the organic solvent DMSO concentration in the test samples was set to 5 % (v/v). 150 µl of each sample was pipetted into microplate wells followed by measurement of light-scattering with a nephelometer at room temperature.

Based on the nephelometric estimation of solubility, the samples at a range of 4-OHE_1 concentrations from 0 to 30 µM were subjected to HPLC analysis with the injection volume of 90 µl to generate a linear standard curve using absorbance at 202 nm (Section 4.8.1.2).

4.5.2 Recombinant human UGT isoforms

Recombinant human UGTs 1A1, 1A3-1A10, 2A1-2A3, 2B4, 2B7, 2B10, 2B11, 2B17, 2B28 were expressed in-house as His-tagged proteins in baculovirus-infected Sf9 insect cells as described previously (Kurkela et al. 2003, Kuuranne et al. 2003, Finel et al. 2005, Kurkela et al. 2007, Sneitz et al. 2009). All the recombinant enzymes were used as UGT-enriched membranes, excluding UGT2B10 and UGT2B11 which were employed as cell homogenates (Troberg et al. 2017). The six His residues at the C-terminus of each UGT protein enabled determination of their relative expression levels by immunodetection using monoclonal anti-His-tag antibody Tetra-His by Qiagen as described earlier (Kurkela et al. 2004 and Kurkela et al. 2007). The values are related to the expression level of UGT2B4 (reference value 1.0) and are listed in Table 7. The total protein concentrations of cell homogenates and membrane preparations were determined by Pierce BCA Protein Assay Kit according to the manufacturer's instructions (ThermoFisher Scientific) using BSA as a standard. The total protein concentrations were used to standardize the amount of enzyme source in the assays and are stated below (Table 7).

Table 7. Relative expression levels of recombinant UGTs used in the activity assay

UGT isoform	Relative expression level	Protein concentration
UGT1A1	3.7	30 mg/ml
UGT1A3	12.6	20 mg/ml
UGT1A4	7.3	25 mg/ml
UGT1A5	9.7	15 mg/ml
UGT1A6	5.1	19 mg/ml
UGT1A7	16.4	20 mg/ml
UGT1A8	11.3	19 mg/ml
UGT1A9	5.6	21.7 mg/ml
UGT1A10	1.1	26 mg/ml
UGT2A1	11.8	23.5 mg/ml
UGT2A2	10.1	25 mg/ml
UGT2A3	9.8	18.5 mg/ml
UGT2B4	1.0	27 mg/ml
UGT2B7	2.7	28 mg/ml
UGT2B10 (cells)	-	25 mg/ml
UGT2B11 (cells)	-	25 mg/ml
UGT2B17	5.2	22 mg/ml
UGT2B28	1.1	19 mg/ml

4.5.3 Preliminary tests

Before glucuronidation assay, preliminary tests were performed to find the most reliable termination method and to show that the formed glucuronide conjugates were stable at room temperature and at -20 °C. Based on studies on 4-OHE_1 glucuronidation (Lépine et al. 2004, Starlard-Davenport et al. 2007), recombinant human UGT1A10 and UGT1A8 were employed as an enzyme source in a ratio 3:1 (approx. 31 µg of total protein) to form both 4-OHE_1 glucuronides. The volume of test incubations was 150 µl with the following composition: 100 mM TRIS-HCl buffer pH 7.5, 5 mM $MgCl_2$, and 50 µM 4-OHE_1. The reactions were started by the addition of UDPGA to final concentration of 5 mM and terminated after 16 h at 37 °C with 4 M PCA (10 % of total volume), methanol, or acetonitrile (both 100 % of total volume). The supernatants were analyzed with HPLC (Section 4.8.1.2) immediately after centrifugation (16,000 g, 10 min) and

after 18 h at room temperature or at -20 °C. No decrease in the chromatogram peak area of both glucuronides was detected after 18 h compared to the directly analyzed samples and 4 M PCA was selected for termination of glucuronidation activity assay reactions. Secondly, the effect of the reducing agent DTT (1 mM) was tested with no apparent benefit for the synthesis of 4-OHE_1 glucuronides (data not shown).

Other small-scale preparatory tests were conducted using UGT1A3, UGT1A8, UGT1A10 and UGT2B7 which activities towards 4-OHE_1 were demonstrated earlier (Lépine et al. 2004 and/or Starlard-Davenport et al. 2007). The purpose was to adjust the incubation time and total protein contents so that the substrate consumption would be below 20 % in glucuronidation screening (data not shown).

4.5.4 Glucuronidation activity assay

The glucuronidation rate of 18 recombinant human UGTs towards 4-OHE_1 was examined in glucuronidation assays. Samples for the activity screening contained 100 mM TRIS-HCl buffer pH 7.5, 5 mM MgCl2, 30 µM 4-OHE_1, 10 µg of total protein of UGT-enriched membrane preparations or cell homogenates, and 5 mM UDPGA in a total volume of 100 µl. The final DMSO concentration was set to 5 % (v/v). The only exception was the incubations of highly active UGT1A10 in which total protein amount was reduced to 5 µg to keep substrate consumption below 20 %. The activity assays were conducted in triplicate for each enzyme source and control incubations, either in the absence of UDPGA or the substrate, were included for UGT1A10 and UGT2B7. In addition, Sf9 insect cells infected with a baculovirus that does not encode any UGT were used as a negative control to detect glucuronides or glucosides formation of which is independent of the tested recombinant UGTs. These incubations contained both UDPGA and the substrate. No non-specific glucuronides or glucosides were detected in any of the control incubations (data not shown).

Because of the large numbers of samples, the experiment was realized in two sets. The basic reaction mixture was prepared by mixing appropriate amounts of water, 500 mM TRIS-HCl pH 7.5, 100 mM $MgCl_2$, and 600 µM 4-OHE_1 DMSO solution in a 5-ml tube (Table 8). The latter was prepared by diluting 2.4 µl of 50 mM 4-OHE_1 stock solution with 197.6 µl of DMSO. 10 µl of enzyme dilution (Table 9) was added to 80 µl of the basic reaction mixture, gently vortexed and kept at 4 °C for 15 min. After that, the samples were pre-warmed at 37 °C for 5 min in a dry block heater and the reaction was started by addition of 10 µl of pre-warmed (37 °C, 5 min) 50 mM UDPGA followed by gentle

vortexing and incubation in a light-protected dry block heater (37 °C, 5 min). The same volume of pre-warmed water (10 µl) was added to control incubations. After 5 min, the reactions were terminated with 10 µl of cold 4 M PCA, the tubes were vortexed, and kept at 4 °C for 15 min. Before analysis, the samples were centrifuged at 16,000 g for 10 min, the supernatants were transferred into vials, and analyzed immediately using HPLC with the injection volume of 90 µl (Section 4.8.1.2).

Table 8. The final composition of incubation mixtures in activity screening

Stock	Added volume	Final concentration
Milli-Q water	50 µl	-
500 mM TRIS-HCl buffer pH 7.5	20 µl	100 mM
100 mM $MgCl_2$	5 µl	5 mM
600 µM 4-OHE_1 in DMSO	5 µl	30 µM, (5 % of DMSO)
Enzyme source (Table 15)	10 µl	0.1 µg/µl
50 mM UDPGA	10 µl	5 mM

Table 9. Dilution of enzyme preparations

UGT isoform	Protein concentration	Enzyme preparation	Water	Final concentration
UGT1A1	30 mg/ml	10 µl	290 µl	1 mg/ml
UGT1A3	20 mg/ml	10 µl	190 µl	1 mg/ml
UGT1A4	25 mg/ml	10 µl	240 µl	1 mg/ml
UGT1A5	15 mg/ml	10 µl	140 µl	1 mg/ml
UGT1A6	19 mg/ml	10 µl	180 µl	1 mg/ml
UGT1A7	20 mg/ml	10 µl	190 µl	1 mg/ml
UGT1A8	19 mg/ml	10 µl	180 µl	1 mg/ml
UGT1A9	21.7 mg/ml	10 µl	207 µl	1 mg/ml
UGT1A10	26 mg/ml	10 µl	510 µl	0.5 mg/ml
UGT2A1	23.5 mg/ml	10 µl	225 µl	1 mg/ml
UGT2A2	25 mg/ml	10 µl	240 µl	1 mg/ml
UGT2A3	18.5 mg/ml	10 µl	175 µl	1 mg/ml
UGT2B4	27 mg/ml	10 µl	260 µl	1 mg/ml
UGT2B7	28 mg/ml	10 µl	270 µl	1 mg/ml

UGT2B10 (cells)	25 mg/ml	10 µl	240 µl	1 mg/ml
UGT2B11 (cells)	25 mg/ml	10 µl	240 µl	1 mg/ml
UGT2B17	22 mg/ml	10 µl	210 µl	1 mg/ml
UGT2B28	19 mg/ml	10 µl	180 µl	1 mg/ml
Bac control	21 mg/ml	10 µl	200 µl	1 mg/ml

Since authentic analytical standards were not available, the HPLC quantification of formed glucuronides was based on the assumption that the parent compound and its glucuronides have closely similar UV absorbance maxima (Troberg et al. 2017). A standard curve prepared from HPLC analyses of a series of 4-OHE_1 concentrations was used to estimate the amount of formed 4-OHE_1 glucuronides (4.5.1). Glucuronidation rates were then calculated as the glucuronide amount formed (picomoles) per milligram of total protein per incubation time in minutes. To obtain normalized glucuronidation rates, the absolute rates were corrected for expression levels of each UGT isoform by dividing the measured rate by the corresponding expression level value (Kurkela et al. 2012).

4.6 Synthesis of 4-OHE_1-3G

Glucuronidation assay with recombinant human UGT enzymes demonstrated the dominant role of UGT1A10 in the formation of 4-OHE_1-3G with high regioselectivity. Therefore, UGT1A10 isoform was selected for the synthesis of 4-OHE_1-3G, even though the second glucuronide was produced as well (see 5.2.2 for results).

4.6.1 Recombinant human UGT1A10

The P4 viral stock of recombinant baculovirus comprising full-length cDNA that encodes UGT1A10 as a His-tagged protein was obtained by following manufacturer's guidelines (Bac-to-Bac® Baculovirus Expression System, Invitrogen) as described previously (Kurkela et al. 2003, Kuuranne et al. 2003, see 4.4.1 for a brief description).

4.6.1.1 Preparation of UGT1A10 cell homogenates

The optimal expression conditions for UGT1A10 expression were determined by infecting parallel 10-ml Sf9 insect cell suspensions at a density of $2x10^6$ cells per ml of cell suspension (HyClone SFX-Insect medium, 5 % FBS) with five different amounts of the P4 viral stock (0.5, 0.75, 1.0, 2.0 and 3.0 µl of baculoviral stock per ml of cell

suspension) in three sets. The infected cells were incubated in 100-ml Erlenmeyer flasks in an incubator shaker set to 27 °C and 120 rpm for 48 h, 72 h, or 96 h. The cells were collected by centrifugation (1,000 g, 16 °C, 5 min), washed twice with 3 ml of PBS, and in the end resuspended in 600 µl of PBS. Total protein concentrations of cell preparations were determined by the BCA method as described in Section 4.4.1.2. The cell homogenates were stored in 1.5-ml microtubes at -20 °C until use.

4.6.1.2 UGT1A10 expression optimization assay

The test samples contained 100 mM TRIS-HCl pH 7.5, 5 mM MgCl2, 30 µM 4-OHE_1, 5 mM UDPGA in a total volume of 100 µl and final DMSO concentration was 5 % (v/v). To keep substrate consumption below 20 %, the amount of enzyme was set to 5 µg of total protein of each cell preparation. The activity assays were performed in duplicate and included single negative control (lacking UDPGA) for each cell homogenate.

The basic reaction mixture contained 2,475 µl of water, 990 µl of 500 mM TRIS-HCl pH 7.5, 247.5 µl of 100 mM $MgCl_2$, and 247.5 µl of 600 µM 4-OHE_1 DMSO solution in a 5-ml tube. The latter was prepared by mixing 3.6 µl of 50 mM 4-OHE_1 solution in DMSO and 296.4 µl of DMSO. 10 µl of each diluted cell homogenate, prepared on ice according to Table 10, was added to 80 µl of the basic reaction, gently vortexed, and kept at 4 °C for 15 min. The pre-incubation of test samples (37 °C, 5 min) was followed by initiation of the reactions with 10 µl of pre-heated 50 mM UDPGA (replaced by 10 µl of water in negative control samples) and gentle vortexing. After 5 min of incubation at 37 °C, the reactions were stopped with 10 µl of cold 4 M PCA, properly vortexed, and kept at 4 °C for 15 min prior to centrifugation at 16,000 g for 10 min. 80 µl of the supernatants was injected into HPLC and analyzed (see 4.8.1.2 for details).

Table 10. Dilution of cell homogenates to 0.5 mg/ml

Sample	Virus stock [µl/ml]	Incubation time [h]	Protein concentration [mg/ml]	Cell homogenate [µl]	Water [µl]
1	0.5	48	22.7	5	222
2	0.75	48	18.9	5	184
3	1.0	48	15.1	5	146
4	2.0	48	18.7	5	182
5	3.0	48	17.6	5	171
6	0.5	72	15.8	5	153
7	0.75	72	17.3	5	168
8	1.0	72	16.7	5	162
9	2.0	72	15.3	5	148
10	3.0	72	14.9	5	144
11	0.5	96	17.6	5	171
12	0.75	96	17.8	5	173
13	1.0	96	13.4	5	129
14	2.0	96	12.5	5	120
15	3.0	96	14.0	5	135

4.6.1.3 Preparation of UGT1A10-enriched membranes

For UGT1A10 protein production, 400 ml of Sf9 insect cell suspension ($2x10^6$ cells/ml) was equally divided into four 250-ml Erlenmeyer flasks and infected with 1.0 µl of the P4 viral stock per ml of cell suspension. After 48 h of incubation at 27 °C on a rotating base at 12 rpm, the cell suspensions were transferred into eight 50-ml centrifuge tubes and the cells were collected by centrifugation (1,200 g, 8 °C, 5 min). The cells were washed twice with 10 ml of PBS, centrifuged after each wash (1,200 g, 8 °C, 5 min), and resuspended in 10 ml. Sonication of cell homogenates was performed to isolate the UGT1A10-enriched membranes.

The cell suspension was equally divided into two 100-ml beakers placed on ice, sonicated seven times with 10s bursts, and centrifuged (3,220 g, 4 °C, 10 min,) to separate the membranes from cell debris. The resulting membrane-containing supernatant was transferred into six pre-cooled ultracentrifuge tubes and the contents of each tube were

adjusted to 20 ml with hypotonic buffer. The membrane pellets were then collected by ultracentrifugation (100,000 g, 4° C, 1h 15 min) and resuspended in a total volume of 7 ml of cold 25 mM TRIS-HCl buffer pH 7.5. Finally, the membrane preparations were homogenized in a glass Potter-Elvehjem homogenizer (3 strokes) and stored in aliquots at -80 °C until use. Assessment of total protein concentration in UGT1A10-enriched membranes was done by the BCA method as described in Section 4.4.1.1.

4.6.2 Determination of the optimal conditions for the synthesis of 4-OHE_1-3G

Several preparatory reactions (100 µl) were made to increase the efficiency of the glucuronide production with an effort to decrease concentration of the costly co-substrate, UDPGA, contents of membranes, and DMSO concentration. The incubation mixtures consisted of 100 mM TRIS-HCl buffer pH 7.5, 5 mM $MgCl_2$, and 1 mM 4-OHE_1 with DMSO concentration set to 5 %, 7 %, or 10 %. The reactions were catalyzed by UGT1A10-enriched membranes that constituted 4 %, 8 %, or 10 % of total volume and initiated by UDPGA in a concentration of 3 mM, 4 mM or 5 mM. 50 µl of the reaction was removed from the mixture after 2 h 30 min at 37 °C and terminated with 5 µl of cold 4 M PCA. 10 µl was subjected to HPLC analysis (see 4.8.1.2 for HPLC method). Since HPLC analysis revealed complete substrate consumption in most of the samples after only 2 h 30 min, the rest of the reaction mixtures was not further analyzed and the optimal conditions were selected based on this single experiment.

4.6.3 Milligram-scale synthesis of 4-OHE_1-3G

4.6.3.1 Synthesis reaction

The reaction volume was increased to 25 ml to yield milligram amounts of 4-OHE_1-3G. The synthesis reaction was performed in a sealed, light-protected 50-ml Erlenmeyer flask and incubated at 37 °C on a rotating base at 210 rpm for 7 h. The reaction mixture contained 100 mM TRIS-HCl buffer pH 7.5, 5 mM $MgCl_2$, 1 mM 4-OHE_1, 7 % DMSO, 8 % of the enzyme source (v/v, 73.8 mg of total protein of UGT1A10-enriched membranes), and 3 mM UDPGA (Table 11). After 7 h of incubation, direct removal of insoluble proteins was achieved by centrifugation (15,963 g, 10 min), the pellets were washed twice with several milliliters of water followed by centrifugation after each wash (15,963 g, 10 min). Finally, the supernatants were combined and subjected to LLE.

Table 11. The final composition of the reaction mixture

Stock	Added volume	Final concentration
500 mM TRIS-HCl buffer pH 7.5	5.000 ml	100 mM
100 mM $MgCl_2$	1.250 ml	5 mM
14.29 mM 4-OHE_1 in DMSO*	1.750 ml	1 mM (7 % of DMSO)
UGT1A10 membranes	2.000 ml	8 % (v/v)
50 mM UDPGA	1.500 ml	3 mM
Milli-Q water	13.500 ml	-

*14.29 mM 4-OHE_1 in DMSO was prepared by diluting 515 µl of 50 mM 4-OHE_1 stock solution with 1287 µl of DMSO.

4.6.3.2 LLE

The unconsumed steroid aglycone (pKa 10.1 ± 0.4) was eliminated by double extraction with an equal amount of dichloromethane with preceding neutralization of the supernatant with 5 M sodium hydroxide solution to pH 7 using pH-indicator strips. 200 µl of the dichloromethane fraction was evaporated, dissolved in 50 µl of a methanol-water mixture (1:1), and 20 µl was injected to HPLC to assure that the ionized glucuronide remained in aqueous fraction.

4.6.3.3 SPE

The aqueous fraction left after LLE was acidified with formic acid to pH 2 (below the pKa of 4-OHE_1-3G that is 2.8 ± 0.7) using pH-indicator strips to enhance glucuronide retention on the reversed-phase sorbent.

The SPE was accomplished with two Oasis HLB cartridges (200 mg, 6 ml, Waters) and vacuum manifold. The pre-condition and equilibration of the SPE cartridges were done with 3 ml of methanol and 3 ml of 2% formic acid in Milli-Q water, respectively. Then the acidified sample was loaded (approx. 14.5 ml per cartridge) and the impurities were washed with a solution containing 2% formic acid in 20% methanol-water mixture. The glucuronides were eluted with 4 ml of 65% aqueous methanol solution including 0.8 ml of 25% aqueous ammonia solution (w/w). In the end, 4 ml of methanol including 0.8 ml of 25% ammonia solution (w/w) were used to flush out the cartridges. All the SPE fractions were collected, analyzed with HPLC (5 µl injected), and the fractions containing glucuronides were mixed. The solvent was evaporated to dryness using rotary evaporator and the residue redissolved in 3.180 ml of a mixture composed of methanol, water,

DMSO, and formic acid in a ratio of 50:45:10:1. The solution was filtered through a syringe filter (Acrodisc®, PTFE Membrane, pore size 0.2 µm) before HPLC purification.

4.6.3.4 HPLC purification

Time-based collection of pure glucuronide fractions was optimized by injecting 10 µl and 100 µl of the sample followed by analysis of chromatograms obtained at the wavelengths of 202, 254, and 277 nm. The whole sample volume was gradually purified in 100-µl injections. The glucuronide fractions were collected at a retention time of 2.86 – 3.17 min (see 4.8.1.2 for details).

4.6.3.5 Reaction yield, purity and structural confirmation

The collected glucuronide fractions were combined and freeze-dried. The lyophilizate was solvated by 5 ml of methanol, transferred to a pre-weighed vial, concentrated, and subsequently kept under vacuum overnight. The vial with the pure sample was weighed and the reaction yield was calculated.

6.67 mg of 4-OHE_1-3G (Mr = 462.49) was dissolved in 288.4 µl of deuterated DMSO to acquire 50 mM stock solution and NMR spectra were recorded at room temperature (see 4.8.2 for details).

The chromatographic purity was determined using HPLC with diode array detector. The 50 µM 4-OHE_1-3G dilution and a blank sample were prepared in the same way, both containing 10 % of methanol in Milli-Q water, and analyzed with HPLC. The injection volume was 5 µl. See Section 4.8.1.2 for a description of used HPLC method.

4.7 Synthesis of 4-OHE_1-4G

The glucuronidation screening assay demonstrated that 4-OHE_1 conjugation with glucuronic acid at position 4 is catalyzed most efficiently by UGT2B7 isoform (see 5.2.2 for results). Recombinant human UGT2B7-enriched membranes, prepared for the synthesis of ETG (Section 4.4.1), were employed for synthesis of 4-OHE_1-4G.

4.7.1 Determination of the optimal conditions for the synthesis of 4-OHE_1-4G

All preparatory incubations were stopped with 4 M PCA (10 % of the reaction volume). Before HPLC analysis, pre-treatment of the samples was done as described in 4.1.1.1 and the injection volume for HPLC examination was 5 µl per sample (see 4.8.1.2 for details).

4.7.1.1 Substrate and DMSO concentration

Small-scale 150-µl incubations were prepared to test substrate conversion to glucuronide at two 4-OHE_1 concentrations (750 µM and 1,000 µM). Five DMSO concentrations (2 %, 5 %, 7 %, 10 %, 15 %; v/v) were tested to determine optimal conditions for the milligram-scale synthesis. The reactions contained 100 mM TRIS-HCl buffer pH 7.5, 5 mM MgCl2, 10 % of membrane preparation (v/v), and were initiated with 5 mM UDPGA. After 20 h on a rotating base at 190 rpm and 37 °C, the reactions were terminated with 4 M PCA and analyzed with HPLC.

4.7.1.2 UDPGA concentration

20-h reactions were started with UDPGA in three final concentrations (3 mM, 4 mM, 5 mM) with an effort to reduce the amount of the expensive co-substrate in the milligram-scale synthesis without affecting the reaction yield. The incubations further consisted of 100 mM TRIS-HCl buffer pH 7.5, 5 mM $MgCl_2$, 1 mM 4-OHE_1, 8 % DMSO (v/v) in a total volume of 100 µl. After 20 h on a rotating base at 190 rpm and 37 °C, the reactions were stopped and analyzed with HPLC.

4.7.1.3 UGT2B7 membrane contents

Eventually, reactions catalyzed by 6 %, 8 %, and 10 % of membrane preparation (v/v) were conducted to select the optimal contents of enzyme source. The reactions contained 100 mM TRIS-HCl buffer pH 7.5, 5 mM MgCl2, 1 mM 4-OHE_1, 8 % DMSO (v/v), 3 mM UDPGA in a total volume of 100 µl and were incubated for 20 h on a rotating base at 190 rpm and 37 °C.

4.7.2 Milligram-scale synthesis of 4-OHE_1-4G

4.7.2.1 Synthesis reaction, LLE and SPE

Based on the small-scale incubations, the 25-ml synthesis reaction was performed in a 100-ml Erlenmeyer flask to produce milligram amounts of 4-OHE_1-4G. The final composition of the mixture was 100 mM TRIS-HCl buffer pH 7.5, 5 mM MgCl2, 1 mM 4-OHE_1, 7 % of DMSO (v/v), 10 % of the enzyme source (v/v, 60.1 mg of total protein of UGT2B7-enriched membranes), and 3 mM UDPGA (Table 12). The reaction flask was protected from light, sealed with parafilm and incubated at 37 °C on a rotating base set to 150 rpm.

Table 12. The final composition of the reaction mixture

Stock	Added volume	Final concentration
500 mM TRIS-HCl buffer pH 7.5	5.000 ml	100 mM
100 mM $MgCl_2$	1.250 ml	5 mM
14.29 mM 4-OHE_1 in DMSO*	1.750 ml	1 mM (7 % of DMSO)
UGT2B7 membranes	2.500 ml	10 % (v/v)
50 mM UDPGA	1.500 ml	3 mM
Milli-Q water	13.000 ml	-

*14.29 mM 4-OHE_1 in DMSO was prepared by diluting 515 µl of 50 mM 4-OHE_1 stock solution with 1287 µl of DMSO.

After 22 h, the reaction mixture was centrifuged in two centrifuge tubes (15,963 g, 10 min), the pellets were washed two times with few milliliters of Milli-Q water and centrifuged after each wash. The supernatants were mixed, and LLE was performed identically as in the case of 4-OHE_1-3G (Section 4.6.3.2). pH of the aqueous phase gained from LLE was adjusted below the pKa of the synthesized glucuronide (2.80 ± 0.70) to enhance its retention on the reversed-phase sorbent. The acidification to pH 2 was accomplished with formic acid using universal pH strips as an indicator. The SPE, including used solvents, copied the SPE procedure described in Section 4.6.3.3. After SPE, all fractions were subjected to HPLC analysis to make sure that the glucuronides were eluted in the elution fraction. The elution fractions were combined, evaporated with a rotary evaporator, and the residue was dissolved in 4.400 ml of a mixture containing water, methanol, DMSO, and formic acid in a ratio of 56:48:5:1 with the use of an ultrasonic bath. Before HPLC purification, the solution was filtered through a syringe filter (Acrodisc®, PTFE Membrane, pore size 0.2 µm).

4.7.2.2 HPLC purification

Chromatograms of 5, 50, 80, and 100µl injections were recorded at the wavelengths of 202, 254, and 277 nm. The chromatograms were analyzed to optimize the time-based fraction collection with the aim to avoid impurities. The whole sample volume was gradually fractionated in 100-µl injections, fractions at the retention time 3.25 – 3.44 min were collected and combined (see 4.8.1.2 for HPLC method).

4.7.2.3 Reaction yield, purity and structural confirmation

The pure glucuronide fraction was freeze-dried and the resulting lyophilizate was dissolved in acetone, transferred to a pre-weighed vial, concentrated, and kept under vacuum overnight. Finally, the vial with the sample was weighed and the mass of the reaction product was calculated.

5.19 mg of 4-OHE_1-4G (Mr = 462.49) was dissolved in 224.4 µl of deuterated DMSO to yield 50 mM stock solution and subjected to NMR analysis. See Section 4.8.2 for details about used NMR spectroscopy method.

HPLC with diode array detector was used to verify the purity of the sample. The 50 µM 4-OHE_1-4G dilution and a blank sample, both containing 10 % of methanol in Milli-Q water, were prepared and subjected to HPLC analysis with the injection volume of 5 µl (see 4.8.1.2 for HPLC method).

4.8 Analytical methods

4.8.1 HPLC methods

For HPLC analyses, the Agilent 1100 Series HPLC system equipped with a G1322A degasser, a G1312A binary pump, a G1313A autosampler, a G1316A thermostatted column compartment, and a G1315B diode array detector was used. HPLC purification of synthesized glucuronides was accomplished by employment of Agilent 1100 Series G1364A automatic fraction collector.

4.8.1.1 EpiT and ETG

EpiT and ETG were separated using Agilent InfinityLab Poroshell 120EC C18 column (100x4.6 mm, 2.7 µm particle size; Agilent Technologies) at 40 °C and a flow rate of 1 ml/min of aqueous 0.1% formic acid and acetonitrile with the following acetonitrile gradient: 0.0 – 2.0 min 33 %, 2.0 – 4.5 min 33 % → 50 %, 4.5 – 8.3 min 50 %, 8.3 – 8.4 min 50 % → 33 %, 8.4 – 10.0 min 33 %. The detection wavelength of 244 nm was used for chromatographic analyses (Figure 5).

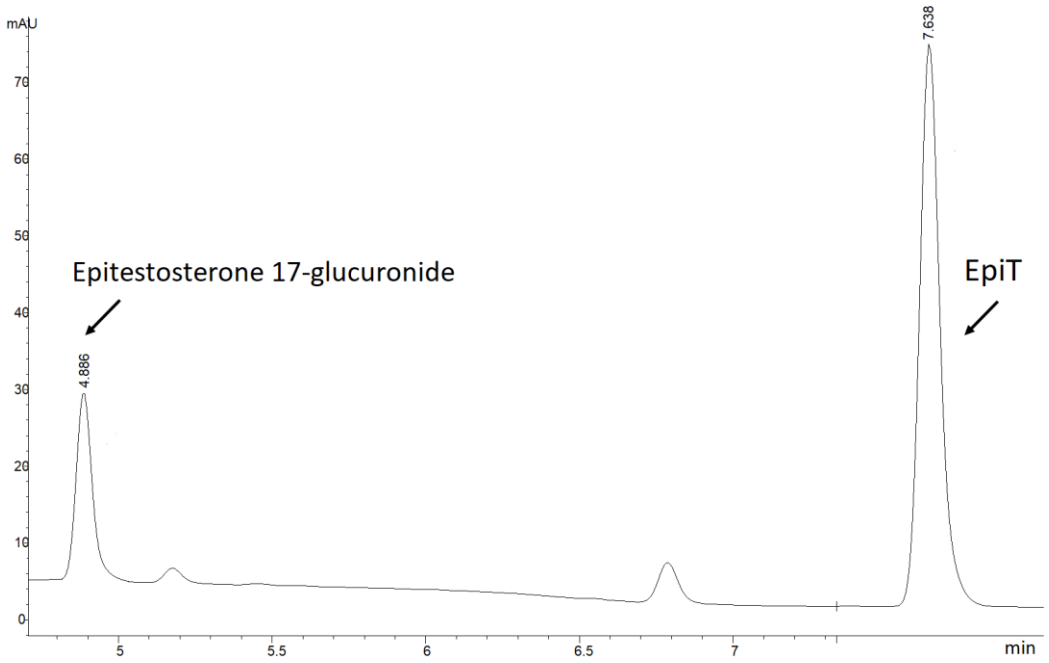

Figure 5. Exemplary chromatographic separation of ETG (retention time 4.89) and EpiT (retention time 7.64)

For HPLC purification, a shorter method was employed with a steeper acetonitrile gradient: 0.0 – 1.0 min 40 %, 1.0 – 2.5 min 40 % → 51%, 2.5 – 2.6 min 51 % → 90 %, 2.6 –3.7 min 90 %, 3.7 – 3.8 min 90 % → 40 %, 3.8 – 5.0 min 40 %.

The purity check of the synthesized ETG was done using the Agilent InfinityLab Poroshell 120EC C18 column at 40 °C and a flow rate of 1 ml/min. The mobile phase consisted of aqueous 0.1% formic acid and acetonitrile with acetonitrile contents as follows: 0.0 – 2.0 min 5 %, 2.0 – 20.0 min 5 % → 95 %, 20.0 – 22.0 min 95 %, 22.0 – 22.5 min 95 % → 5 %, 22.5 – 25.0 min 5 %. The chromatograms obtained at detection wavelengths of 200 nm, 215 nm, 244 nm, 280 nm, and 350 nm were analyzed.

4.8.1.2 4-OHE$_1$ and 4-OHE$_1$ glucuronides

The parent compound, 4-OHE$_1$, and its regioisomeric glucuronides, 4-OHE$_1$-3G and 4-OHE$_1$-4G, were separated with Kinetex Pentafluorophenyl column (75x4.6 mm, 2.6 µm particle size; Phenomenex) at 50 °C and a flow rate of 2 ml/min (Figure 6). The mobile phase was composed of aqueous 0.1% formic acid and acetonitrile with the following acetonitrile gradient: 0.0 – 1.0 min 20 %, 1.0 – 4.0 min 20 % → 25 %, 4.0 – 5.5 min 25 → 40 %, 5.5 – 5.7 min 40 % → 75 %, 5.7 – 6.7 min 75 %, 6.7 – 6.8 75 % → 20 %, 6.8 – 8.0 20 %. The detection wavelengths of 202 nm and 277 nm were used for

chromatographic analyses. For HPLC purification, the same HPLC method employing the detection wavelengths of 202 nm, 254 nm, and 277 nm was used.

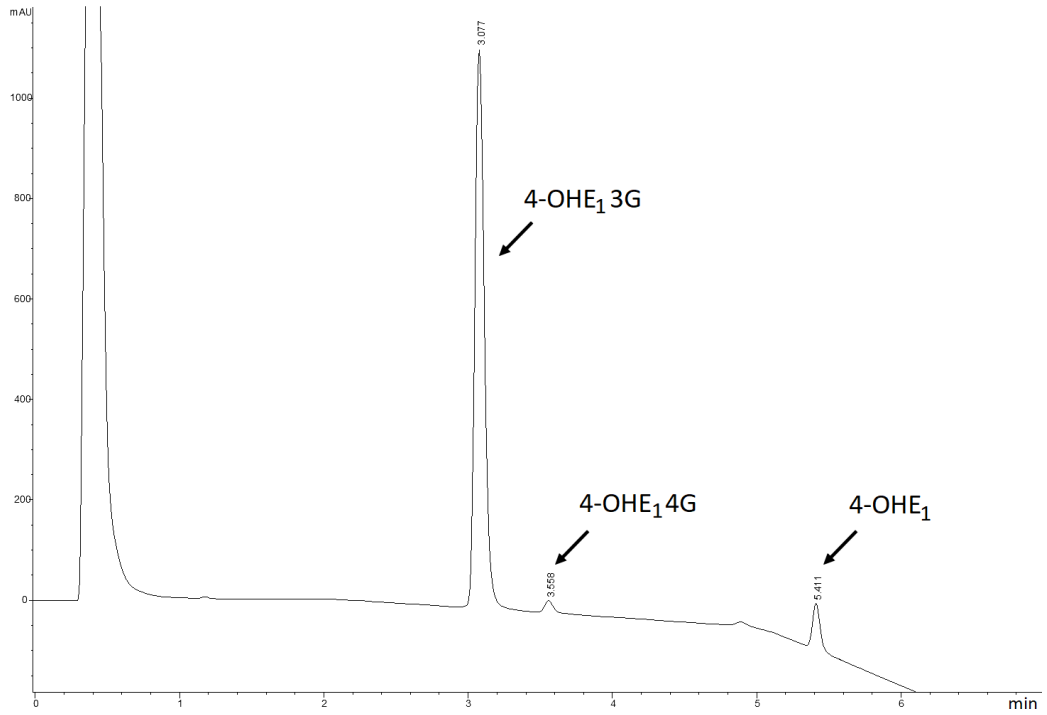

Figure 6. Exemplary chromatographic separation of 4-OHE_1-3G (retention time 3.08), 4-OHE_1-4G (retention time 3.56) and 4-OHE_1 (retention time 5.41) at 202 nm

The purity of synthesized 4-OHE_1 glucuronides was examined with Kinetex Pentafluorophenyl column at 50 °C and a flow rate set to 2 ml/min of aqueous 0.1% formic acid and acetonitrile with the following acetonitrile gradient: 0.0 – 2.0 min 5 %, 2.0 – 20.0 min 5 % → 95 %, 20.0 – 22.0 min 95 %, 22.0 – 22.5 min 95 % → 5 %, 22.5 – 25.0 min 5 %. The whole spectrum between 200 nm and 400 nm was recorded and the chromatograms obtained at detection wavelengths of 202 nm, 225 nm, 254 nm, and 277 nm were thoroughly checked for impurities.

4.8.2 NMR spectroscopy

^{1}H and ^{13}C NMR spectra and COSY, HSQC, and HMBC spectra were acquired on the NMR Bruker Ascend™ 400 MHz Spectrometer. Chemical shifts were related to the DMSO signal (δ = 2.50 ppm in ^{1}H spectra and 39.5 ppm in ^{13}C). The NMR data were analyzed using MestReNova software.

4.9 Data analysis and software

The HPLC chromatograms were analyzed using Agilent ChemStation software for LC (Agilent Technologies) on Windows XP Professional.

MestReNova 12.0.3 that was provided by Mestrelab Research S.L. was employed in NMR data analyses.

The pKa values of all substances were calculated using ACD/Labs Software V11.02, © 1994 – 2018 ACD/Labs.

The experimental data and graphs were processed using GraphPad Prism version 7.00 for Windows (GraphPad Software, La Jolla, California, USA; www.graphpad.com). The GraphPad software was used for calculations of mean values and standard deviations (SD) of duplicate and triplicate samples, and statistical analyses.

The figures presented in this thesis were created in ChemDraw Professional version 16.0.1.4 by PerkinElmer Inc. and Inkscape version 0.92 by Free Software Foundation, Inc.

5. Results

5.1 Synthesis of ETG

5.1.1 Recombinant human UGT2B7

5.1.1.1 Protein concentration of UGT2B7 cell homogenates

The calibration curve (Figure 7) was constructed by measuring absorbances of a series of BSA standard samples and the linear regression equation was used to calculate the protein concentration of the samples (Table 12). The total protein concentrations were used to standardize the amount of enzyme source in the activity assay.

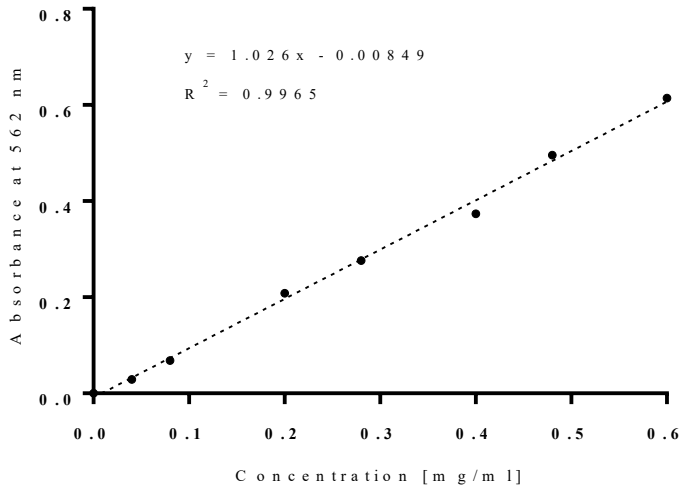

Figure 7. Calibration curve with linear regression equation and correlation coefficient R^2

Table 12. Protein concentration of UGT2B7 cell homogenates

Sample	Virus infection volume [µl/ml]	Incubation time [h]	Protein concentration [mg/ml] ± SD
1	0.5	48	25.1 ± 1.1
2	1.0	48	25.3 ± 1.7
3	2.0	48	24.7 ± 1.4
4	3.0	48	24.0 ± 1.6
5	0.5	72	23.9 ± 0.3
6	1.0	72	23.6 ± 1.4
7	2.0	72	27.6 ± 2.1
8	3.0	72	23.4 ± 2.1

5.1.1.2 UGT2B7 expression optimization assay

The optimal expression conditions for the production of UGT2B7-enriched membranes were determined by comparison of ETG formed during 20-min incubation by individual UGT2B7 cell homogenates prepared using two incubation times and four virus infection volumes. Based on the results (Figure 8), the Sf9 cells were infected with 1.0 µl of virus stock per ml of cell suspension and cultured for three days to obtain active enzyme source for glucuronide production.

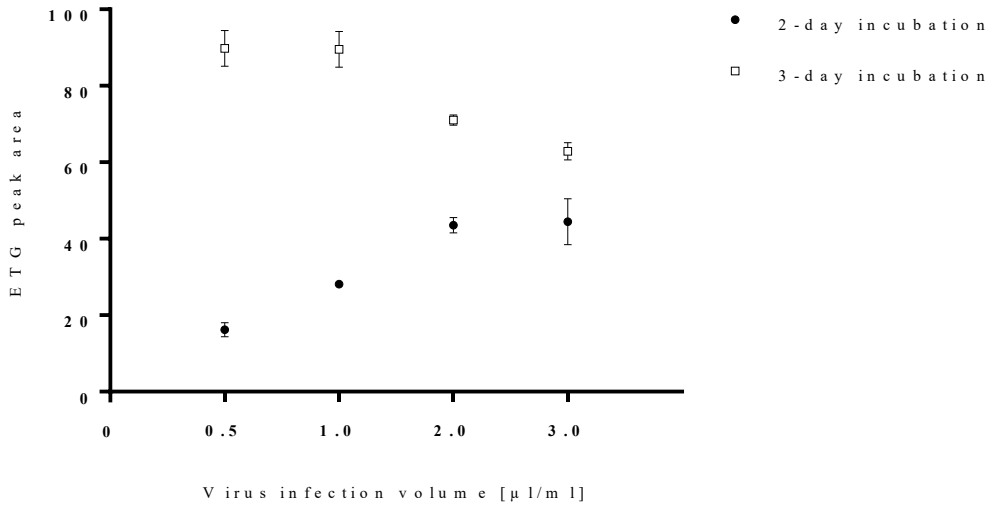

Figure 8. Comparison of UGT2B7 cell homogenates
Each point stands for the mean value of duplicate samples, error bars symbolize SD.

5.1.1.3 Protein concentration of UGT2B7-enriched membrane preparations

The total protein concentrations of membrane preparations, assessed by the BCA method, were used to standardize the amount of enzyme source in the activity comparison test. The calibration curve (Figure 9) was generated and the linear regression equation was used to determine the protein concentration of the samples (Table 13).

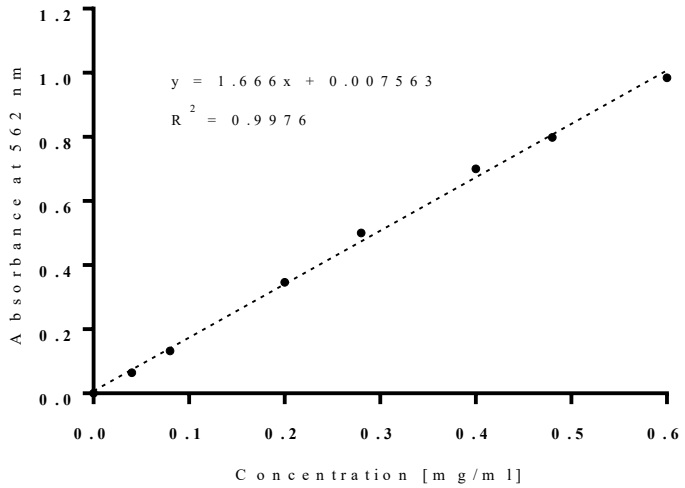

Figure 9. Calibration curve with linear regression equation and correlation coefficient R^2

Table 13. Protein concentration and yield of UGT2B7 membrane preparations

Membrane preparation method	**Protein concentration [mg/ml] ± SD**	**Approximate total protein yield [mg]**
Osmotic lysis	14.9 ± 0.4	52.2
Sonication	33.2 ± 0.6	149.4

5.1.1.4 Activity comparison of UGT2B7 membrane preparations

The formation of ETG during 10-min incubation by the equal protein amount of UGT2B7-enriched membranes, prepared either by osmotic lysis or sonication, was compared. The data were analyzed using the unpaired non-parametric Mann-Whitney test at 95% confidence level. The test showed no significant difference between the two datasets (Figure 10).

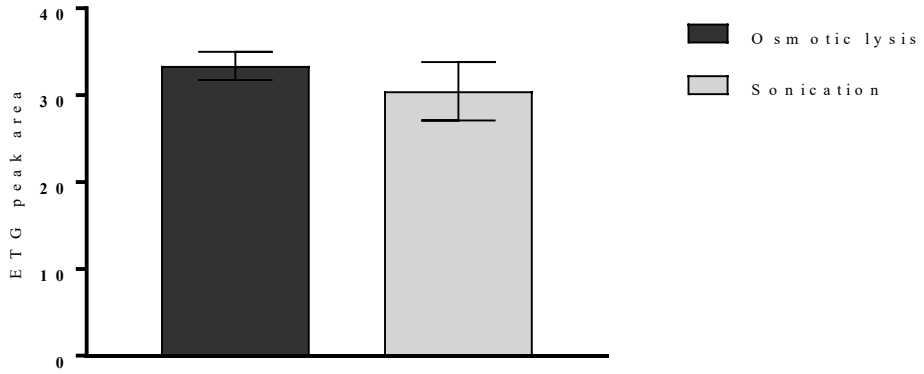

Figure 10. Comparison of ETG formed by UGT2B7-enriched membranes prepared with the employment of osmotic lysis and sonication

The ETG peak areas are expressed as the mean of triplicate samples ± SD.

5.1.2 Determination of the optimal conditions for the synthesis of ETG

5.1.2.1 Buffer type and DMSO concentration

The effect of buffer type and DMSO concentration on the formation of ETG in 24-h incubations in the presence of 500 µM substrate was evaluated. Since the samples containing 100 mM TRIS-HCl buffer pH 7.5 yielded higher amounts of ETG than those with 50 mM PB pH 7.4 (Figure 11), TRIS-HCl buffer was used for further optimization of synthesis conditions and large-scale synthesis. No indication that the generation of ETG would be greatly affected by DMSO in the concentration range of 5 – 10 % (v/v) was demonstrated in the preliminary tests. For further tests and milligram-scale reaction, 7.5% DMSO concentration (v/v) was selected and substrate concentration was increased to 750 µM as there was no substrate detected in the samples after 24 h.

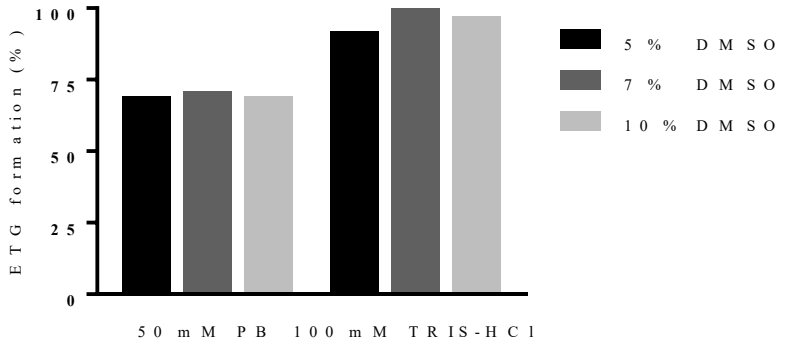

Figure 11. Effect of buffer type and DMSO concentration (v/v) on ETG formation

The formation of ETG in each sample is expressed as a percentage of ETG formed in the sample containing 100 mM TRIS-HCl buffer pH 7.5 and 7 % of DMSO (v/v).

5.1.2.2 UDPGA concentration

The substrate consumptions in the test reactions initiated by UDPGA in the final concentration of 5 mM, 4 mM, and 3 mM were 99.3 %, 99.3 %, and 95.5 %, respectively. To ensure the effective utilization of this costly cofactor without affecting the glucuronide yield, the concentration of 4 mM was selected as optimal for the milligram-scale synthesis.

5.1.2.3 UGT2B7 membrane contents

The effect of UGT2B7 membrane contents on the formation of ETG in 24-h incubations in the presence of 750 μM substrate is shown in Figure 12. For the milligram-scale synthesis of ETG, UGT2B7-enriched membranes in the concentration of 8 % (v/v) were employed.

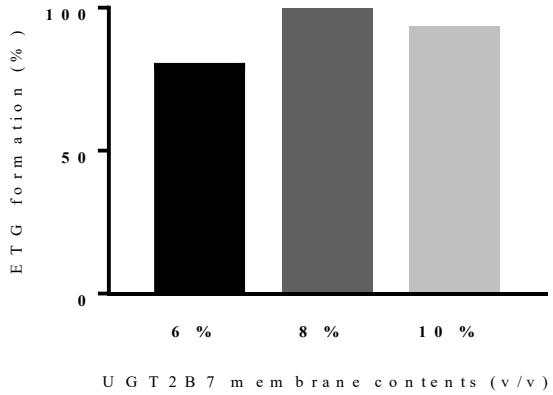

Figure 12. Effect of membrane contents on ETG formation

The formation of ETG is expressed as a percentage of ETG formed in the sample containing 8 % of UGT2B7 membrane preparations (v/v).

5.1.3 Milligram-scale synthesis of ETG

5.1.3.1 LLE and SPE

The absence of ETG peak in the chromatograms of the dichloromethane fractions indicated that the ionized glucuronide remained in the aqueous phase. On the other hand, the unconsumed substrate was completely extracted to the dichloromethane fraction.

The HPLC analysis of SPE fractions demonstrated that the overwhelming majority of ETG (99.33 %) was eluted in the elution fraction (75% methanol-water solution with ammonium hydroxide).

5.1.3.2 Reaction yield

The milligram amount (6.31 mg) of pure and dry ETG ammonium salt was obtained in this study (Figure 13), which was sufficient for accurate weighing and structural confirmation by NMR (Section 5.1.3.3). The overall reaction yield was 69.9 %.

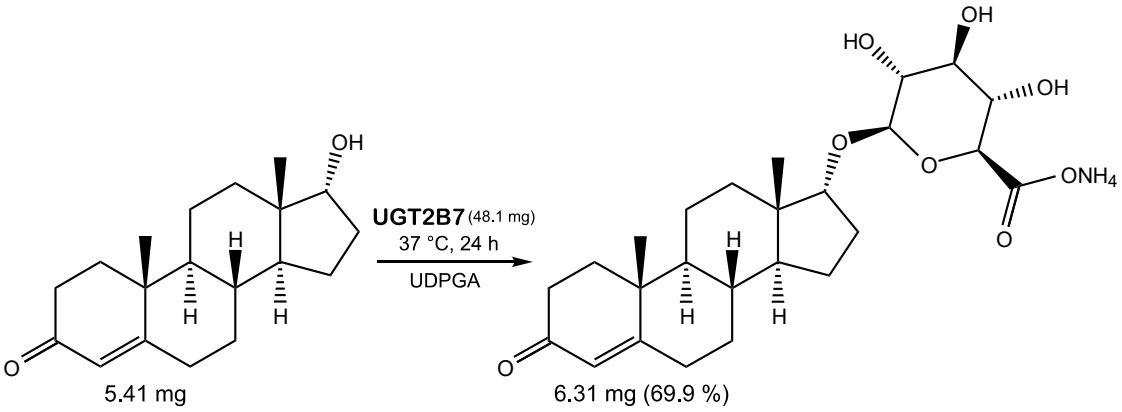

Figure 13. Synthesis of ETG

5.1.3.3 Structural confirmation

The ^{1}H and ^{13}C NMR spectra of EpiT were assigned based on COSY, HSQC, and HMBC spectra. The three-bond correlation of H1' of the glucuronide (δ_{GH1} = 4.07 ppm) and C17 of the aglycone (δ_{C17} = 84.39 ppm) was observed in the HMBC spectra indicated that the glucuronic acid is glycosidically linked at position 17 (Figure 14). β-configuration of the anomeric proton was identified by the analysis of the coupling constant between H1' and H2' of the glucuronide moiety (J_{GH1GH2} = 7.7 Hz). Other protons of the β-glucuronide moiety appeared in the carbohydrate ring proton region between 2.8 – 3.2 ppm. The NMR data confirmed that the synthesized compound is ETG.

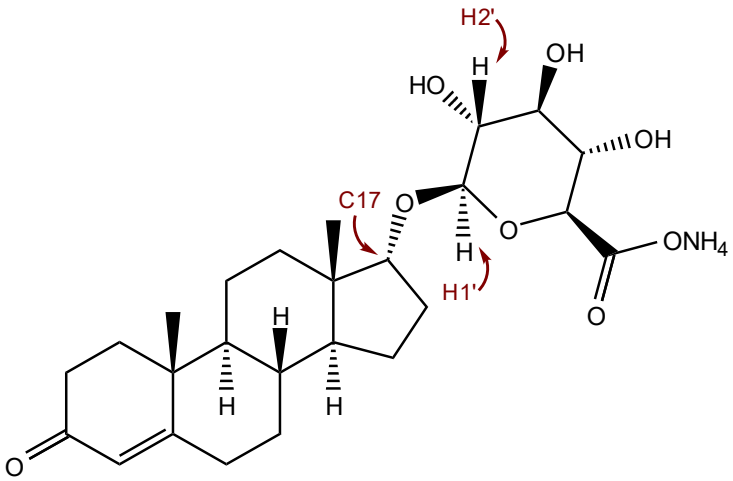

Figure 14. Chemical structure of ETG

5.1.3.4 Purity of ETG

The purity of the synthesis product was characterized by HPLC. The analysis of chromatograms showed only one intense peak corresponding to the ETG (Figure 15). No extra peaks were detected in comparison to blank sample indicating that the synthesized product is highly pure.

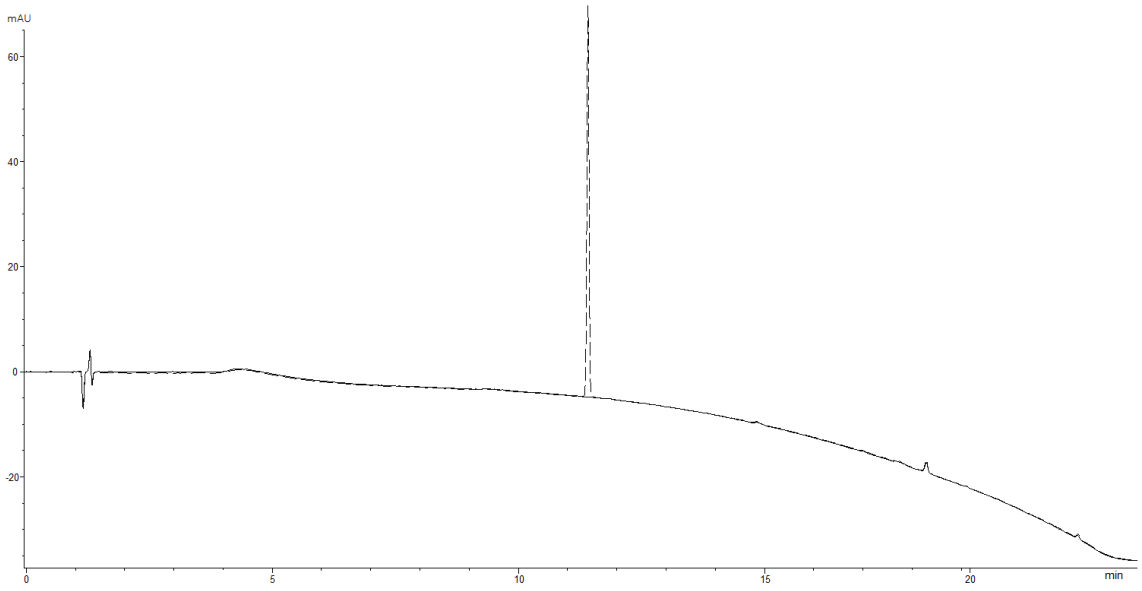

Figure 15. Determination of the purity of ETG

The overlapping chromatograms of the test and blank sample obtained at the wavelength of 244 nm demonstrate the presence of a single glucuronide peak and high purity of the synthesis product.

5.2 4-OHE$_1$ glucuronidation activity assay

5.2.1 Solubility of 4-OHE$_1$ and calibration curve

To obtain relevant glucuronidation data and quantify glucuronidation activity, the solubility of the substrate, 4-OHE$_1$, was assessed and a calibration curve was generated. The measured nephelometric data were related to the sample with 0 µM concentration of 4-OHE$_1$ (1.0) and the relative values were: 5 µM, 1.3; 10 µM, 1.1; 15 µM, 1.1; 20 µM, 1.3; 25 µM, 1.3; 50 µM, 1.5, 75 µM, 9.5; 100 µM, 15.9; 200 µM, 39.5; 300 µM, 47.5. Subsequent HPLC analyses of the samples within the concentration range from 0 to 50 µM provided a linear calibration curve up to 30 µM with the correlation coefficient R^2 = 0.9992 (Figure 16). For precise quantification of low amounts of 4-OHE$_1$ and its glucuronides, a calibration curve at the concentration range of 0.1 to 2 µM was used (Figure 17).

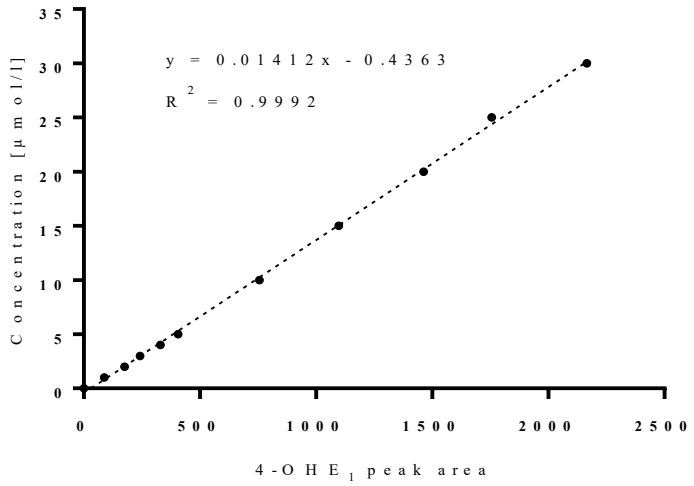

Figure 16. Calibration curve at the concentration range of 0 to 30 µM with linear regression equation and correlation coefficient R^2 used for quantification of 4-OHE_1 glucuronides in glucuronidation screening assay

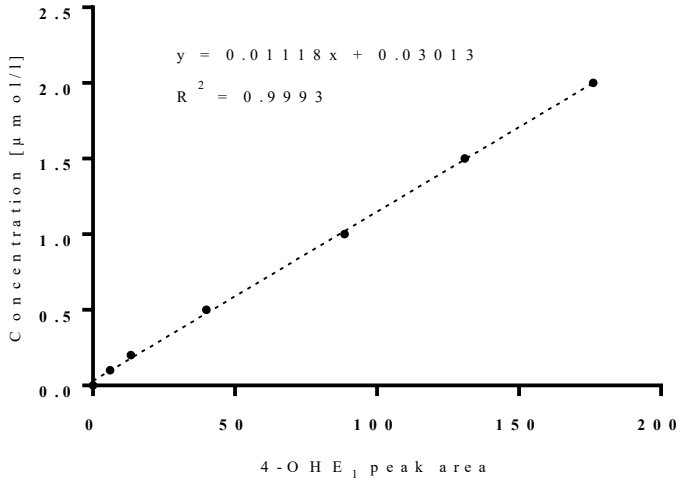

Figure 17. Calibration curve at the concentration range of 0 to 2 µM with linear regression equation and correlation coefficient R^2 generated for precise quantification of low amounts of 4-OHE_1 glucuronides

5.2.2 Glucuronidation screening assay

A set of 18 recombinant human UGTs were tested to select the most convenient isoform for the enzymatic synthesis of 4-OHE_1 glucuronides. The measured (absolute) glucuronidation rates towards 4-OHE_1 in the presence of a single substrate concentration

(30 μM) are shown in Figure 18. The recombinant human UGT preparations may significantly differ in their expression levels, and hence in the actual amount of active enzyme per mg total protein in the sample. To normalize expression differences and achieve more reliable comparison among the activities of individual UGT isoforms, the actual glucuronidation rates were divided by the relative expression level of each UGT preparation to yield normalized activities (Figure 19). The values of measured and normalized glucuronidation rates are presented in Tables 14 and 15, separately for each glucuronide.

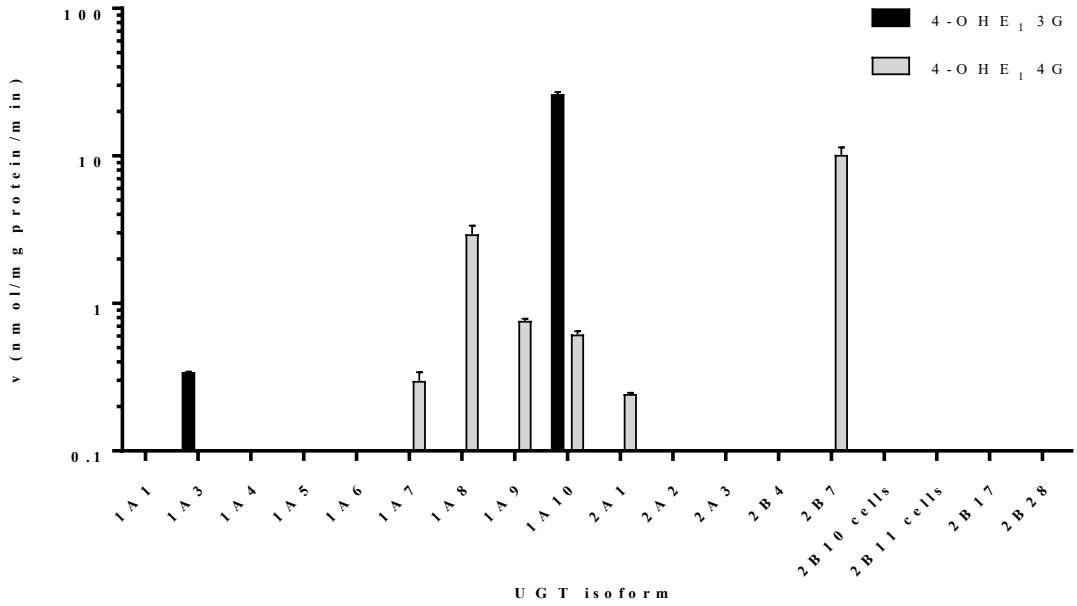

Figure 18. Measured glucuronidation rates of 4-OHE_1 by recombinant human UGTs

The glucuronidation rate values are expressed as the mean of triplicate samples ± SD. The Y-axis values are presented on a logarithmic scale.

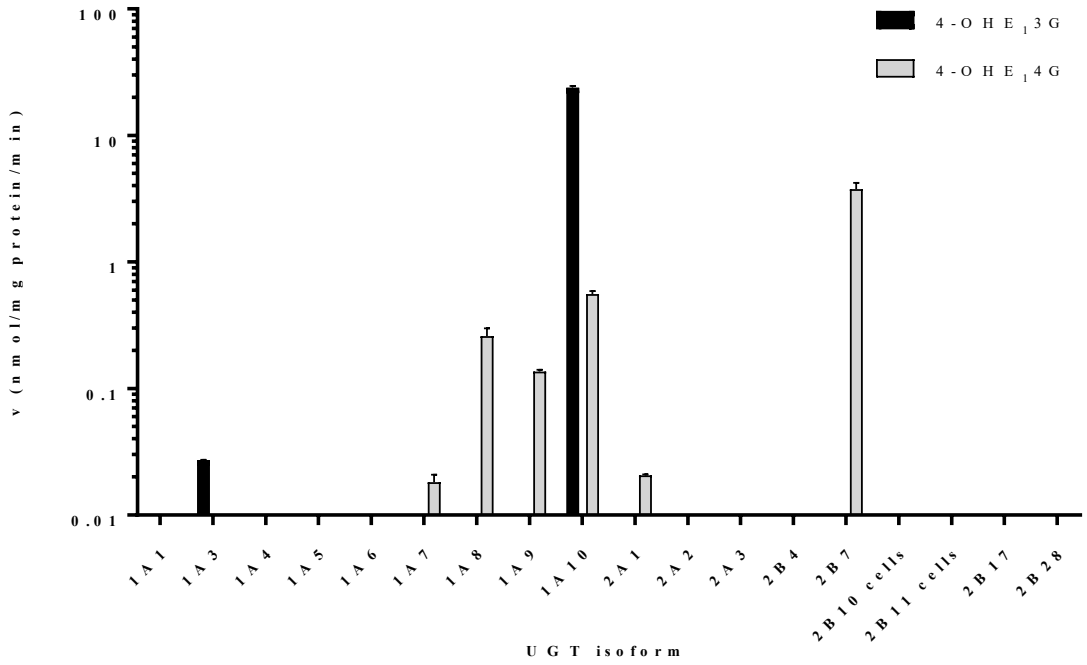

Figure 19. Normalized glucuronidation rates of 4-OHE_1 by recombinant human UGTs

The glucuronidation rates were corrected with respect to the relative expression levels of individual UGT enzymes and expressed as the mean of triplicate samples ± SD. Note that the Y-axis is logarithmic.

Table 14. Formation of 4-OHE_1-3G

The values represent the mean of three replicates ± SD.

UGT isoform	Actual glucuronidation rates [pmol·mg^{-1}·min^{-1}]	Normalized glucuronidation rates [pmol·mg^{-1}·min^{-1}]
UGT1A3	341.3 ± 3.1	27.1 ± 0.2
UGT1A10	26,198.6 ± 840.2	23,816.9 ± 763.9

Table 15. Formation of 4-OHE_1-4G

The values are expressed as the mean of triplicate samples ± SD.

UGT isoform	Actual glucuronidation rates [pmol·mg^{-1}·min^{-1}]	Normalized glucuronidation rates [pmol·mg^{-1}·min^{-1}]
UGT1A7	298.3 ± 42.8	18.2 ± 2.6
UGT1A8	2,943.5 ± 430.1	260.5 ± 38.1
UGT1A9	760.9 ± 28.2	135.9 ± 5.0
UGT1A10	614.5 ± 34.4	558.6 ± 31.3
UGT2A1	243.0 ± 4.6	20.6 ± 0.4
UGT2B7	10,148.7 ± 1,278.7	3,758.8 ± 473.6

From the recombinant human UGTs included in the assay, UGT1A10 exhibited the highest 4-OHE_1 glucuronidation rates at 3-OH, whereas UGT2B7 was the most active isoform in the formation of 4-OHE_1-4G. Unlike UGT2B7 that catalyzed glucuronidation of 4-OHE_1 exclusively at position 4, UGT1A10 produced both glucuronides, even though the formation of 4-OHE_1-4G was catalyzed at much lower rates (558.6 ± 31.3 pmol·mg^{-1}·min^{-1}) than the formation of 4-OHE_1-3G (23,816.9 ± 763.9 pmol·mg^{-1}·min^{-1}). Apart from UGT1A10, UGT1A3 was the only isoform producing 4-OHE_1-3G specifically but at much lower rates, only 27.1 ± 0.2 pmol·mg^{-1}·min^{-1}. In addition to UGT1A10 and UGT2B7, the conjugation of 4-OHE_1 at position 4 was catalyzed by isoforms UGT1A7, UGT1A8, UGT1A9, and UGT2A1.

Based on the data obtained from the glucuronidation assay, highly regioselective UGT1A10 was selected to produce milligrams of 4-OHE_1-3G and for the synthesis of 4-OHE_1-4G, strictly regioselective UGT2B7 was chosen as a biocatalyst.

5.3 Synthesis of 4-OHE_1-3G

5.3.1 Recombinant human UGT1A10

5.3.1.1 Protein concentration of UGT1A10 cell homogenates

Total protein concentrations of cell homogenates were assessed by the BCA method. The calibration curve (Figure 20) was constructed by measuring absorbances of a series of BSA standards and the protein concentrations of the samples were calculated using the linear regression equation (Table 16). The total protein concentrations were used to standardize the amount of UGT1A10 cell homogenates in the activity assay.

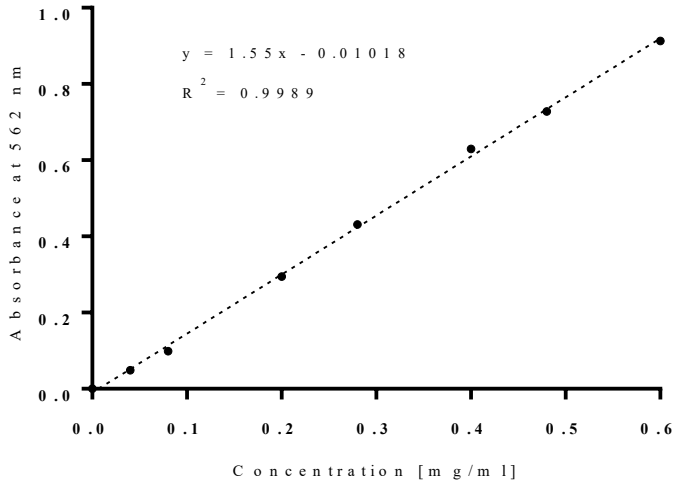

Figure 20. Calibration curve with linear regression equation and correlation coefficient R^2

Table 16. Protein concentration of UGT1A10 cell homogenates

Sample	Virus infection volume [µl/ml]	Incubation time [h]	Protein concentration [mg/ml] ± SD
1	0.5	48	22.7 ± 0.3
2	0.75	48	18.9 ± 1.0
3	1.0	48	15.1 ± 1.0
4	2.0	48	18.7 ± 1.0
5	3.0	48	17.6 ± 1.8
6	0.5	72	15.8 ± 1.1
7	0.75	72	17.3 ± 1.0
8	1.0	72	16.7 ± 0.6
9	2.0	72	15.3 ± 0.9
10	3.0	72	14.9 ± 1.7
11	0.5	96	17.6 ± 0.5
12	0.75	96	17.8 ± 0.8
13	1.0	96	13.4 ± 1.4
14	2.0	96	12.5 ± 0.2
15	3.0	96	14.0 ± 0.3

5.3.1.2 UGT1A10 expression optimization assay

The optimal expression conditions for the production of UGT1A10-enriched membranes were determined by comparison of the formation of 4-OHE_1-3G during 5-min incubation (represented by 4-OHE_1-3G peak area) by 5 μg of UGT1A10 cell homogenates. Based on the results (Figure 21) considering the advantage of 2-day incubation time, the Sf9 cells were infected with 1.0 μl of P4 baculoviral stock per ml of cell suspension and incubated for two days to obtain membrane preparation with the highest portion of active enzyme per mg of total protein.

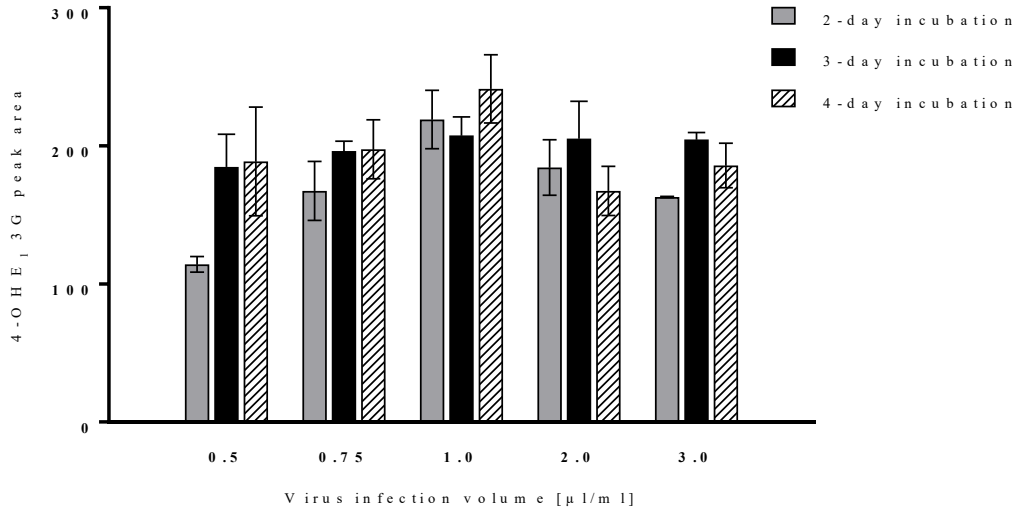

Figure 21. Comparison of UGT1A10 cell homogenates

The Y-axis represents 4-OHE_1-3G chromatogram peak area and the height of the columns stands for the mean value of duplicate samples with error bars symbolizing SD.

5.3.1.3 Protein concentration of UGT1A10-enriched membrane preparation

The total protein concentration of membrane preparation was assessed by the BCA method. The calibration curve was generated using linear regression in GraphPad Prism and the linear regression equation ($y = 1.323x + 0.001707$, $R^2 = 0.9982$) was used to calculate the protein concentration of UGT1A10 membranes which was 36.9 ± 3.2 mg/ml.

5.3.2 Determination of the optimal conditions for the synthesis of 4-OHE_1-3G

HPLC analysis of test reactions with different contents of UDPGA, DMSO, and UGT1A10 membranes revealed nearly identical results with complete substrate consumption after only 2 h 30 min. The only exceptions were samples catalyzed by UGT1A10-enriched membranes that constituted 4 % of total reaction volume (Figure 22).

The results point to the exceptionally high activity of UGT1A10 in the formation of 4-OHE_1-3G and allowed to reduce the concentration of expensive UDPGA in the milligram-synthesis reaction to 3 mM without an apparent decrease in the glucuronide yield. DMSO concentration was set to 7 % and UGT1A10 membranes were employed in the concentration of 8 % (v/v).

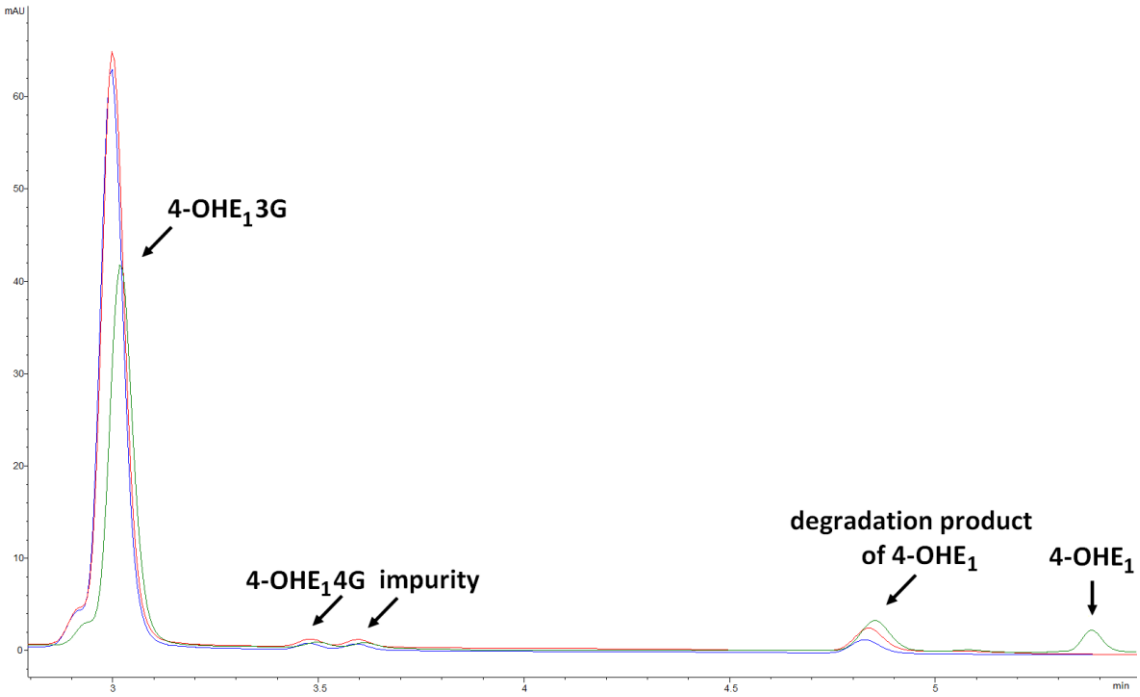

Figure 22. Chromatographic comparison of optimization reactions

Figure 22 represents three overlapping chromatograms of samples catalyzed by UGT1A10 membrane preparations that constituted 4 % (green line), 8 % (blue line), and 10 % (red line) of total reaction volume. The chromatogram of the sample containing 4 % of membranes (v/v) demonstrated the lowest formation of 4-OHE_1-3G with incomplete substrate consumption (represented by green 4-OHE_1 peak). The reactions catalyzed by 8 % or 10 % of the enzyme source showed almost identical results with no substrate left.

5.3.3 Milligram-scale synthesis of 4-OHE_1-3G

5.3.3.1 LLE and SPE

No peak of 4-OHE_1-3G was noticed in the chromatograms of the dichloromethane fractions indicating that the ionized glucuronide remained in the aqueous phase. Even if there was no substrate peak left, a peak at a retention time of 4.9 min, presumably a degradation product of 4-OHE_1, was found in the chromatograms of both dichloromethane fractions and aqueous fractions.

The HPLC analysis of SPE fractions indicated that the majority of 4-OHE_1-3G (over 99 %) was eluted in the elution fraction consisting of 65 % aqueous methanol solution with ammonium hydroxide. The elution fraction further contained a putative degradation product of 4-OHE_1 and a trace of 4-OHE_1-4G. To separate these compounds from the desired 4-OHE_1-3G, the elution fractions from both cartridges were combined, evaporated under nitrogen, and subjected to HPLC purification after reconstitution.

5.3.3.2 HPLC purification

The chromatograms measured at a detection wavelength of 254 nm revealed the presence of impurity eluting close to 4-OHE_1-3G. Time-based collection of glucuronide fractions was made with the effort to avoid collection of the impurity. The center of the peak, approximately 90 % of the total peak area, was collected while the rest of the peak was avoided (Figure 23).

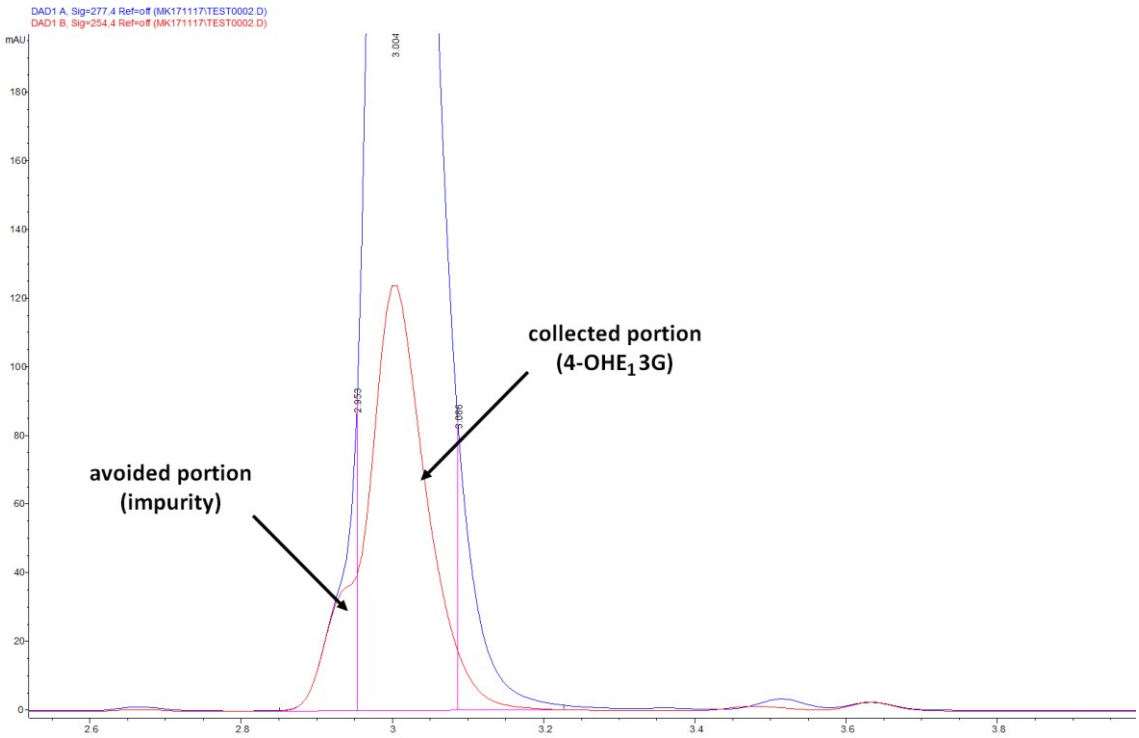

Figure 23. Representative chromatograms of HPLC purification

The chromatograms obtained at detection wavelengths of 277 nm (blue line) and 254 nm (red line) depict the time-based collection of the fraction containing 4-OHE_1-3G with the aim to avoid collection of structure-related impurity.

5.3.3.3 Reaction yield

6.67 mg of pure and dry 4-OHE_1-3G was obtained in the milligram-scale reaction (Figure 24). The amount was sufficient for accurate weighing and structural confirmation by NMR (Section 5.3.3.4). The final reaction yield was 57.7 % of the theoretical yield.

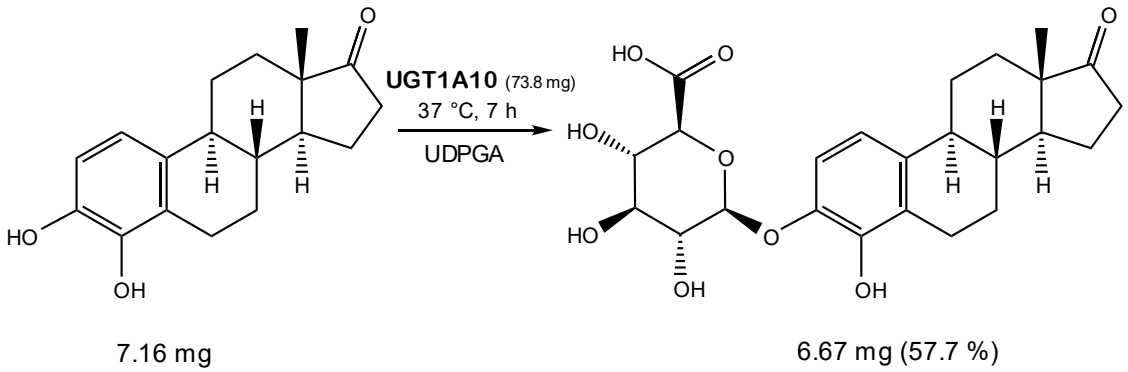

Figure 24. Synthesis of 4-OHE_1-3G

5.3.3.4 Structural confirmation

The ^{1}H and ^{13}C NMR spectra of 4-OHE_1-3G were assigned for structural confirmation. The ^{13}C signals and their corresponding ^{1}H resonances were identified with the aid of the HSQC, HMBC and COSY spectra. There was an interglycosidic correlation in HMBC spectrum between H1 of the glucuronide (δ_{GH1} = 4.67 ppm) and C3 of the aglycone (δ_{C3} = 144.74 ppm) confirming that the glucuronide moiety is conjugated to 4-OHE_1 at position 3 (Figure 25). The anomericity of glucuronide moiety was determined from the vicinal coupling constant J_{GH1GH2} = 7.1 Hz that is a typical value between two axial protons indicating the β-configuration. Other protons of the β-glucuronide moiety appeared in the carbohydrate ring proton region between 3.3 – 3.8 ppm. The NMR data confirmed that the synthesized compound is 4-OHE_1-3G.

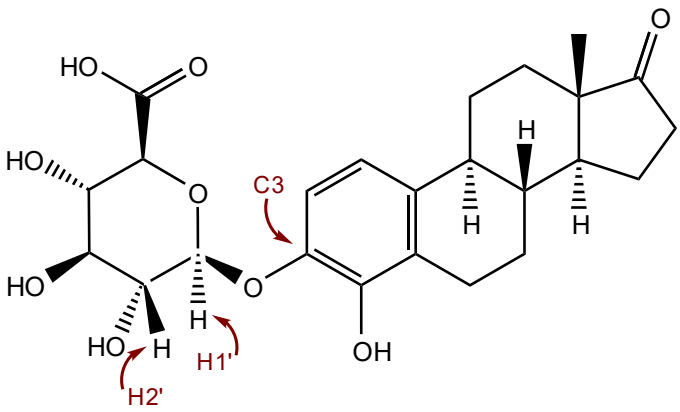

Figure 25. Chemical structure of 4-OHE1-3G

5.3.3.5 Purity of 4-OHE$_1$-3G

The purity of the synthesis product was checked with HPLC. The chromatograms of a sample containing 4-OHE$_1$-3G and a blank sample differed in a single peak belonging to 4-OHE$_1$-3G. No extra peaks were found in the sample chromatogram in comparison to blank chromatogram indicating the high purity of the synthesized steroid glucuronide (Figure 26).

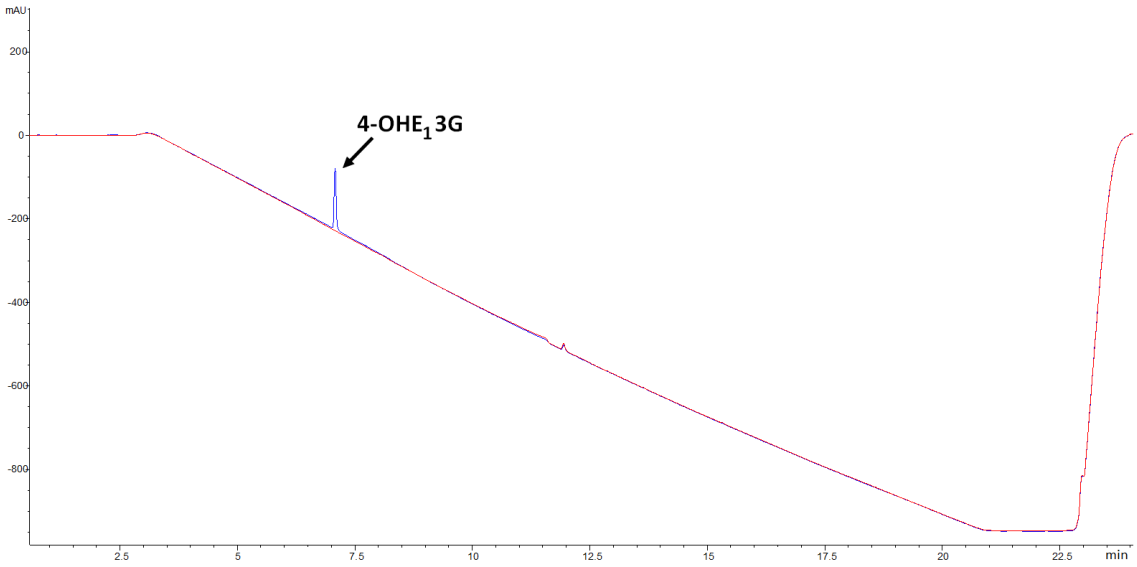

Figure 26. Chromatographic characterization of 4-OHE$_1$-3G purity

The overlapping chromatograms of the test and blank sample at the wavelength of 202 nm show the presence of a single peak corresponding to 4-OHE$_1$-3G indicating its high purity.

5.4 Synthesis of 4-OHE$_1$-4G

5.4.1 Determination of the optimal conditions for the synthesis of 4-OHE$_1$-4G

5.4.1.1 Substrate and DMSO concentration

The HPLC chromatograms demonstrated complete substrate utilization after 24 h at both 4-OHE$_1$ concentrations (750 μM and 1,000 μM). The effect of DMSO concentration on the formation of 4-OHE$_1$-4G at the presence of 1,000 μM substrate concentration is presented in Figure 27. A small peak at the retention time of 4.7 min, presumably corresponding to a degradation product of 4-OHE$_1$, was present in all chromatograms and its peak area constituted approximately 0.2 % of the glucuronide peak. Based on these observations, DMSO concentration of 7 % (v/v) and 1 mM substrate concentration were used in further optimization tests and milligram-scale reaction.

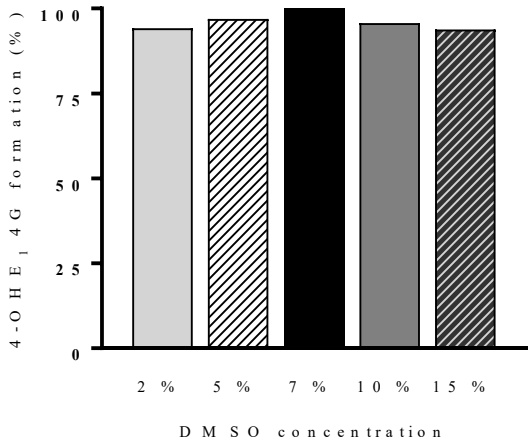

Figure 27. Effect of different DMSO concentration (v/v) on the formation of 4-OHE$_1$-4G

The formation of 4-OHE$_1$-4G in each sample is expressed as a percentage of 4-OHE$_1$-4G formed in the sample containing 7 % of DMSO (v/v).

5.4.1.2 UDPGA concentration

The formation of 4-OHE$_1$-4G in the reactions initiated by UDPGA in the concentration of 5 mM, 4 mM, and 3 mM is depicted in Figure 28. Since the reaction yield in the sample containing 3 mM UDPGA seemed unaffected, this concentration of the costly co-substrate was preferred in further optimization reaction in the milligram-scale synthesis.

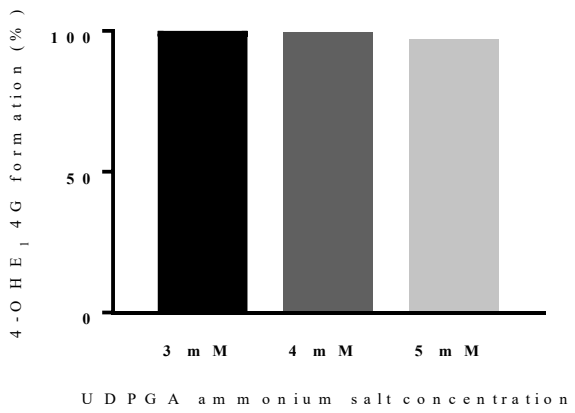

Figure 28. Comparison of 4-OHE_1-4G production in reactions containing different concentrations of UDPGA

The formation of 4-OHE_1-4G is depicted as a percentage of the chromatogram glucuronide peak formed in the sample containing 3 mM UDPGA (100 %).

5.4.1.3 UGT2B7 membrane contents

4-OHE_1 glucuronidation at position 4 catalyzed by 6 % and 8 % of UGT2B7 membranes (v/v) reached 89.9 % and 92.4 % of the glucuronide amount produced in the sample containing 10 % of this enzyme source. Hence, UGT2B7-enriched membranes in the concentration of 10 % (v/v) were employed as a catalyst in the milligram-scale synthesis.

5.4.2 Milligram-scale synthesis of 4-OHE_1-4G

5.4.2.1 LLE and SPE

The chromatograms of dichloromethane and aqueous fractions confirmed that the majority of 4-OHE_1-4G (> 99 %) remained unextracted in the aqueous phase. No peak of 4-OHE_1 was noticed in the chromatograms of both fractions indicating its complete consumption in the reaction. A small peak at a retention time of 4.8 min was present in the chromatograms of both dichloromethane and aqueous fractions. This peak most likely corresponded to a degradation product of 4-OHE_1.

The HPLC analysis of SPE fractions demonstrated that most of the glucuronide (> 99 %) was eluted in the elution fraction consisting of 65% aqueous methanol solution with the addition of ammonium hydroxide. No extra peaks were detected in the elution fraction.

5.4.2.2 HPLC purification

Test injections revealed the presence of another peak at a retention time close to the retention time of 4-OHE$_1$-4G. Since the peaks were merged into one peak in higher injection volumes at the detection wavelengths of 202 nm and 277 nm, the time-based collection of glucuronide fractions was optimized using the chromatograms obtained at the detection wavelength of 254 nm, in which they were only partly overlapping. Approximately 70 % of the total peak area was collected while the rest of the peak was avoided (Figure 29).

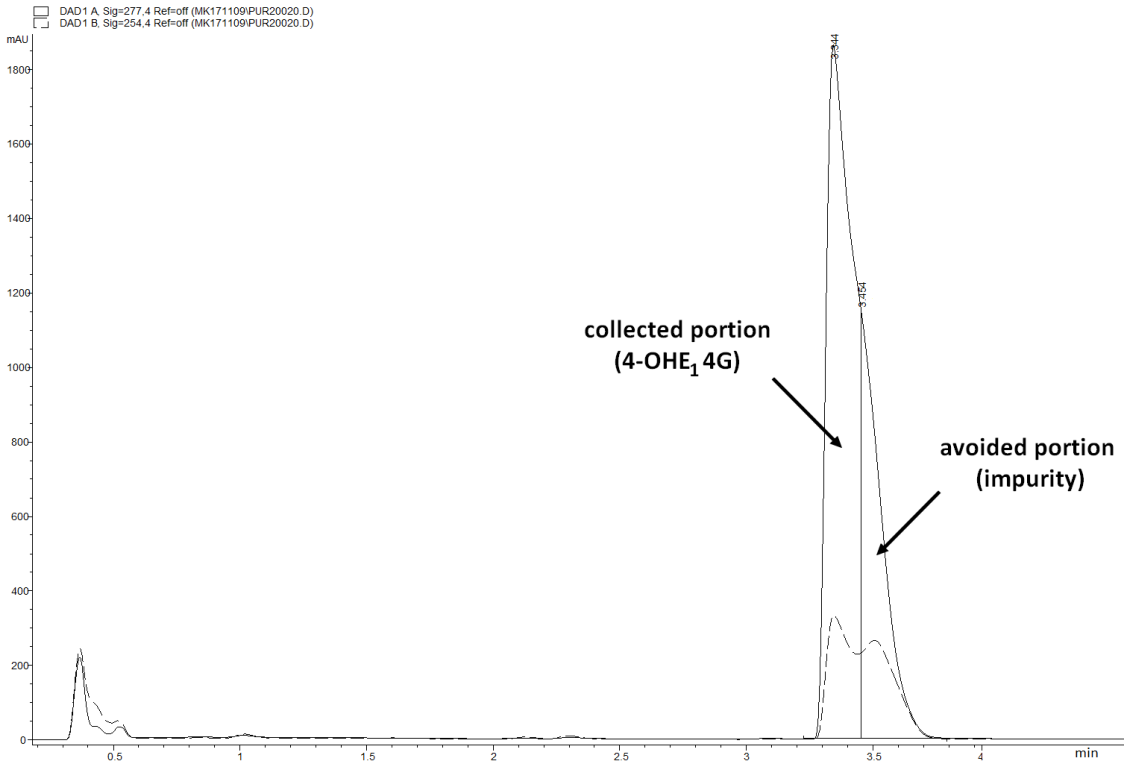

Figure 29. Illustrative chromatograms of HPLC purification

The chromatograms obtained at detection wavelengths of 277 nm (solid line) and 254 nm (dashed line) depict the time-based collection of the fraction containing 4-OHE$_1$-4G with the aim to avoid collection of structure-related impurity.

5.4.2.3 Reaction yield

The amount of pure 4-OHE$_1$-4G obtained in the milligram-scale reaction (5.19 mg) accounted for 44.9 % of the theoretical yield and was sufficient for accurate weighing and structural confirmation by NMR (Section 5.4.2.4). The reaction scheme is depicted in Figure 30.

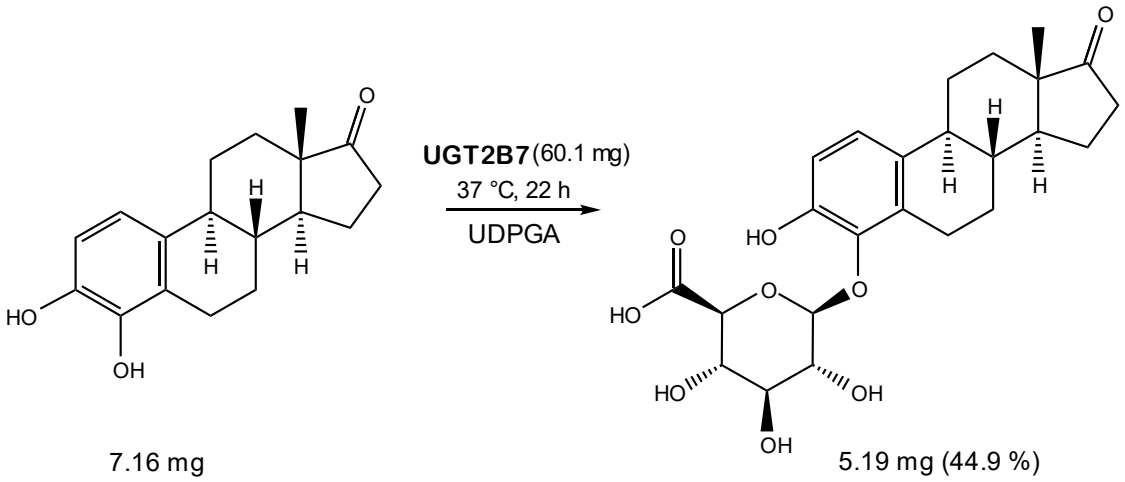

Figure 30. Synthesis of 4-OHE$_1$-4G

5.4.2.4 Structural confirmation

The ^{1}H and ^{13}C NMR spectra of 4-OHE$_1$-4G were assigned with the aid of COSY, HSQC, and HMBC. The presence of HMBC three-bond interglycosidic correlation between H1 of the glucuronide (δ_{GH1} = 4.62 ppm) and C4 of the aglycone (δ_{C4} = 147.34 ppm) confirmed that the glucuronide moiety is conjugated to 4-OHE$_1$ at position 4. The analysis of the coupling constant between GH1 and GH2 (J_{GH1GH2} = 7.3) revealed the expected β-configuration of the anomeric glucuronide conjugate. Other protons of the glucuronide moiety were found in the region between 3.3 – 3.8 that are the typical values for the protons of carbohydrate ring.

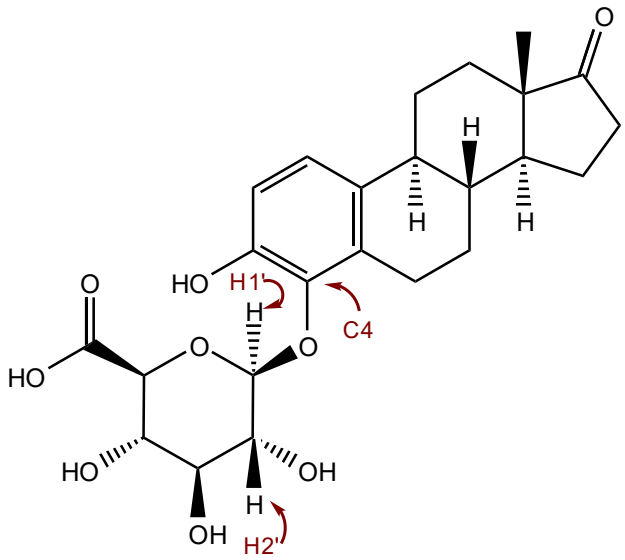

Figure 31. Chemical structure of 4-OHE$_1$-4G

5.4.2.5 Purity of 4-OHE$_1$-4G

The purity of the synthesis product was examined with HPLC. Only one intense peak corresponding to 4-OHE$_1$-4G was detected in the analyzed chromatograms. No extra peaks were found in the chromatogram of the test sample in comparison to chromatogram of the blank sample indicating the high purity of the synthesized steroid glucuronide (Figure 32).

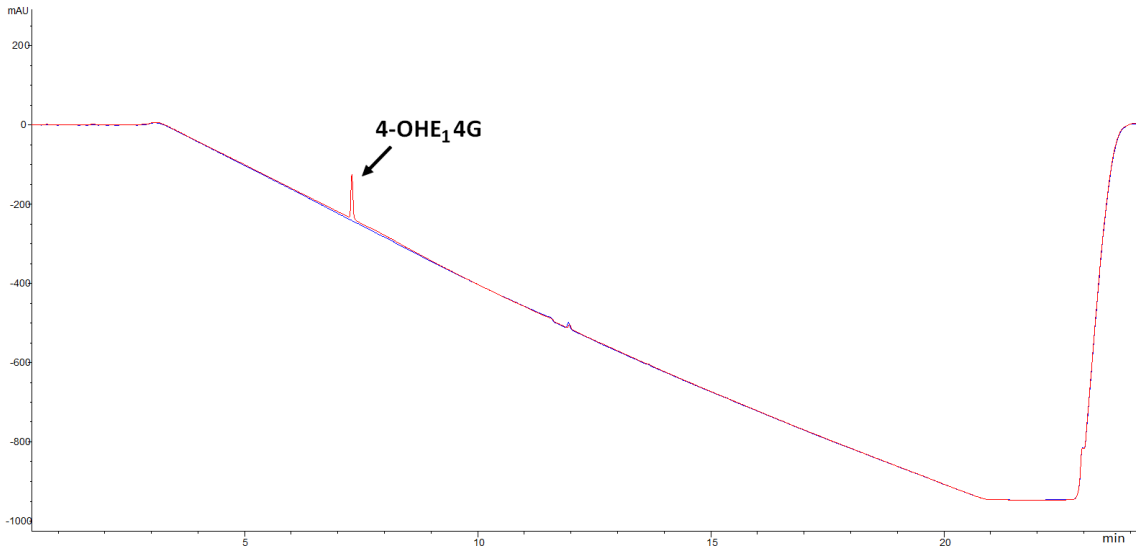

Figure 32. Chromatographic characterization of 4-OHE$_1$-4G purity

The overlapping chromatograms of the test and blank sample at the wavelength of 202 nm display the presence of a single intense peak corresponding to 4-OHE$_1$-4G indicating the high purity of the sample.

6. Discussion

Both chemical and enzymatic methods have been employed in the synthesis of steroid glucuronides so far. Chemical methods based on Königs-Knorr reaction or more recent procedures (Stachulski and Meng 2013) require additional protection and deprotection steps, often suffer from poor yields, and numerous side products are formed in addition to the desired β-anomeric conjugate. Chemical synthesis may be disadvantageous especially when the compound possesses several possible glucuronidation sites. The unwanted glucuronidation sites have to be protected to avoid a mixture of mono- and poly glucuronides. To overcome these drawbacks of chemical synthesis, recombinant human UGT enzymes were used as catalysts for the synthesis of glucuronides in this study. One of the major advantages in comparison to chemical synthesis was the formation of solely biologically relevant β-anomers. In the case of 4-OHE_1 with two conjugation sites, the synthesis of both glucuronides was conveniently achieved by selecting UGT isoforms that regioselectively produced one of the two possible isomers.

UGT2B7 was selected to produce ETG based on glucuronidation data from the earlier study (Sten et al. 2009). In the case of 4-OHE_1, a set of recombinant human UGTs was tested to evaluate their glucuronidation activity towards this substrate. UGT1A10 exhibited the highest 4-OHE_1 glucuronidation rates at 3-OH, whereas UGT2B7 was the most active isoform in the formation of 4-OHE_1-4G (Figure 17) and thus, these isoenzymes were employed in the syntheses of the respective glucuronides. Despite high amino sequence homology among UGT1A7, UGT1A8, UGT1A9, and UGT1A10, only UGT1A10 was capable of formation of both 4-OHE_1 glucuronides (Tukey and Strassburg 2000). This observation is in contradiction to the results from another study on glucuronidation of catechol estrogens which reported no catalytic activity of UGT1A10 microsomes towards 4-OHE_1 (Lépine et al. 2004). The reason for this divergence is most likely the origin of UGT1A10. Previously, Troberg et al. 2017 that the activity of UGT1A10 is often underestimated due to limited activity of commercially available UGT1A10 used by Lépine et al. 2004. In a more recent study, UGT1A10, UGT2B7, and UGT1A8 were reported as the most effective enzymes in the glucuronidation of 4-OHE_1 (Starlard-Davenport et al. 2007). These findings, mainly the identification of UGT1A10 as the most effective isoform in 4-OHE_1 glucuronidation, are in a good agreement with here presented observations. In addition to formerly announced catalytic activities of UGT1A1, UGT1A3, UGT1A7, UGT1A8, UGT1A9, UGT1A10, and UGT2B7, three

members of UGT2A family have been tested for glucuronidation of 4-OHE_1 in this study with a novel recognition of the extrahepatic UGT2A1 as a catalyst of 4-OHE_1 glucuronidation at position 4.

Although UGT1A10 was the most efficient isoform in 4-OHE_1 glucuronidation with a clear preference for 3-OH, this observation may not be relevant for 4-OHE_1 glucuronidation in human liver considering that the expression of UGT1A10, which is expressed mainly in small intestine, colon and nasal epithelium, is very low (Ohno and Nakajin 2009) or none in HLM (Court et al. 2012). UGT2B7 is probably the most dominant isoform involved in 4-OHE_1 glucuronidation in human liver with the strictly regioselective formation of 4-OHE_1-4G. The relative contribution of individual UGT isoforms in the conjugation of 4-OHE_1 at tissue levels and clinical significance of glucuronidation as a way of inactivation of genotoxic 4-OHE_1, especially in hormone-responsive tissues, are still unknown and need to be determined in future studies.

Since the synthesis reaction yield depends on the activity of the enzymatic preparation used as catalysts, small-scale preliminary experiments were performed before each *in vitro* enzymatic synthesis. Expression optimization assays were performed before UGT2B7 and UGT1A10 expression with the aim to get a maximum of active enzyme in a low amount of protein to avoid binding of the substrate and glucuronide product to proteins present in the reaction mixture. The concentration of organic solvent is another parameter that is beneficial to optimize. The inclusion of organic solvent (e.g. DMSO, methanol) helps to overcome poor solubility of steroid aglycones and achieve their higher concentrations in the aqueous reaction mixture. On the other hand, these solvents may have an inhibitory effect on enzyme activity and the solvent sensitivity may differ greatly among individual isoenzymes (Kuuranne et al. 2003). The solubility issues in the syntheses of EpiT and 4-OHE_1 glucuronides was partly resolved by the presence of 7.5 % and 7 % of DMSO, respectively, with the enzyme retaining useful activity as seen in preliminary trials. Another way to overcome this limitation could be simply by the gradual addition of the substrate in several steps. The inclusion of solubilizing agent β-cyclodextrin or temporary introduction of polar substituents (e.g. O-(carboxymethyl)oxime group) have also been used to improve aqueous solubility of steroidal aglycones and acquire higher overall yields in the enzymatical syntheses of steroid glucuronides (Kashima et al. 2010, Wilkinson et al. 2011). Although there are many parameters that can be optimized, optimization conducted before each milligram-

scale synthesis in this study was sufficient for the effective synthesis of glucuronide conjugates by recombinant human UGTs.

A relatively simple procedure based on LLE with dichloromethane, SPE, and HPLC purification was used to extract and purify the synthesized glucuronides from the reaction mixtures. Even if the HPLC analysis of the SPE elution fractions indicated that the glucuronide product was almost free from impurities, HPLC purification may be advantageous in the case of structure-related impurities with similar physicochemical properties, especially when low purity or unstable substrate is used.

The optimized procedure allowed the selective production of β-glucuronides of two steroid substrates in milligram amounts. 6.31 mg of ETG was obtained after 24-h incubation with the overall reaction yield 69.9 %. In comparison, chemical synthesis employing a modification of Königs-Knorr reaction lasting two days produced approximately 1.16 g of ETG and the reaction yield was 50 % (Sanaullah and Bowers 1996). In another study, ETG was synthesized enzymatically using the glucuronylsynthase derived from *E.coli* resulting in very low yield (0.45 mg) and only 28% substrate conversion (Ma et al. 2014). Taken altogether, the enzymatic procedure presented here is a practical way for the rapid production of milligrams of ETG, however, the chemical method would be probably preferred when larger amounts are required, irrespective of the additional deprotection and purification steps.

4-OHE_1 glucuronides were produced regioselectively using recombinant human UGT1A10 (4-OHE_1-3G) and UGT2B7 (4-OHE_1-4G). The amount of 4-OHE_1-3G acquired after only 7 h was 6.67 mg and accounted for 57.7 % of the theoretical yield. The reaction was highly regioselective, and thus the yield was not significantly affected by the formation of the other glucuronide. 5.19 mg of 4-OHE_1-4G was synthesized in a 22-h reaction. The relatively low reaction yield (44.9 %) was most probably caused by 30% loss during HPLC purification that was aimed to separate the glucuronide from the structure-related impurity.

The results indicate that EpiT and 4-OHE_1 glucuronides are easily producible with recombinant human UGT enzymes employed as reaction catalysts. The milligram amounts that were recovered after extraction and purification are sufficient for numerous analyses and experiments.

7. Conclusions

- Highly regioselective UGT1A10 isoform was selected to produce 4-OHE_1-3G and UGT2B7 was employed in the synthesis of 4-OHE_1-4G. The choice of recombinant human UGT isoforms for the syntheses was based on the measurement of glucuronidation rates of 18 recombinant human UGTs towards 4-OHE_1.

- Optimal expression conditions for the production of UGT2B7- and UGT1A10-enriched membranes were determined. UGT2B7 membrane preparations with comparable activities were acquired using both osmotic lysis and sonication. Because of the higher total protein yield, sonication was performed to isolate the UGT1A10-enriched membranes.

- An enzymatic method for synthesis of ETG, 4-OHE_1-3G, and 4-OHE_1-4G, using recombinant human UGTs was developed and optimized. The optimized procedure was successfully used to produce 5 – 7 mg pure steroid glucuronide conjugates with the overall reaction yields ranging from 45 % to 70 %.

- Synthesis products were purified using LLE, SPE and HPLC purification. NMR analyses confirmed chemical structures of the synthesized glucuronide metabolites and HPLC analyses indicated high purity of the samples.

8. Abbreviations

4-OHE_1	4-hydroxyestrone
4-OHE_1-3G	4-hydroxyestrone 3-O-(β-D-glucuronide)
4-OHE_1-4G	4-hydroxyestrone 4-O-(β-D-glucuronide)
AAS	anabolic androgenic steroids
AZT	3′-azido-3′-deoxythymidine
BCA	bicinchoninic acid
BSA	bovine serum albumin
CAS RN	Chemical Abstracts Service Registry Number
cDNA	complementary DNA
COSY	homonuclear correlation spectroscopy
CYP	cytochrome P450
DMSO	dimethyl sulfoxide
DTT	dithiothreitol
E_1	estrone
E_2	17β-estradiol
EC	Enzyme Commission
EpiT	epitestosterone
ER	endoplasmic reticulum
ETG	epitestosterone glucuronide
FBS	fetal bovine serum
GC-MS	gas chromatography-mass spectrometry
GT	glycosyltransferase
HIM	human intestinal microsomes
HKM	human kidney microsomes
HLM	human liver microsomes
HSA	human serum albumin
HSD	hydroxysteroid dehydrogenase
HMBC	heteronuclear multiple-bond correlation spectroscopy
HSQC	heteronuclear single-quantum correlation spectroscopy

HPLC	high-performance liquid chromatography
IFABP	intestinal fatty acid binding protein
IMER	immobilized enzyme reactor
LC-MS	liquid chromatography-mass spectrometry
LC-MS/MS	liquid chromatography-tandem mass spectrometry
LC-NMR	liquid chromatography-nuclear magnetic resonance spectroscopy
LLE	liquid-liquid extraction
MS	mass spectrometry
MS/MS	tandem mass spectrometry
NMR	nuclear magnetic resonance
NSAIDs	nonsteroidal anti-inflammatory drugs
SLC	solute carrier
SPE	solid phase extraction
PB	phosphate buffer
PBS	phosphate buffer saline
PCA	perchloric acid
PCR	polymerase chain reaction
PDE	phosphodiesterase
ROS	reactive oxygen species
RT-PCR	reverse transcription-polymerase chain reaction
qRT-PCR	quantitative reverse transcription-polymerase chain reaction
T/E	testosterone/epitestosterone
TRIS	tris(hydroxymethyl)aminomethane
UDP	uridine diphosphate
UDPGA	UDP-α-D-glucuronic acid
UGDH	UDP-glucose 6-dehydrogenase
UGT	UDP-glucuronosyltransferase

9. References

1. BELLEMARE, Véronique, FAUCHER, Frédérick, BRETON, Rock and LUU-THE, Van. Characterization of 17α-hydroxysteroid dehydrogenase activity (17α-HSD) and its involvement in the biosynthesis of epitestosterone. *BMC Biochemistry.* July 2005. 6, art. 12. ISSN: 14712091. DOI: 10.1186/1471-2091-6-12.
2. BLAIR, Ian A. Analysis of estrogens in serum and plasma from postmenopausal women: Past present, and future. *Steroids.* April 2010. 75(4-5), pp. 297-306. ISSN: 0039-128X. DOI: 10.1016/j.steroids.2010.01.012.
3. BRANDON, Esther F.A., RAAP, Christiaan D., MEIJERMAN, Irma, BEIJNEN, Jos H. and SCHELLENSA, Jan H.M. An update on in vitro test methods in human hepatic drug biotransformation research: Pros and cons. *Toxicology and Applied Pharmacology.* June 2003. 189(3), pp. 233-246. ISSN: 0041-008X. DOI: 10.1016/S0041-008X(03)00128-5.
4. CATLIN, Don H., LEDER, Benjamin Z., AHRENS, Brian D., HATTON, Caroline K. and Joel S. FINKELSTEIN. Effects of androstenedione administration on epitestosterone metabolism in men. *Steroids.* 2002. 67(7), pp. 559-564. ISSN: 0039-128X. DOI: 10.1016/S0039-128X(02)00005-3.
5. CAVALIERI, Ercole, CHAKRAVARTI, Dhubajyoti, GUTTENPLAN, Joseph, HART, Elizabeth, INGLE, James, JANKOWIAK, Ryszard, MUTI, Paola, ROGAN, Eleanor, RUSSO, Jose, SANTEN, Richard and SUTTER, Thomas. Catechol estrogen quinones as initiators of breast and other human cancers: Implications for biomarkers of susceptibility and cancer prevention. *Biochimica et Biophysica Acta - Reviews on Cancer.* August 2006. 1766(1), pp. 63-78. ISSN: 0304-419X. DOI: 10.1016/j.bbcan.2006.03.001.
6. CHANG, Jae H., YOO, Phillip, LEE, Theresa, KLOPF, Wendy and TAKAO, Denise. The role of pH in the glucuronidation of raloxifene, mycophenolic acid and ezetimibe. *Molecular Pharmaceutics.* August 2009. 6(4), pp. 1216-1227. ISSN: 1543-8384. DOI: 10.1021/mp900065b.
7. CHANG, Aram, SINGH, Shanteri, PHILLIPS, George N. and THORSON, Jon S. Glycosyltransferase structural biology and its role in the design of catalysts for glycosylation. *Current Opinion in Biotechnology.* December 2011. 22(6), pp. 800-808. ISSN: 0958-1669. DOI: 10.1016/j.copbio.2011.04.013.

8. CHATZISTEFANIDIS, Dimitrios, GEORGIOU, Ioannis, KYRITSIS, Athanassios P. and MARKOULA, Sofia. Functional impact and prevalence of polymorphisms involved in the hepatic glucuronidation of valproic acid. *Pharmacogenomics*. July 2012. 13(9), pp. 1055-1071. ISSN: 1462-2416. DOI: 10.2217/pgs.12.78.
9. COURT, Michael H., ZHANG, Xiuling, DING, Xinxin, YEE, Karen K., HESSE, Leah M. and FINEL, Moshe. Quantitative distribution of mRNAs encoding the 19 human UDP-glucuronosyltransferase enzymes in 26 adult and 3 fetal tissues. *Xenobiotica.* March 2012. 42(3), pp. 266-277. ISSN: 0049-8254. DOI: 10.3109/00498254.2011.618954.
10. CSALA, Miklós, STAINES, Adam G., BÁNHEGYI, Gábor, MANDL, József, COUGHTRIE, Michael W.H. and BURCHELL, Brian. Evidence for multiple glucuronide transporters in rat liver microsomes. *Biochemical Pharmacology.* October 2004. 68(7), pp. 1353-1362. ISSN: 0006-2952. DOI: 10.1016/j.bcp.2004.05.055.
11. DÖRING, Barbara and PETZINGER, Ernst. Phase 0 and phase III transport in various organs: Combined concept of phases in xenobiotic transport and metabolism. *Drug Metabolism Reviews*. January 2014. 46(3), pp. 261-282. ISSN: 1097-9883. DOI: 10.3109/03602532.2014.882353.
12. D'UVA, Gabriele, BACI, Denisa, ALBINI, Adriana and NOONAN, Douglas M. Cancer chemoprevention revisited: Cytochrome P450 family 1B1 as a target in the tumor and the microenvironment. *Cancer Treatment Reviews.* February 2018. 63, pp. 1-18. ISSN: 0305-7372. DOI: 10.1016/j.ctrv.2017.10.013.
13. DRĂGAN, Călin-Aurel, BUCHHEIT, Daniela, BISCHOFF, Daniel, EBNER, Thomas and BUREIK, Matthias. Glucuronide production by whole-cell biotransformation using genetically engineered fission yeast Schizosaccharomyces pombe. *Drug Metabolism and Disposition.* March 2010. 38(3), pp. 509-515. ISSN: 0090-9556. DOI: 10.1124/dmd.109.030965.
14. EENOO, Peter Van and DELBEKE, Frans T. Metabolism and excretion of anabolic steroids in doping control-New steroids and new insights. *Journal of Steroid Biochemistry and Molecular Biology.* November 2006. 101(4-5), pp. 161-178. ISSN: 0960-0760. DOI: 10.1016/j.jsbmb.2006.06.024.
15. ENGTRAKUL, Juntyma J., FOTI, Robert S., STRELEVITZ, Timothy J. and FISHER, Michael B. Altered AZT (3′-azido-3′-deoxythymidine) glucuronidation kinetics in liver microsomes as an explanation for underprediction of in vivo

clearance: Comparison to hepatocytes and effect of incubation environment. *Drug Metabolism and Disposition.* November 2005. 33(11), pp. 1621-1627. ISSN: 0090-9556. DOI: 10.1124/dmd.105.005058.

16. FABREGAT, Andreu, POZO, Oscar J., MARCOS, Josep, SEGURA, Jordi and VENTURA, Rosa. Use of LC-MS/MS for the open detection of steroid metabolites conjugated with glucuronic acid. *Analytical Chemistry.* May 2013. 85(10), pp. 5005-5014. ISSN: 0003-2700. DOI: 10.1021/ac4001749.
17. FALLON, John K., NEUBERT, Hendrik, GOOSEN, Theunis C. and SMITH, Philip C. Targeted precise quantification of 12 human recombinant uridine-diphosphate glucuronosyl transferase 1A and 2B isoforms using nano-ultra-high-performance liquid chromatography/tandem mass spectrometry with selected reaction monitoring. *Drug Metabolism and Disposition.* December 2013. 41(12), pp. 2076-2080. ISSN: 0090-9556. DOI: 10.1124/dmd.113.053801.
18. FINEL, Moshe, LI, Xin, GARDNER-STEPHEN, Dione, BRATTON, Stacie, MACKENZIE, Peter I. and RADOMINSKA-PANDYA, Anna. Human UDP-glucuronosyltransferase 1A5: Identification, expression, and activity. *Journal of Pharmacology and Experimental Therapeutics.* December 2005. 315(3), pp. 1143-1149. ISSN: 0022-3565. DOI: 10.1124/jpet.105.091900.
19. FINEL, Moshe and KURKELA, Mika. The UDP-glucuronosyltransferases as oligomeric enzymes. *Current Drug Metabolism.* January 2008. 9(1), pp. 70-76. ISSN: 1389-2002. DOI: 10.2174/138920008783331158.
20. FISHER, Michael B., CAMPANALE, Kristina, ACKERMANN, Bradley L., VANDENBRANDEN, Mark and WRIGHTON, Steven A. In vitro glucuronidation using human liver microsomes and the pore-forming peptide alamethicin. *Drug Metabolism and Disposition.* 2000. 28(5), pp. 560-566. ISSN: 0090-9556.
21. FUHRMAN, Barbara J., SCHAIRER, Catherine, GAIL, Mitchell H., BOYD-MORIN, Jennifer, XU, Xia, SUE, Laura Y., BUYS, Saundra S., ISAACS, Claudine, KEEFER, Larry K., VEENSTRA, Timothy D., BERG, Christine D., HOOVER, Robert N. and ZIEGLER, Regina G. Estrogen metabolism and risk of breast cancer in postmenopausal women. *Journal of the National Cancer Institute.* February 2012. 104(4), pp. 326-339. ISSN: 0027-8874. DOI: 10.1093/jnci/djr531.
22. FUHRMAN, Barbara J., XU, Xia, FALK, Roni T., DALLAL, Cher M., VEENSTRA, Timothy D., KEEFER, Larry K., GRAUBARD, Barry I., BRINTON, Louise A., ZIEGLER, Regina G. and GIERACH, Gretchen L. Assay reproducibility

and interindividual variation for 15 serum estrogens and estrogen metabolites measured by liquid chromatography-tandem mass spectrometry. *Cancer Epidemiology Biomarkers and Prevention.* December 2014. 23(12), pp. 2649-2657. ISSN: 1055-9965. DOI: 10.1158/1055-9965.EPI-14-0438.

23. FUJIWARA, Ryoichi and ITOH, Tomoo. Extensive protein-protein interactions involving UDP-glucuronosyltransferase (UGT) 2B7 in human liver microsomes. *Drug Metabolism and Pharmacokinetics.* 2014. 29(3), pp. 259-265. ISSN: 1347-4367. DOI: 10.2133/dmpk.DMPK-13-RG-096.
24. FUJIWARA, Ryoichi, YOKOI, Tsuyoshi and NAKAJIMA, Miki. Structure and protein-protein interactions of human UDP-glucuronosyltransferases. *Frontiers in Pharmacology.* October 2016. 7(OCT), art. 388. ISSN: 1663-9812. DOI: 10.3389/fphar.2016.00388.
25. GE, Shufan, TU, Yifan and HU, Ming. Challenges and opportunities with predicting *in vivo* phase II metabolism via glucuronidation from *in vitro* data. *Current Pharmacology Reports.* December 2016. 2(6), pp. 326-338. ISSN: 2198-641X. DOI: 10.1007/s40495-016-0076-8.
26. GESTL, Shelley A., GREEN, Mitchell D., SHEARER, Debra A., FRAUENHOFFER, Elizabeth, TEPHLY, Thomas R. and WEISZ, Judith. Expression of UGT2B7, a UDP-glucuronosyltransferase implicated in the metabolism of 4-hydroxyestrone and all-trans retinoic acid, in normal human breast parenchyma and in invasive and in situ breast cancers. *American Journal of Pathology.* 2002. 160(4), pp. 1467-1479. ISSN: 0002-9440. DOI: 10.1016/S0002-9440(10)62572-2.
27. GHAYEE, Hans K. and AUCHUS, Richard J. Basic concepts and recent developments in human steroid hormone biosynthesis. *Reviews in Endocrine and Metabolic Disorders.* December 2007. 8(4), pp. 289-300. ISSN: 1389-9155. DOI: 10.1007/s11154-007-9052-2.
28. GIBSON, G. Gordon and SKETT, Paul. *Introduction to Drug Metabolism.* Third Edition. United Kingdom: Nelson Thornes Publishers, 2001. ISBN 0-7487-6011-3.
29. GIRARD, Hugo, LÉVESQUE, Eric, BELLEMARE, Judith, JOURNAULT, Kim, CAILLIER, Bertrand and GUILLEMETTE, Chantal. Genetic diversity at the UGT1 locus is amplified by a novel 3′ alternative splicing mechanism leading to nine additional UGT1A proteins that act as regulators of glucuronidation activity.

Pharmacogenetics and Genomics. December 2007. 17(12), pp. 1077-1089. ISSN: 1744-6872. DOI: 10.1097/FPC.0b013e3282f1f118.

30. GREAVES, Ronda F., JEVALIKAR, Ganesh, HEWITT, Jacqueline K. and ZACHARIN, Margaret R. A guide to understanding the steroid pathway: New insights and diagnostic implications. *Clinical Biochemistry.* January 2015. 47(15), pp. 5-15. ISSN: 0009-9120. DOI: 10.1016/j.clinbiochem.2014.07.017.
31. GUILLEMETTE, Chantal, LÉVESQUE, Éric, HARVEY, Mario, BELLEMARE, Judith and MENARD, Vincent. UGT genomic diversity: Beyond gene duplication. *Drug Metabolism Reviews.* February 2010. 42(1), pp. 22-42. ISSN: 0360-2532. DOI: 10.3109/03602530903210682.
32. GUILLEMETTE, Chantal, LÉVESQUE, Éric and ROULEAU, Michéle. Pharmacogenomics of human uridine diphospho-glucuronosyltransferases and clinical implications. *Clinical Pharmacology and Therapeutics.* September 2014. 96(3), pp. 324-339. ISSN: 0009-9236. DOI: 10.1038/clpt.2014.126.
33. HU, Dong G., MACKENZIE, Peter I., MCKINNON, Ross A. and MEECH, Robyn. Genetic polymorphisms of human UDP-glucuronosyltransferase (UGT) genes and cancer risk. *Drug Metabolism Reviews.* January 2016. 48(1), pp. 47-69. ISSN: 0360-2532. DOI: 10.3109/03602532.2015.1131292.
34. IKUSHIRO, Shin-Ichi, EMI, Yoshikazu and IYANAGI, Takashi. Activation of glucuronidation through reduction of a disulfide bond in rat UDP-glucuronosyltransferase 1A6. *Biochemistry.* October 2002. 41(42), pp. 12813-12820. ISSN: 0006-2960. DOI: 10.1021/bi0262451.
35. IKUSHIRO, Shin-ichi, NISHIKAWA, Miyu, MASUYAMA, Yuuka, SHOUJI, Tadashi, FUJII, Miharu, HAMADA, Masahiro, NAKAJIMA, Noriyuki, FINEL, Moshe, YASUDA, Kaori, KAMAKURA, Masaki and SAKAKI, Toshiyuki. Biosynthesis of drug glucuronide metabolites in the budding yeast saccharomyces cerevisiae. *Molecular Pharmaceutics.* July 2016. 13(7), pp. 2274-2282. ISSN: 1543-8384. DOI: 10.1021/acs.molpharmaceut.5b00954.IOANNIDES, Costas. Xenobiotic Metabolism: An Overview. In: Costas IOANNIDES, ed. *Enzyme Systems that Metabolise Drugs and Other Xenobiotic*. United Kingdom: John Wiley & Sons, Ltd, 2002, pp. 1-32. ISBN 0-471-89466-4.
36. IZUKAWA, Takeshi, NAKAJIMA, Miki, FUJIWARA, Ryoichi, YAMANAKA, Hiroyuki, FUKAMI, Tatsuki, TAKAMIYA, Masataka, AOKI, Yasuhiro, IKUSHIRO, Shin-ichi, SAKAKI, Toshiyuki and YOKOI, Tsuyoshi. Quantitative

analysis of UDP-glucuronosyltransferase (UGT) 1A and UGT2B expression levels in human livers. *Drug Metabolism and Disposition.* August 2009. 37(8), pp. 1759-1768. ISSN: 0090-9556. DOI: 10.1124/dmd.109.027227.

37. JANCOVA, Petra, ANZENBACHER, Pavel and ANZENBACHEROVA, Eva. Phase II drug metabolising enzymes. *Biomedical Papers.* June 2010. 154(2), pp. 103-116. ISSN: 1213-8118. DOI: 10.5507/bp.2010.017.
38. KAMIMORI, Hiroshi, OZAKI, Yoshihisa, OKABAYASHI, Yoshito, UENO, Kyoji and NARITA, Shigeru. Synthesis of acylglucuronides of drugs using immobilized dog liver microsomes octadecylsilica particles coated with phospholipid. *Analytical Biochemistry.* June 2003. 317(1), pp. 99-106. ISSN: 0003-2697. DOI: 10.1016/S0003-2697(03)00111-8.
39. KASHIMA, Yousuke, KITADE, Takashi, KASHIMA, Yuuko and OKABAYASHI, Yoshito. Development of an automated synthesis system for preparation of glucuronides using a solid-phase extraction column loaded with microsomes. *Chemical and Pharmaceutical Bulletin.* March 2010. 58(3), pp. 354-358. ISSN: 0009-2363. DOI: 10.1248/cpb.58.354.
40. KASHIMA, Yousuke and OKABAYASHI, Yoshito. Development of a rapid and detailed structural identification system with an on-line immobilized enzyme reactor integrated into LC-NMR. *Chemical and Pharmaceutical Bulletin.* March 2010. 58(3), pp. 423-425. ISSN: 0009-2363. DOI: 10.1248/cpb.58.423.
41. KASPERSEN, Frans M. and BOECKEL, Constant A.A. van. A review of the methods of chemical synthesis of sulphate and glucuronide conjugates. *Xenobiotica*. 1987. 17(12), pp. 1451-1471. ISSN: 0049-8254. DOI: 10.3109/00498258709044005.
42. KAUR-ATWAL, Gushinder, REYNOLDS, James C., MUSSELL, Christopher, CHAMPARNAUD, Elodie, KNAPMAN, Tom W., ASHCROFT, Alison E., O'CONNOR, Gavin, CHRISTIE, Steven D. R. and CREASER, Colin S. Determination of testosterone and epitestosterone glucuronides in urine by ultra performance liquid chromatography-ion mobility-mass spectrometry. *Analyst.* October 2011. 136(19), pp. 3911-3916. ISSN: 0003-2654. DOI: 10.1039/c1an15450h.
43. KOBAYASHI, Tsutomu, SLEEMAN, Judith E., COUGHTRIE, Michael W. H. and BURCHELL, Brian. Molecular and functional characterization of microsomal UDP-glucuronic acid uptake by members of the nucleotide sugar transporter (NST) family.

Biochemical Journal. December 2006. 400(2), pp. 281-289. ISSN: 0264-6021. DOI: 10.1042/BJ20060429.

44. KURKELA, Mika, GARCÍA-HORSMAN, J. Arturo, LUUKKANEN, Leena, MÖRSKY, Saila, TASKINEN, Jyrki, BAUMANN, Marc, KOSTIAINEN, Risto, HIRVONEN, Jouni and FINEL, Moshe. Expression and characterization of recombinant human UDP-glucuronosyltransferases (UGTs): UGT1A9 is more resistant to detergent inhibition than the other UGTs and was purified as an active dimeric enzyme. *Journal of Biological Chemistry.* February 2003. 278(6), pp. 3536-3544. ISSN: 0021-9258. DOI: 10.1074/jbc.M206136200.
45. KURKELA, Mika, HIRVONEN, Jouni, KOSTIAINEN, Risto and FINEL, Moshe. The interactions between the N-terminal and C-terminal domains of the human UDP-glucuronosyltransferases are partly isoform-specific, and may involve both monomers. *Biochemical Pharmacology.* December 2004. 68(12), pp. 2443-2450. ISSN: 0006-2952. DOI: 10.1016/j.bcp.2004.08.019.
46. KURKELA, Mika, PATANA, Anne-Sisko, MACKENZIE, Peter I., COURT, Michael H., TATE, Christopher G., HIRVONEN, Jouni, GOLDMAN, Adrian and FINEL, Moshe. Interactions with other human UDP-glucuronosyltransferases attenuate the consequences of the Y485D mutation on the activity and substrate affinity of UGT1A6. *Pharmacogenetics and Genomics.* February 2007. 17(2), pp. 115-126. ISSN: 1744-6872. DOI: 10.1097/FPC.0b013e328011b598.
47. KUURANNE, Tiia, KURKELA, Mika, THEVIS, Mario, SCHÄNZER, Wilhelm, FINEL, Moshe and KOSTIAINEN, Risto. Glucuronidation of anabolic androgenic steroids by recombinant human UDP-glucuronosyltransferases. *Drug Metabolism and Disposition.* September 2003. 31(9), pp. 1117-1124. ISSN: 0090-9556. DOI: 10.1124/dmd.31.9.1117.
48. KUURANNE, Tiia, SAUGY, Martial and BAUME, Norbert. Confounding factors and genetic polymorphism in the evaluation of individual steroid profiling. *British Journal of Sports Medicine.* 2014. 48(10), pp. 848-855. ISSN: 0306-3674. DOI: 10.1136/bjsports-2014-093510.
49. LÉPINE, Johanie, BERNARD, Olivier, PLANTE, Marie, TÊTU, Bernard, PELLETIER, Georges, LABRIE, Fernand, BÉLANGER, Alain and GUILLEMETTE, Chantal. Specificity and regioselectivity of the conjugation of estradiol, estrone, and their catecholestrogen and methoxyestrogen metabolites by human uridine diphospho-glucuronosyltransferases expressed in endometrium.

Journal of Clinical Endocrinology and Metabolism. October 2004. 89(10), pp. 5222-5232. ISSN: 0021-972X. DOI: 10.1210/jc.2004-0331.

50. LIEHR, Joachim G. and RICCI, Mary J. 4-Hydroxylation of estrogens as marker of human mammary tumors. *Proceedings of the National Academy of Sciences of the United States of America.* April 1996. 93(8), pp. 3294-3296. ISSN: 0027-8424. DOI: 10.1073/pnas.93.8.3294.
51. LIU, Yuejian and COUGHTRIE, Michael W. H. Revisiting the latency of uridine diphosphate-glucuronosyltransferases (UGTs) - How does the endoplasmic reticulum membrane influence their function? *Pharmaceutics.* September 2017. 9(3), art. 32. ISSN: 1999-4923. DOI: 10.3390/pharmaceutics9030032.
52. LUUKKANEN, Leena, KILPELÄINEN, Ilkka, KANGAS, Heli, OTTOILA, Pekka, ELOVAARA, Eivor and TASKINEN, Jyrki. Enzyme-assisted synthesis and structural characterization of nitrocatechol glucuronides. *Bioconjugate Chemistry.* January 1999. 10(1), pp. 150-154. ISSN: 1043-1802. DOI: 10.1021/bc980064n.
53. MA, Paul, KANIZAJ, Nicholas, CHAN, Shu-Ann, OLLIS, David L. and MCLEOD, Malcolm D. The Escherichia coli glucuronylsynthase promoted synthesis of steroid glucuronides: Improved practicality and broader scope. *Organic and Biomolecular Chemistry.* August 2014. 12(32), pp. 6208-6214. ISSN: 1477-0520. DOI: 10.1039/c4ob00984c.
54. MACKENZIE, Peter I., BOCK, Karl W., BURCHELL, Brian, GUILLEMETTE, Chantal, IKUSHIRO, Shin-ichi, IYANAGI, Takashi, MINERS, John O., OWENS, Ida S. and NEBERT, Daniel W. Nomenclature update for the mammalian UDP glycosyltransferase (UGT) gene superfamily. *Pharmacogenetics and Genomics*. October 2005. 15(10), pp. 677-685. ISSN: 1744-6872. DOI: 10.1097/01.fpc.0000173483.13689.56.
55. MAGDALOU, Jacques, FOURNEL-GIGLEUX, Sylvie and OUZZINE, Mohamed. Insights on membrane topology and structure/function of UDP-glucuronosyltransferases. *Drug Metabolism Reviews*. February 2010. 42(1), pp. 154-161. ISSN: 0360-2532. DOI: 10.3109/03602530903209270.
56. MANEVSKI, Nenad, TROBERG, Johanna, SVALUTO-MOREOLO, Paolo, DZIEDZIC, Klaudyna, YLI-KAUHALUOMA, Jari and FINEL, Moshe. Albumin stimulates the activity of the human UDP-glucuronosyltransferases 1A7, 1A8, 1A10, 2A1 and 2B15, but the effects are enzyme and substrate dependent. *PLoS ONE.*

January 2013. 8(1), art. e54767. ISSN: 1932-6203. DOI: 10.1371/journal.pone.0054767.

57. MEECH, Robyn, MINERS, John O., LEWIS, Benjamin C. and MACKENZIE, Peter I. The glycosidation of xenobiotics and endogenous compounds: Versatility and redundancy in the UDP glycosyltransferase superfamily. *Pharmacology and Therapeutics*. May 2012. 134(2), pp. 200-218. ISSN: 0163-7258. DOI: 10.1016/j.pharmthera.2012.01.009.
58. MILEY, Michael J., ZIELINSKA, Agnieszka K., KEENAN, Jeffrey E., BRATTON, Stacie M., RADOMINSKA-PANDYA, Anna and REDINBO, Matthew R. Crystal structure of the cofactor-binding domain of the human phase II drug-metabolism enzyme UDP-glucuronosyltransferase 2B7. *Journal of Molecular Biology.* June 2007. 369(2), pp. 498-511. ISSN: 0022-2836. DOI: 10.1016/j.jmb.2007.03.066.
59. MILLER, Walter L. and AUCHUS, Richard J. The molecular biology, biochemistry, and physiology of human steroidogenesis and its disorders. *Endocrine Reviews.* February 2011. 32(1), pp. 81-151. ISSN: 0163-769X. DOI: 10.1210/er.2010-0013.
60. MINERS, John O., SMITH, Paul A., SORICH, Michael J., MCKINNON, Ross A. and MACKENZIE, Peter I. Predicting Human Drug Glucuronidation Parameters: Application of In Vitro and In Silico Modeling Approaches. *Annual Review of Pharmacology and Toxicology*. 2004. 44, pp. 1-25. ISSN: 0362-1642. DOI: 10.1146/annurev.pharmtox.44.101802.121546.
61. MITRA, Partha S., BASU, Nikhil K. and OWENS, Ida S. Src supports UDP-glucuronosyltransferase-2B7 detoxification of catechol estrogens associated with breast cancer. *Biochemical and Biophysical Research Communications.* May 2009. 382(4), pp. 651-656. ISSN: 0006-291X. DOI: 10.1016/j.bbrc.2009.03.054.
62. MULLEN, Jenny E., THÖRNGREN, John-Olof, SCHULZE, Jenny J., ERICSSON, Magnus, GÅREVIK, Nina, LEHTIHET, Mikael and EKSTRÖM, Lena. Urinary steroid profile in females – the impact of menstrual cycle and emergency contraceptives. *Drug Testing and Analysis.* July 2017. 9(7), pp. 1034-1042. ISSN: 1942-7603. DOI: 10.1002/dta.2121.
63. NIWA, Toshiro, MURAYAMA, Norie, IMAGAWA, Yurie and YAMAZAKI, Hiroshi. Regioselective hydroxylation of steroid hormones by human cytochromes P450. Drug *Metabolism Reviews.* May 2015. 47(2), pp. 89-110. ISSN: 0360-2532. DOI: 10.3109/03602532.2015.1011658.

64. ODA, Shingo, NAKAJIMA, Miki, HATAKEYAMA, Masahiko, FUKAMI, Tatsuki and YOKOI, Tsuyoshi. Preparation of a specific monoclonal antibody against human UDP-glucuronosyltransferase (UGT) 1A9 and evaluation of UGT1A9 protein levels in human tissues. *Drug Metabolism and Disposition.* August 2012. 40(8), pp. 1620-1627. ISSN: 0090-9556. DOI: 10.1124/dmd.112.045625.
65. ODA, Shingo, FUKAMI, Tatsuki, YOKOI, Tsuyoshi and NAKAJIMA, Miki. A comprehensive review of UDP-glucuronosyltransferase and esterases for drug development. *Drug Metabolism and Pharmacokinetics.* February 2015. 30(1), pp. 30-51. ISSN: 1347-4367. DOI: 10.1016/j.dmpk.2014.12.001.
66. OHNO, Shuji and NAKAJIN, Shizuo. Determination of mRNA expression of human UDP-glucuronosyltransferases and application for localization in various human tissues by real-time reverse transcriptase-polymerase chain reaction. *Drug Metabolism and Disposition.* January 2009. 37(1), pp. 32-40. ISSN: 0090-9556. DOI: 10.1124/dmd.108.023598.
67. OLESON, Lauren and COURT, Michael H. Effect of the β-glucuronidase inhibitor saccharolactone on glucuronidation by human tissue microsomes and recombinant UDP- glucuronosyltransferases. *Journal of Pharmacy and Pharmacology.* September 2008. 60(9), pp. 1175-1182. ISSN: 0022-3573. DOI: 10.1211/jpp.60.9.0009.
68. RADOMINSKA-PANDYA, Anna, BRATTON, Stacie M and LITTLE, Joanna M. A historical overview of the heterologous expression of mammalian UDP-glucuronosyltransferase isoforms over the past twenty years. *Current Drug Metabolism.* April 2005. 6(2), pp. 141-160. ISSN: 1389-2002. DOI: 10.2174/1389200053586127.
69. RADOMINSKA-PANDYA, Anna, BRATTON, Stacie M., REDINBO, Matthew R. and MILEY, Michael J. The crystal structure of human UDP-glucuronosyltransferase 2B7 C-terminal end is the first mammalian UGT target to be revealed: The significance for human UGTs from both the 1A and 2B families. *Drug Metabolism Reviews.* February 2010. 42(1), pp. 128-139. ISSN: 0360-2532. DOI: 10.3109/03602530903209049.
70. RANE, Anders and EKSTRÖM, Lena. Androgens and doping tests: Genetic variation and pit-falls. *British Journal of Clinical Pharmacology.* July 2012. 74(1), pp. 3-15. ISSN: 0306-5251. DOI: 10.1111/j.1365-2125.2012.04294.x.

71. REZVANPOUR, Atoosa and DON-WAUCHOPE, Andrew C. Clinical implications of estrone sulfate measurement in laboratory medicine. *Critical Reviews in Clinical Laboratory Sciences.* February 2017. 54(2), pp. 73-86. ISSN: 1040-8363. DOI: 10.1080/10408363.2016.1252310.
72. RODWELL, Victor W., BENDER David A., BOTHAM, Kathleen M., KENNELLY Peter J. and WEIL, P. Anthony. *Harper's illustrated biochemistry*. 30th edition. New York: McGraw-Hill Education, 2015. ISBN 978-0-07-182534-4.
73. ROWLAND, Andrew, GAGANIS, Paraskevi, ELLIOT, David J., MACKENZIE, Peter I., KNIGHTS, Kathleen M. and MINERS, John O. Binding of inhibitory fatty acids is responsible for the enhancement of UDP-glucuronosyltransferase 2B7 activity by albumin: Implications for in vitro-in vivo extrapolation. *Journal of Pharmacology and Experimental Therapeutics.* April 2007. 321(1), pp. 137-147. ISSN: 0022-3565. DOI: 10.1124/jpet.106.118216.
74. ROWLAND, Andrew, KNIGHTS, Kathleen M., MACKENZIE, Peter I. and MINERS, John O. Characterization of the binding of drugs to human intestinal fatty acid binding protein (IFABP): Potential role of IFABP as an alternative to albumin for in vitro-in vivo extrapolation of drug kinetic parameters. *Drug Metabolism and Disposition.* July 2009. 37(7), pp. 1395-1403. ISSN: 0090-9556. DOI: 10.1124/dmd.109.027656.
75. ROWLAND, Andrew, MINERS, John O. and MACKENZIE, Peter I. The UDP-glucuronosyltransferases: Their role in drug metabolism and detoxification. *International Journal of Biochemistry and Cell Biology.* June 2013. 45(6), pp. 1121-1132. ISSN: 1357-2725. DOI: 10.1016/j.biocel.2013.02.019.
76. ROWLAND, Andrew, MACKENZIE, Peter I. and MINERS, John O. Transporter-mediated uptake of UDP-glucuronic acid by human liver microsomes: Assay conditions, kinetics, and inhibition. *Drug Metabolism and Disposition.* January 2015. 43(1), pp. 147-153. ISSN: 0090-9556. DOI: 0.1124/dmd.114.060509.
77. SAKAI-KATO, Kumiko, KATO, Masaru and TOYO'OKA, Toshimasa. On-line drug-metabolism system using microsomes encapsulated in a capillary by the sol-gel method and integrated into capillary electrophoresis. *Analytical Biochemistry.* October 2002. 308(2), pp. 278-284. ISSN: 0003-2697. DOI: 10.1016/S0003-2697(02)00231-2.

78. SAMAVAT, Hamed and KURZER, Mindy S. Estrogen metabolism and breast cancer. *Cancer Letters.* January 2015. 356(2), pp. 231-243. ISSN: 0304-3835. DOI: 10.1016/j.canlet.2014.04.018.
79. SANAULLAH and BOWERS, Larry D. Facile synthesis of [16,16,17-$^{2}H_3$]-testosterone, -epitestosterone and their glucuronides and sulfates. *Journal of Steroid Biochemistry and Molecular Biology.* May 1996. 58(2), pp. 225-234. ISSN: 0960-0760. DOI: 10.1016/0960-0760(96)00025-8.
80. SATO, Yuichiro, NAGATA, Masanori, TETSUKA, Kazuhiro, TAMURA, Kouichi, MIYASHITA, Aiji, KAWAMURA, Akio and USUI, Takashi. Optimized methods for targeted peptide-based quantification of human uridine 5'-diphosphate-glucuronosyltransferases in biological specimens using liquid chromatography-tandem mass spectrometry. *Drug Metabolism and Disposition.* May 2014. 42(5), pp. 885-889. ISSN: 0090-9556. DOI: 10.1124/dmd.113.056291.
81. SIMPSON, Evan R., RUBIN, Gary L., CLYNE, Colin D., ROBERTSON, Kelli M., O'DONNELL, Liza, DAVIS, Susan R. and JONES, Margaret E. Local estrogen biosynthesis in males and females. *Endocrine-Related Cancer.* June 1999. 6(2), pp. 131-137. ISSN: 1351-0088. DOI: 10.1677/erc.0.0060131.
82. SIMPSON, Evan R. Sources of estrogen and their importance. *Journal of Steroid Biochemistry and Molecular Biology.* September 2003. 86(3-5), pp. 225-230. ISSN: 0960-0760. DOI: 10.1016/S0960-0760(03)00360-1.
83. SNEITZ, Nina, COURT, Michael H., ZHANG, Xiuling, LAAJANEN, Kaisa, YEE, Karen K., DALTON, Pamela, DING, Xinxin and FINEL, Moshe. Human UDP-glucuronosyltransferase UGT2A2: CDNA construction, expression, and functional characterization in comparison with UGT2A1 and UGT2A3. *Pharmacogenetics and Genomics.* December 2009. 19(12), pp. 923-934. ISSN: 1744-6872. DOI: 10.1097/FPC.0b013e3283330767.
84. STACHULSKI, Andrew V. and JENKINS, Gareth N. The synthesis of O-glucuronides. *Natural Product Reports.* April 1998. 15(2), pp. 173-186. ISSN: 0265-0568.
85. STACHULSKI, Andrew V. and MENG, Xiaoli. Glucuronides from metabolites to medicines: A survey of the in vivo generation, chemical synthesis and properties of glucuronides. *Natural Product Reports.* June 2013. 30(6), pp. 806-848. ISSN: 0265-0568. DOI: 10.1039/c3np70003h.

86. STÁRKA, Luboslav. Epitestosterone. *Journal of Steroid Biochemistry and Molecular Biology.* October 2003. 87(1), pp. 27-34. ISSN: 0960-0760. DOI: 10.1016/S0960-0760(03)00383-2.
87. STARLARD-DAVENPORT, Athena, XIONGA, Yan, BRATTON, Stacie, GALLUS-ZAWADA, Anna, FINEL, Moshe and RADOMINSKA-PANDYA, Anna. Phenylalanine90 and phenylalanine93 are crucial amino acids within the estrogen binding site of the human UDP-glucuronosyltransferase 1A10. *Steroids.* January 2007. 72(1), pp. 85-94. ISSN: 0039-128X. DOI: 10.1016/j.steroids.2006.11.016.
88. STARLARD-DAVENPORT, Athena, LYN-COOK, Beverly and RADOMINSKA-PANDYA, Anna. Novel identification of UDP-glucuronosyltransferase 1A10 as an estrogen-regulated target gene. *Steroids.* January 2008. 73(1), pp. 139-147. ISSN: 0039-128X. DOI: 10.1016/j.steroids.2007.09.007.
89. STEN, Taina, QVISEN, Saana, UUTELA, Päivi, LUUKKANEN, Leena, KOSTIAINEN, Risto and FINEL, Moshe. Prominent but reverse stereoselectivity in propranolol glucuronidation by human UDP-glucuronosyltransferases 1A9 and 1A10. *Drug Metabolism and Disposition.* 2006. 34(9), pp. 1488-1494. ISSN: 0090-9556. DOI: 10.1124/dmd.106.010371.
90. STEN, Taina, BICHLMAIER, Ingo, KUURANNE, Tiia, LEINONEN, Antti, YLI-KAUHALUOMA, Jari and FINEL, Moshe. UDP-glucuronosyltransferases (UGTs) 2B7 and UGT2B17 display converse specificity in testosterone and epitestosterone glucuronidation, whereas UGT2A1 conjugates both androgens similarly. *Drug Metabolism and Disposition.* February 2009. 37(2), pp. 417-423. ISSN: 0090-9556. DOI: 10.1124/dmd.108.024844.
91. STINGL, Julia C., BARTELS, Henning, VIVIANI, Roberto, LEHMANNA, Marie L. and BROCKMÖLLER, Jürgen. Relevance of UDP-glucuronosyltransferase polymorphisms for drug dosing: A quantitative systematic review. *Pharmacology and Therapeutics.* January 2014. 141(1), pp. 92-116. ISSN: 0163-7258. DOI: 10.1016/j.pharmthera.2013.09.002.
92. STRAHM, Emmanuel, MULLEN, Jenny E., GÅREVIK, Nina, ERICSSON, Magnus, SCHULZE, Jenny J., RANE, Anders and EKSTRÖM, Lena. Dose-dependent testosterone sensitivity of the steroidal passport and GC-C-IRMS analysis in relation to the UGT2B17 deletion polymorphism. *Drug Testing and Analysis.* November 2015. 7(11), pp. 1063-1070. ISSN: 1942-7603. DOI: 10.1002/dta.1841.

93. The International Conference on Harmonisation of Technical Requirements for Registration of Pharmaceuticals for Human Use. *Guidance on nonclinical safety studies for the conduct of human clinical trials and marketing authorization for pharmaceuticals M3(R2)* [online]. June 2009. [cit. 2018-03-26]. Available from: http://www.ich.org/fileadmin/Public_Web_Site/ICH_Products/Guidelines/Multidisciplinary/M3_R2/Step4/M3_R2__Guideline.pdf.
94. Thermo Fisher Scientific Inc. *User Guide: Pierce BCA Protein Assay Kit (MAN0011430 Rev. A)* [online]. 2013. [cit. 2018-06-01]. Available from: http://tools.thermofisher.com/content/sfs/manuals/MAN0011430_Pierce_BCA_Protein_Asy_UG.pdf
95. THIBAUDEAU, Jean, LÉPINE, Johanie, TOJCIC, Jelena, DUGUAY, Yannick, PELLETIER, Georges, PLANTE, Marie, BRISSON, Jacques, TÊTU, Bernard, JACOB, Simon, PERUSSE, Louis, BÉLANGER, Alain and GUILLEMETTE, Chantal. Characterization of common UGT1A8, UGT1A9, and UGT2B7 variants with different capacities to inactivate mutagenic 4-hydroxylated metabolites of estradiol and estrone. *Cancer Research.* January 2006. 66(1), pp. 125-133. ISSN: 0008-5472. DOI: 10.1158/0008-5472.CAN-05-2857.
96. TOURANCHEAU, Alan, MARGAILLAN, Guillaume, ROULEAU, Mélanie, GILBERT, Isabelle, VILLENEUVE, Lyne, LÉVESQUE, Éric, DROIT, Arnaud, and GUILLEMETTE, Chantal. Unravelling the transcriptomic landscape of the major phase II UDP-glucuronosyltransferase drug metabolizing pathway using targeted RNA sequencing. *Pharmacogenomics Journal.* February 2016. 16(1), pp. 60-70. ISSN: 1470-269X. DOI: 10.1038/tpj.2015.20.
97. TROBERG, Johanna, JÄRVINEN, Erkka, GE, Guang-Bo, YANG, Ling and FINEL, Moshe. UGT1A10 is a high activity and important extrahepatic enzyme: Why has its role in intestinal glucuronidation been frequently underestimated? *Molecular Pharmaceutics.* September 2017. 14(9), pp. 2875-2883. ISSN: 1543-8384. DOI: 10.1021/acs.molpharmaceut.6b00852.
98. TUKEY, Robert H. and STRASSBURG, Christian P. Human UDP-glucuronosyltransferases: Metabolism, expression, and disease. *Annual Review of Pharmacology and Toxicology.* 2000. 40, pp. 581-616. ISSN: 0362-1642. DOI: 10.1146/annurev.pharmtox.40.1.581.

99. UGT Nomenclature Committee. *UGT alleles nomenclature – Pharmacogenomics* [online]. June 2005. [cit. 2017-12-06]. Available from: https://www.pharmacogenomics.pha.ulaval.ca/ugt-alleles-nomenclature/.
100. VENKATAKRISHNAN, Karthik, MOLTKE, Lisa L. von, OBACH, Ronald S. and GREENBLATT, David J. Drug metabolism and drug interactions: Application and clinical value of in vitro models. *Current Drug Metabolism.* October 2003. 4(5), pp. 423-459. ISSN: 1389-2002. DOI: 10.2174/1389200033489361.
101. WADE, Leroy G. and SIMEK, Jan W. Alkyl Halides. Nucleophilic Substitution. In: *Organic Chemistry, Global Edition.* Ninth Edition. United Kingdom: Pearson Education Limited, 2016. ISBN: 1-292-15110-2.
102. WALIA, Gurinder, SMITH, Alexander D., RICHES, Zoe, COLLIER, Abby C. and COUGHTRIE, Michael W.H. The effects of UDP-sugars, UDP and Mg2+on uridine diphosphate glucuronosyltransferase activity in human liver microsomes. *Xenobiotica.* September 2017. pp. 1-9. ISSN: 0049-8254. DOI: 10.1080/00498254.2017.1376260.
103. WALSKY, Robert L., BAUMAN, Jonathan N., BOURCIER, Karine, GIDDENS, Georgina, LAPHAM, Kimberly, NEGAHBAN, Andre, RYDER, Tim F., OBACH, Roland S., HYLAND, Ruth and GOOSEN, Theunis C. Optimized assays for human UDP-glucuronosyltransferase (UGT) activities: Altered alamethicin concentration and utility to screen for UGT inhibitors. *Drug Metabolism and Disposition.* May 2012. 40(5), pp. 1051-1065. ISSN: 0090-9556. DOI: 10.1124/dmd.111.043117.
104. WESTERLIND, Kim C., GIBSON, Kristin J., EVANS, Glenda L. and TURNER, Russel T. The catechol estrogen, 4-hydroxyestrone, has tissue-specific estrogen actions. *Journal of Endocrinology.* 2000. 167(2), pp. 281-287. ISSN: 0022-0795. DOI: 10.1677/joe.0.1670281.
105. WEUSTEN, Jos J.A.M., LEGEMAAT, G., WOUW, Marianne P. M. E., SMALS, Anthony G.H., KLOPPENBORG, Peter W.C. and BENRAAD, Theo J. The mechanism of the synthesis of 16-androstenes in human testicular homogenates. *Journal of Steroid Biochemistry.* May 1989. 32(5), pp. 689-694. ISSN: 0022-4731. DOI: 10.1016/0022-4731(89)90513-X.
106. WILKINSON, Shane M., WATSON, Morgan A., WILLIS, Anthony C. and MCLEOD, Malcolm D. Experimental and kinetic studies of the Escherichia coli glucuronylsynthase: An engineered enzyme for the synthesis of glucuronide

conjugates. *Journal of Organic Chemistry.* April 2011. 76(7), pp. 1992-2000. ISSN: 0022-3263. DOI: 10.1021/jo101914s.

107. World Anti-Doping Agency. *Prohibited List - World Anti-Doping Agency* [online]. January 2018. [cit. 2018-02-10]. Available from: https://www.wada-ama.org/sites/default/files/prohibited_list_2018_en.pdf

108. WU, Baojian, BASU, Sumit, MENG, Shengnan, WANG, Xiaoqiang, ZHANG, Shuxing and Ming HU. Regioselective sulfation and glucuronidation of phenolics: Insights into the structural basis. *Current Drug Metabolism.* November 2011. 12(9), pp. 900-916. ISSN: 1389-2002. DOI: 10.2174/138920011797470100.

109. YAGER, James D. Mechanisms of estrogen carcinogenesis: The role of E2/E1-quinone metabolites suggests new approaches to preventive intervention - A review. *Steroids.* May 2015. Part A, pp. 56-60. ISSN: 0039-128X. DOI: 10.1016/j.steroids.2014.08.006.

110. YANG, Na, SUN, Runbin, LIAO, Xiaoying, AA, Jiye and WANG, Guangji. UDP-glucuronosyltransferases (UGTs) and their related metabolic cross-talk with internal homeostasis: A systematic review of UGT isoforms for precision medicine. *Pharmacological Research.* July 2017. 121, pp. 169-183. ISSN: 1043-6618. DOI: 10.1016/j.phrs.2017.05.001.

111. ZAMRAZILOVÁ, Ludmila, SOSVOROVÁ, Lucie, HERÁČEK, Jiří, SOBOTKA, Vladimír and HAMPL, Richard. The content of five sex steroids in human testis. *Physiological Research.* 2012. 61(2), pp. 221-225. ISSN: 1802-9973.

112. ZHANG, Hongbo, TOLONEN, Ari, ROUSU, Timo, HIRVONEN, Jouni and FINEL, Moshe. Effects of cell differentiation and assay conditions on the UDP-glucuronosyltransferase. *Drug Metabolism and Disposition.* March 2011. 39(3), pp. 456-464. ISSN: 0090-9556. DOI: 10.1124/dmd.110.036582.

113. ZHANG, Hongbo, PATANA, Anne-Sisko, MACKENZIE, Peter I., IKUSHIRO, Shinichi, GOLDMAN, Adrian and FINEL, Moshe. Human UDP-glucuronosyltransferase expression in insect cells: Ratio of active to inactive recombinant proteins and the effects of a C-terminal his-tag on glucuronidation kinetics. *Drug Metabolism and Disposition.* October 2012. 40(10), pp. 1935-1944. ISSN: 0090-9556. DOI: 10.1124/dmd.112.046086.

114. ZHU, Bao T. and CONNEY, Allan H. Functional role of estrogen metabolism in target cells: Review and perspectives. *Carcinogenesis.* January 1998. 19(1), pp. 1-27. ISSN: 0143-3334. DOI: 10.1093/carcin/19.1.1.